Ferdowsi University of Mashhad

Print ISSN 2008-9147
Online ISSN 2717-3364
Numbers: 24

JCMR

Journal of Cell and Molecular Research

Volume 12, Number 2, (Winter) 2021

بسم الله الرحمن الرحیم

Issuance License No. 124/902-27.05.2008 from Ministry of Culture and Islamic Guidance
Scientific Research Issuance License No. 161675 from the Ministry of Science, Research and Technology, Iran

Journal of Cell and Molecular Research (JCMR)

Volume 12, Number 2, (Winter) 2021

JCMR Office: Department of Biology, Faculty of Sciences, Ferdowsi University of Mashhad, Mashhad, Iran.
Postal Code: 9177948953
P.O. Box: 917751436
Tel: +98-513-8804063/+98-9156996326
Fax: +98-513-8795162
E-mail: jcmr@um.ac.ir
Online Submission: https://jcmr.um.ac.ir

Table of Contents

Journal of Cell and Molecular Research (2021) 12 (2), 49-55 DOI: 10.22067/jcmr.2021.67052.0

Research Article

LncRNA *HOXD-AS1* Is Upregulated in Ovarian Cancer

Seyedeh Nahid Fotuhi [1], Mohammad Khalaj-Kondori [1,*], Hadis Karimi [2]

[1] *Department of Animal Biology, Faculty of Natural Sciences, University of Tabriz, Tabriz, Iran*
[2] *Department of Biology, Science and Research Branch, Islamic Azad University, Tehran, Iran*

Received 6 November 2020 Accepted 12 March 2021

Abstract

Patients with ovarian cancer are mostly diagnosed at advanced stages which leads to poor prognosis and high mortality rate. Deregulation of lncRNA *HOXD-AS1* expression associates with cancer development and metastasis. However, the expression level of this lncRNA in ovarian cancer is not determined.50 paired ovarian tumors and their adjusted normal tissues were included in the study. Total RNA was extracted by TRIzol® Reagent and reverse-transcribed to cDNA using PrimeScript II cDNA synthesis kit. The expression levels of *HOXD-AS1* were quantified by qRT-PCR and compared. The Roc curve analysis was used to evaluate the capacity of *HOXD-AS1* as a biomarker for ovarian cancer. We observed that lncRNA *HOXD-AS1* was significantly upregulated in ovarian tumors compared to their adjusted normal tissues ($p<0.003$). Moreover, the ROC curve analysis revealed that the lncRNA *HOXD-AS1* expression level could discriminate tumoral and non-tumoral tissues with 85% sensitivity and 88% specificity. The lncRNA *HOXD-AS1* expression level might be considered as a potential biomarker for ovarian cancer development.

***Keywords*:** Ovarian cancer, Biomarker, lncRNA, *HOXD-AS1*, Gene expression

Introduction

Ovarian cancer (OC) can be the most lethal gynecological cancer and the seventh most common malignancy worldwide (Zhang et al., 2019). According to the researches, many countries show a high age-standardized incidence rate of ovarian cancer (Momenimovahed et al., 2019; Zhang et al., 2019). Despite this severe disease is one of the most mortality determinants in women, improved diagnostic methods have caused its incidence and mortality to be decreasing during the last few decades (La Vecchia, 2001; Razi et al., 2016). Although, there is no specific and sensitive screening method for ovarian cancer, small tumors are still the most important prognostic factors. This disease is usually diagnosed after metastasis of cancer, so the survival rate is a bit low (Knutson et al., 2015; LaDuca et al., 2019). Nowadays, molecular biomarkers are considerably growing and scientists attempt to introduce them as a diagnostic tool for severe diseases (Bignotti et al., 2006; Liu et al., 2014). Using these biomarkers leads to early-stage diagnosis which is prominent factor to improve survival (Ditto et al., 2019). In this regard, researchers are trying to discover novel diagnostic biomarkers/panels for early diagnosis of ovarian cancer. Therefore, many molecular biomarkers/panels have been recognized (Dochez et al., 2019; Zhang et al., 2011). For instance, the combination of serum *CA125* and *HE4* comes to be one of the most popular markers which have been studied (Dochez et al., 2019), but markers should possess high sensitivity and specificity (Jacobs and Bast Jr, 1989); and still need further validation.

Homeobox (HOX) genes play an essential role in embryonic development and oncogenesis. The *HOX* clusters contain various non-protein-coding RNAs, including some lncRNAs (Li et al., 2019). *HOXD-Antisense1* (*HOXD-AS1*) is encoded by the HOXD cluster on human chromosome 2q31.2 in an antisense manner (Goode et al., 2010). It is evolutionary conserved among hominids and shows all bona fide features of a gene. *HOXD-AS1* is activated by PI3K/AKT pathway and plays an important role in cell differentiation (Yarmishyn et al., 2014). Knock-down of *HOXD-AS1* confirmed that it can control the expression of clinically significant protein-coding genes which are the hallmarks of metastatic cancer. Moreover, studies

*Corresponding author's e-mail address:
khalaj@tabrizu.ac.ir, khalaj49@gmail.com

revealed that *HOXD-AS1* is usually overexpressed in hepatocellular carcinoma as well as patients with metastatic cancer (Soshnikova and Duboule, 2009; Yuan et al., 2014). *HOXD-AS1* activates a GTPase protein in the MERK/ERK signaling cascade, leading to metastasis through impeding of the apoptosis (Fang and Fullwood, 2016). Here, we compared the expression levels of *HOXD-AS1* in 50 ovarian tumors and their paired adjusted normal tissues. Moreover, the potency of HOXD-AS1 as an ovarian cancer biomarker was evaluated with ROC curve analysis.

Materials and Methods

Study subjects

50 women with ovarian cancer who had been referred to AL-Zahra Hospital of Tabriz were included in the study. After surgical operation, 50 paired ovarian tumor and marginal non-tumor samples were collected. The samples were diagnosed and approved by the pathologist. None of the patients had received chemotherapy before sampling. The study protocol was approved by the Clinical Research Ethics Committee and all subjects signed the informed consent according to the approved guidelines of AL-Zahra Hospital. Clinical information was collected from hospital records as well as by patient interviews. Table 1 represents the clinicopathologic data of the samples.

Total RNA purification

All tissue samples were collected in RNase/DNase free tubes. Samples were snap-frozen in liquid nitrogen and stored at −80°C. For RNA extraction, 30-40 mg of tissue sample was pulverized under liquid nitrogen using pestle and mortar. TRIzol® Reagent (Ambion) was used to extract total RNA from the samples according to the manufacturer's instructions. Protein and DNA contamination was eliminated by RNA Purification Kit (TIANGEN, Beijing, China). The RNA purification was evaluated by a NanoDrop ND-1000 spectrophotometer at 260 and 280 nm and the integrity of the samples was assessed by 1% gel electrophoresis.

qRT-PCR

The RNA samples were treated with DNase I according to the manufacturer's instructions (Takara, Japan). 500 ng total RNA was used for reverse transcription reaction using PrimeScript II cDNA synthesis kit (Takara, Japan). The cDNAs were applied for amplification of lncRNA *HOXD-AS1* using primers; 5′- TAATGCCAAGAACTCCCAG -3′ (forward) and 5′- GTATTCAAGGGACAGTCACAG -3′ (reverse) as well as *GAPDH* using primers; 5′- GAGAAGTATGACAACAGCCTC-3′ (forward) and 5′- TGAGTCCTTCCACGATAC -3′ (reverse) as an internal control. Quantification of the *HOXD-AS1* expression level was done by SYBR- Ampliqon (RealQ Plus 2x Master Mix Green) with an Applied Biosystems Step One Plus system using $2^{-\Delta CT}$ method (Livak and Schmittgen, 2001). The Real-time PCR reactions were run at 95°C for 10 min, followed by 40 cycles of 95°C for 20 sec, 62°C for 25 sec and 72°C for 25 sec, in 20 µl total volumes. All amplification reactions were done in duplicate format.

Statistical analysis

The data were analyzed with SPSS 24.0 (USA). The student *t*-test was used for comparison of the *HOXD-AS1* expression levels between the tumor and

Table 1. Clinicopathologic data
The clinical data are written as percentage and numbers of patients in each group for disease stage.
RMI: risk of malignancy index

	Non-tumor marginal tissue	Ovarian tumor tissue
	n = 50	n = 50
Age, years	50 (33 – 68)	50 (33 – 68)
Preoperative RMI	57 (0-1740)	4327 (33–53,000)
Disease Stage		Stage I: (n=17; 6.8%) Stage II: (n= 15; 4.9%) Stage III: (n=12; 43.9%) Stage IV: (n=6; 47.8%)
CA 125 by FIGO class: U/mL		Stage I: 66 Stage II: 229 Stage III: 910 Stage IV: 891

non-tumor control groups. Differences were considered significant at p value <0.05. Receiver-operating characteristic (ROC) curves and area under the curve (AUC) were used to assess the possibility of using *HOXD-AS1* as a diagnostic tool for detecting ovarian cancer.

Results

HOXD-AS1 expression is upregulated in ovarian cancer

The lncRNA *HOXD-AS1* expression in ovarian tumor tissues was quantified and compared with that of paired non-tumor marginal tissues by qRT-PCR. The results showed that the expression of *HOXD-AS1* in carcinoma tissues was significantly higher (p < 0.003) than those of the non-tumor marginal tissues (Figure 1A). Further correlation analysis revealed that the *HOXD-AS1* expression level was positively correlated with the disease stage (r = 0.3271, P <0.001) (Figure 1B).

HOXD-AS1 expression level might serve as a biomarker for ovarian cancer diagnosis

The biomarker capacity of the *HOXD-AS1* expression level for ovarian cancer was evaluated with the receiver operating characteristics (ROC) curve analysis. The ROC curve analysis showed an AUC (area under the curves) of 0.88 (P < 0.0001, 95% CI 0.8141- 0.9495). This analysis revealed that the *HOXD-AS1* expression level could discriminate ovarian tumor and non-tumor tissues with 85% sensitivity and 88% specificity (Figure 2A). The corresponding dot plot with the data distribution is depicted in Figure 2B.

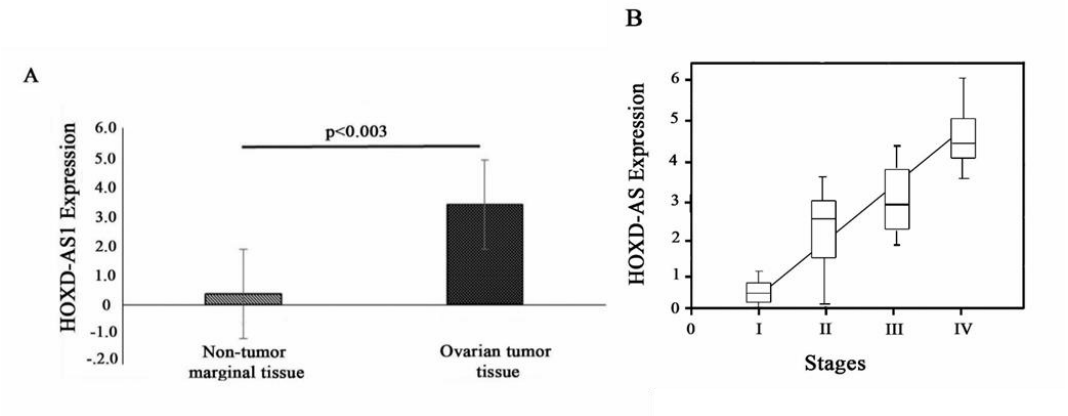

Figure 1. A) The expression of *HOXD-AS1* in carcinoma tissues was significantly higher (P< 0.003) than those of the non-tumor marginal tissues. B) The expression level shows positive correlation with disease stages.

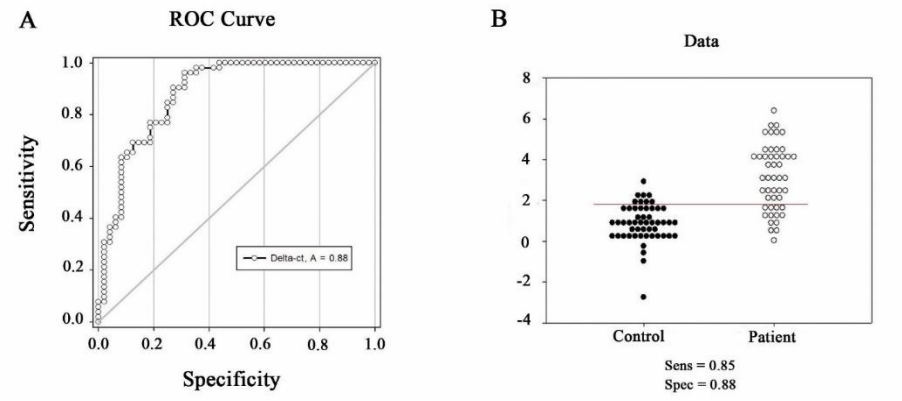

Figure 2. A) The data show that the *HOXD-AS1* expression level could discriminate ovarian tumor and non-tumor tissues with 85% sensitivity and 88% specificity. B) The corresponding dot plot showing the relative expression data distribution.

Discussion

LncRNAs are cis-/trans-regulating factors that their deregulation could result in aberrant gene expression (Chi et al., 2017). These deregulations could promote tumor development, progression, and metastasis of various type of cancers (Prensner et al., 2013; Yang et al., 2013; Yuan et al., 2014). Deregulation of the *HOXD-AS1* expression has been already reported in different cancers including bladder, cervical, colorectal, gastric, ovarian, prostate, and non-small cell lung cancers as well as hepatocellular carcinoma, melanoma, and osteosarcoma (Xie et al., 2019).

Here we compared the expression level of *HOXD-AS1* in ovarian tumor and non-tumor tissues to find out whether it may implicate with ovarian cancer development. Results showed that lncRNA *HOXD-AS1* was significantly upregulated in ovarian cancer and suggested its potential role in the ovarian cancer development. These findings are in line with the reports by Dong et al., where they observed a significant overexpression of *HOXD-AS1* in epithelial ovarian cancer tissues (Dong et al., 2019). Moreover, overexpression of this lncRNA was reported in an epithelial ovarian cancer cell line (Zhang et al., 2017). Further research has revealed that *HOXD-AS1* promotes cell proliferation, invasion, and epithelial-mesenchymal transition in epithelial ovarian cancer cells (Dong et al., 2019; Wang et al., 2018; Zhang et al., 2017), as well as invasion and metastasis in hepatocellular carcinoma cells (Wang et al., 2017).

Involving in the MEK\ERK signaling cascade (Larman et al., 2011; Yaginuma et al., 1992), *HOXD-AS1* also acts as an oncogene and changes oncogenic processes such as cell proliferation, differentiation, apoptosis, invasion, and metastasis (Wang et al., 2018; Xie et al., 2019). Consistently, we found out a positive correlation between this lncRNA expression level and the tumor stage (Figure 1B), implying that the elevated levels of *HOXD-AS1* may contribute to tumor progression. This evidence suggests that *HOXD-AS1* might be considered as a novel prognostic biomarker for malignant tumors (Dong et al., 2019).

To evaluate the biomarker capacity of this lncRNA for ovarian cancer development, we used ROC curve analysis. The results showed that the expression level of lncRNA *HOXD-AS1* could discriminate ovarian tumor and non-tumor samples with 85% sensitivity and 88% specificity. Therefore, *HOXD-AS1* expression level might serve as a potential biomarker for ovarian cancer development.

Although numerous studies have been published on the potential possibility of noncoding RNAs as cancer biomarkers (Russell et al., 2019; Sheng et al., 2020; Taylor and Gercel-Taylor, 2008), there is no certain lncRNA biomarker to diagnose ovarian cancer. However, some lncRNAs such as *MALAT1* (Zou et al., 2016), *SNHG15* (Qu et al., 2019), *ATB* (Yuan et al., 2020), *HOXA10*, and *HOXA11* (Fiegl et al., 2008; Vosseler et al., 2009) have been introduced as potential biomarkers for the ovarian cancer diagnosis.

In conclusion, this study approved that the lncRNA *HOXD-AS1* was significantly upregulated in ovarian cancer and its expression level might be considered as a potential biomarker for ovarian cancer development.

Acknowledgement

This study was supported by the research deputy of University of Tabriz. Authors appreciate all patients involved in the study.

Conflict of interest

The authors declare that they have no competing interests.

References

Bignotti E., Tassi R. A., Calza S., Ravaggi A., Romani C., Rossi E., et al. (2006) Differential gene expression profiles between tumor biopsies and short-term primary cultures of ovarian serous carcinomas: identification of novel molecular biomarkers for early diagnosis and therapy. Gynecologic oncology 103:405-416.

Chi J.-s., Li J.-z., Jia J.-j., Zhang T., Liu X.-m., and Yi, L. (2017). Long non-coding RNA ANRIL in gene regulation and its duality in atherosclerosis. Current Medical Science 37: 816-822.

Ditto A., Leone Roberti Maggiore U., Bogani G., Martinelli F., Chiappa V., Evangelista M. T., et al. (2019). Predictive factors of recurrence in patients with early-stage epithelial ovarian cancer. International Journal of Gynecology & Obstetrics 145:28-33.

Dochez V., Caillon H., Vaucel E., Dimet J., Winer N., and Ducarme G. (2019). Biomarkers and algorithms for diagnosis of ovarian cancer: CA125, HE4, RMI and ROMA, a review. Journal of ovarian research 12:28.

Dong S., Wang R., Wang H., Ding Q., Zhou X., Wang J.,et al. (2019). HOXD-AS1 promotes the epithelial to mesenchymal transition of ovarian cancer cells by regulating miR-186-5p and PIK3R3. Journal of Experimental & Clinical Cancer Research 38:110.

Fang Y., and Fullwood M. J. (2016). Roles, functions, and mechanisms of long non-coding RNAs in cancer. Genomics, proteomics & bioinformatics 14: 42-54.

Fiegl H., Windbichler G., Mueller-Holzner E., Goebel G., Lechner M., Jacobs I. J., and Widschwendter M. (2008). HOXA11 DNA methylation—a novel prognostic biomarker in ovarian cancer. International journal of cancer 123: 725-729.

Goode E. L., Chenevix-Trench G., Song H., Ramus S. J., Notaridou M., Lawrenson K., et al. (2010). A genome-wide association study identifies susceptibility loci for ovarian cancer at 2q31 and 8q24. Nature genetics 42: 874-879.

Jacobs I., and Bast Jr R. C. (1989). The CA 125 tumour-associated antigen: a review of the literature. Human reproduction 4: 1-12.

Knutson K. L., Karyampudi L., Lamichhane P., and Preston C. (2015). RETRACTED ARTICLE: Targeted immune therapy of ovarian cancer. Cancer and Metastasis Reviews 34: 53-74.

La Vecchia C. (2001). Epidemiology of ovarian cancer: a summary review. European Journal of Cancer Prevention 10: 125-129.

LaDuca H., Polley E. C., Yussuf A., Hoang L., Gutierrez S., Hart S. N.,et al. (2019). A clinical guide to hereditary cancer panel testing: evaluation of gene-specific cancer associations and sensitivity of genetic testing criteria in a cohort of 165,000 high-risk patients. Genetics in Medicine, 1-9.

Larman H. B., Zhao Z., Laserson U., Li M. Z., Ciccia A., Gakidis M. A. M., et al. (2011). Autoantigen discovery with a synthetic human peptidome. Nature biotechnology 29: 535-541.

Li L., Wang Y., Song, G., Zhang X., Gao S., and Liu H. (2019). HOX cluster-embedded antisense long non-coding RNAs in lung cancer. Cancer letters 450:14-21.

Liu R., Wang X., Aihara K., & Chen L. (2014). Early diagnosis of complex diseases by molecular biomarkers, network biomarkers, and dynamical network biomarkers. Medicinal research reviews 34, 455-478.

Livak K. J., and Schmittgen T. D. (2001). Analysis of relative gene expression data using real-time quantitative PCR and the $2^{-\Delta\Delta CT}$ method. methods 25:402-408.

Momenimovahed Z., Tiznobaik A., Taheri S., and Salehiniya H. (2019). Ovarian cancer in the world: epidemiology and risk factors. International journal of women's health 11:287.

Prensner J. R., Iyer M. K., Sahu A., Asangani I. A., Cao Q., Patel L., et al. (2013). The long noncoding RNA SChLAP1 promotes aggressive prostate cancer and antagonizes the SWI/SNF complex. Nature genetics 45:1392.

Qu C., Dai C., Guo Y., Qin R., and Liu J. (2019). Long noncoding RNA SNHG15 serves as an oncogene and predicts poor prognosis in epithelial ovarian cancer. OncoTargets and therapy 12, 101.

Razi S., Ghoncheh M., Mohammadian-Hafshejani A., Aziznejhad H., Mohammadian M., and Salehiniya H. (2016). The incidence and mortality of ovarian cancer and their relationship with the Human Development Index in Asia. ecancermedicalscience 10.

Russell M. R., Graham C., D'Amato A., Gentry-Maharaj A., Ryan A., Kalsi J. K.,et al. (2019). Diagnosis of epithelial ovarian cancer using a combined protein biomarker panel. British journal of cancer 121: 483.

Sheng R., Li X., Wang Z., and Wang X. (2020). Circular RNAs and their emerging roles as diagnostic and prognostic biomarkers in ovarian cancer. Cancer Letters 473:139-147.

Soshnikova N., and Duboule D. (2009). Epigenetic temporal control of mouse Hox genes in vivo. Science 324: 1320-1323.

Taylor D. D., and Gercel-Taylor C. (2008). MicroRNA signatures of tumor-derived exosomes as diagnostic biomarkers of ovarian cancer. Gynecologic oncology 110:13-21.

Vosseler S., Lederle W., Airola K., Obermueller E., Fusenig, N. E., and Mueller M. M. (2009). Distinct progression-associated expression of tumor and stromal MMPs in HaCaT skin SCCs correlates with onset of invasion. International journal of cancer 125: 2296-2306.

Wang H., Huo X., Yang X.-R., He,J., Cheng,L., Wang N.,et al. (2017). STAT3-mediated upregulation of lncRNA HOXD-AS1 as a ceRNA facilitates liver cancer metastasis by regulating SOX4. Molecular cancer 16: 136.

Wang Y., Zhang W., Wang Y., and Wang S. (2018). HOXD-AS1 promotes cell proliferation, migration and invasion through miR-608/FZD4 axis in ovarian cancer. American journal of cancer research 8: 170.

Xie S., Yang Y., Zhang J., Zhou S., Xie S., and Hua Y. (2019). HOXD-AS1: a novel oncogenic long intergenic non-coding RNA in humans. European review for medical and pharmacological sciences 23: 2898-2907.

Yaginuma Y., Yamashita K., Kuzumaki N., Fujita M., and Shimizu T. (1992). ras oncogene product p21 expression and prognosis of human ovarian tumors. Gynecologic oncology 46: 45-50.

Yang L., Lin C., Jin C., Yang J. C., Tanasa B., Li W., et al. (2013). lncRNA-dependent mechanisms of androgen-receptor-regulated gene activation programs. Nature 500: 598-602.

Yarmishyn A. A., Batagov A. O., Tan J. Z., Sundaram G. M., Sampath P., Kuznetsov V. A., and Kurochkin I. V. (2014). HOXD-AS1 is a novel lncRNA encoded in HOXD cluster and a marker of neuroblastoma progression revealed via integrative analysis of noncoding transcriptome. BMC genomics 15: S7.

Yuan D., Zhang X., Zhao Y., Qian H., Wang H., He C., et al. (2020). Role of lncRNA-ATB in ovarian cancer and its mechanisms of action. Experimental and Therapeutic Medicine 19: 965-971.

Yuan J.-h., Yang F., Wang F., Ma J.-z., Guo Y.-j., Tao Q.-f., et al. (2014). A long noncoding RNA activated by TGF-β promotes the invasion-metastasis cascade in hepatocellular carcinoma. Cancer cell 25: 666-681.

Zhang B., Cai F. F., and Zhong X. Y. (2011). An overview of biomarkers for the ovarian cancer diagnosis. European Journal of Obstetrics & Gynecology and Reproductive Biology 158: 119-123.

Zhang Y., Dun Y., Zhou S., and Huang X.-H. (2017). LncRNA HOXD-AS1 promotes epithelial ovarian cancer cells proliferation and invasion by targeting miR-133a-3p and activating Wnt/β-catenin signaling pathway. Biomedicine & Pharmacotherapy 96: 1216-1221.

Zhang Y., Luo G., Li M., Guo P., Xiao Y., Ji H., and Hao Y. (2019). Global patterns and trends in ovarian cancer incidence: age, period and birth cohort analysis. BMC cancer 19: 984.

Zou A., Liu R., and Wu X. (2016). Long non-coding RNA MALAT1 is up-regulated in

ovarian cancer tissue and promotes SK-OV-3 cell proliferation and invasion. Neoplasma 63, 865.

Journal of Cell and Molecular Research (2021) 12 (2), 56-64 DOI: 10.22067/jcmr.2021.68924.1003

Research Article

Cloning and Expression of a Fusion Protein Containing Highly Epitopic Regions of *Clostridium perfringens* Epsilon Toxin and *Clostridium novyi* Alpha Toxin

Mohsen Mehrvarz [1], Mohsen Fathi Najafi [1,*], Taghi Zahraei Salehi [2], Behjat Majidi [1]

[1] *Education and Extension Organization (AREEO), Agricultural Research, Razi Vaccine and Serum Research Institute, Mashhad Branch, Mashhad, Iran*

[2] *Department of Microbiology and Immunology, Faculty of Veterinary Medicine University of Tehran, Tehran, Iran*

Received 16 February 2021 Accepted 13 March 2021

Abstract

Clostridium perfringens and *novyi* species are two important toxin-producing pathogens which pose a risk to the livestock health. Epsilon and alpha toxins are major toxins of these two pathogens, respectively. Advances in current vaccine industrialization lead to the utilization of toxin epitopes instead of the whole pathogen/toxoids to produce novel vaccines. In the present study, bioinformatics approaches were applied to design a fused protein containing both toxin fragments of interest with the highest antigenicity score for B-cells. To do so different specialized algorithms including I-TASSER, IEDB, ElliPro, PyDock and CLC Main Workbench were applied. The chimeric protein was successfully cloned, expressed, and purified using an immobilized-metal affinity chromatography for His-tagged proteins. During *in vivo* experiments on rabbits, the levels of immunization provided by the recombinant protein or native alpha and epsilon toxins were compared based on serological studies. Results indicated that the designed protein was able to stimulate effective immune responses against both alpha and epsilon toxins. This can be used as a proper strategy to design novel peptide-based subunit vaccines.

***Keywords*:** Clostridium, Alpha toxin, Epsilon-toxin, Fusion protein, ELISA, Immunization

Introduction

Clostridium novyi (*C. novyi*) type B is the causative agent of infectious necrotic hepatitis (black disease, German Bradsot), especially in sheep. The major pathological determinant of the disease is the edema-inducing and lethal exotoxin alpha (2178 aa, MW: 250 kDa) which is produced by *C. novyi* type B (Busch et al., 2000). *Clostridium perfringens* produces four main lethal toxins (alpha, beta, epsilon, and iota) which are divided into 5 toxin types (A–E). Spores and toxins of *Clostridium perfringens* (*C. perfringens*) have reportedly been considered as biological warfare agents. Epsilon-toxin (ETX), a 34-kDa pore-forming protein, is considered as the major virulence factor of both type B and D strains. It was ranked as the third most potent Clostridium-derived toxin after botulinum and tetanus toxins (Alves et al., 2014). Enterotoxaemia can cause acute or super acute disease, with the sudden death of the affected animals. It provokes huge economic losses when large numbers of livestock are affected (Souzaet al., 2010). Considering the high lethality levels of these pathogens, efficient vaccination is highly desirable. Different vaccines were introduced to prevent the disease. Traditional vaccines are composed of live attenuated or fixed whole pathogens and carry native protein antigens. Although, these vaccines prevent the disease, some challenges such as the variable levels of the immune- and inflammatory responses induction following their application remains unsolved (Adhikari et al., 2012).

The latest progress in the evolution of vaccine formulations is the development of epitope-based vaccines (Palatnik-de-Sousa et al., 2018). The main benefit of immunization with these vaccines is the ability to effective stimulation of immune system with minimal structure of antigen and without any undesirable effects (Oscherwitz, 2016).

Previous studies confirmed that antibodies act more specifically when they are in contact with the epitopes of an antigen rather than the whole antigen (Watts, 2004). Hence, in the present study, we detected the antigenic regions of *C. novyi* alpha-toxin and *C. perfringens* epsilon-toxin to design a fusion peptide. In the chimeric protein these fragments were fused by a properly designed linker

*Corresponding author's e-mail address: najafiii99@gmail.com

sequence. During *in vivo* experiments, the immunogenic capacity of the new peptide was compared with native alpha and epsilon toxins.

Fusion of different antigens from two or more pathogenic sources is a technology which is proposed for concurrent induction of the immunity against different pathogens. Putting both antigens in just one protein, not only makes the immunization faster and cheaper, but also in some cases makes it more effective (Schmidt, 2009). Moreover, the combination of vaccines is economically preferred when we consider its direct and indirect

consequences such as costs of extra injections, delayed or missed vaccinations, and additional handling and storage steps (Chandran et al., 2010). Epitope-based vaccines have been demonstrated to induce protection against many infectious diseases. For example, Pilechian et al designed a fusion protein of beta end epsilon toxins derived from type B and D of *C.perfringens* (Pilechian et al., 2011). In another study, a recombinant protein vaccine from *Pseudomonas aeruginosa* A and B flagellin epitopes was produced which caused less inflammation and infection in mice compared to the control samples (Weimer et al., 2009).

Materials and Methods

Bioinformatics

The most complete gene sequence of the alpha-toxin was introduced as Z48636.1 *C.novyi* in NCBI database with 6836 bps length. The gene sequence of epsilon toxin was obtained from NCBI with accession number of pCP8533etx and 1098 bps length.

The gene sequence of alpha toxin was obtained from NCBI with accession number of Z48636.1 and 6836 bps length and for epsilon toxin,

To determine the antigenicity of alpha and epsilon-toxins, their secondary structures and some other essential parameters were obtained from CLC Main Workbench 5 offline software. Reverse translation of the above mentioned gene sequences were applied as the input data to obtain the secondary structures of the proteins. Primer pairs and the linker sequence were selected according to our previous results obtained via bioinformatics (Noshahri et al, 2016, Mehrvarz et al, 2020). The designed construct was subjected to CLC Main Workbench and bioinformatics tools analysis to reveal its binding affinity with the major histocompatibility complex II (MHC-II) DRBI polymorphism in *Ovis*. Docking analysis was

Table 1. The first 10 highest scored MHC-II peptide binding results according to IEDB algorithm and similarity level of the sequences with previously identified sequences of the DRBI allele.

Allele	Start	End	length	peptide	IEDB rank
DRBI	108	122	15	GLQKISDKYYFNDN	76
DRBI	150	164	15	WFNNNKERYYFDSEG	66
DRBI	321	335	15	SDTVNKSDLNEDGIT	63
DRBI	36	50	15	KKGYQEIEGERYYFN	58
DRBI	5	19	15	HYKNIPGDTEFEYGW	51
DRBI	374	388	15	EKSNDSNIVKYRSLS	50
DRBI	271	284	15	PANTTVEVIAYLKKV	46
DRBI	250	264	15	TNTNTNSKEITHNVP	43
DRBI	160	174	15	FDSEGRLLTGYQVIG	41
DRBI	86	100	15	YTGWLTIDGNKYYFQ	35

performed using Pydock online software (https://life.bsc.es/servlet/pydock/).

Evaluation of ALE linear and structure-based epitopes was performed by Ellipro and Discotope online softwares, respectively (Table 1 and Figure 1). For both Pydock and IEDB (www.iedb.org) softwares, the PDB files of the fragments and proteins were obtained from I-TASSER online software (https://zhanglab.ccmb.med.umich.edu/I-TASSER/).

common phenol-chloroform method. The quality and quantity of DNA samples were determined by agarose gel electrophoresis and Nanodrop spectrophotometric method (260 nm), respectively.

The polymerase chain reaction (PCR) experiments were performed as follows: Initial denaturation (94°C, 5 min), denaturation (94 °C, 30 sec), annealing (53 °C and 55°C, 30 sec for epsilon and alpha toxin, respectively), extension (72 °C, 30 sec), and final extension (72 °C, 5 min). Primer sequences are shown in the Table 2. Fragments which were amplified by PCR, were cloned into pTZ57R vector by TA cloning system (CloneJET PCR Cloning Kit.,

Table 2. Primer sequences applied to perform PCR experiment. The linker sequence is also shown

Primer name	Sequence (5´-3´)
AHEF*-Forward	AATGGAGAGCTTCATTACAAAAAT
AHEF-Reverse	AAGAAGGGTTAAAGGTAAATATAA
EHEF*-Forward	AAAAATACTGATACAGTAACTGCAACTACTAC
EHEF-Reverse	AAAATAAGGACCACGGAATTATCTTTCTGAGG
Linker	GGATCCGGCAACTACAACCTGAAGAGCAACCAATATGAAGCTGAGCTC

*Abbreviations: AHEF (alpha high epitopic region), EHEF (epsilon high epitopic region)

Bacterial culture and molecular studies

C. perfringens (CN409) and *C. novyi* (CN804) bacterial strains were obtained from Razi Vaccine and Serum Research Institute, Mashhad, Iran. Both bacteria were cultured anaerobically in the liver extract medium prepared by Anomax instrument (Mart® microbiology B.V., Netherlands) at 37°C, pH 7.5 for 16 h. Bacterial DNA was extracted by the

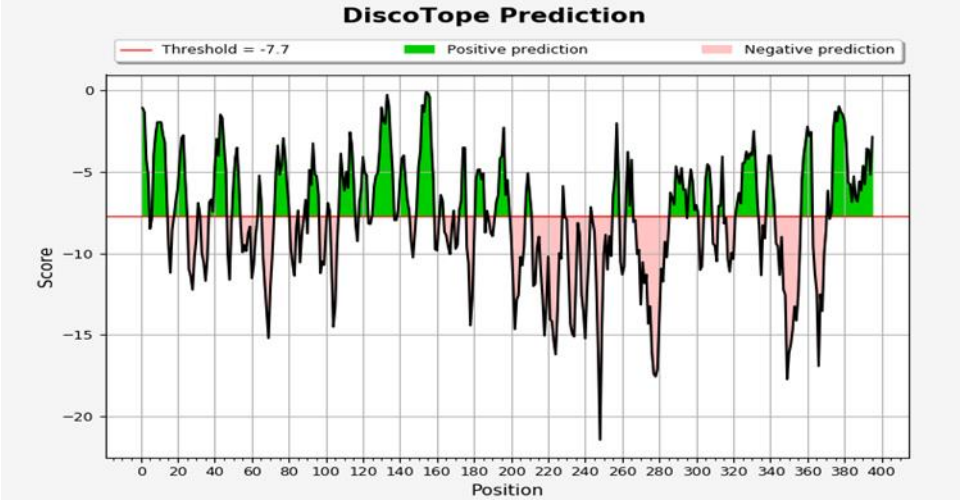

Figure 1. Structure-based antibody prediction for ALE fusion protein epitopes by Discotope according to Discotope score. The score is calculated through combining the contact numbers with propensity scores (PS). DiscoTope scores above the threshold (green regions) indicates positive predictions and that below the threshold (pink regions) indicates negative predictions .

K1231, Thermo scientific, USA). *Escherichia coli* DH5a competent cells were prepared and transformed by the recombinant plasmids using methods described by Sambrook (Sambrook et al., 2012).

To select cells containing recombinant plasmids,

they were cultured in the presence of ampicillin (100 µg/ml), IPTG (Isopropyl β- d-1-thiogalactopyranoside), and X-Gal (5-Bromo-4-Chloro-3-Indolyl β-D-Galactopyranoside). White colonies, which are supposed to carry recombinant plasmids, were cultured. Then, their plasmids were extracted to confirm the validity of the cloning based on PCR experiments for epsilon and alpha toxin sequences. Other rounds of PCR studies were performed using M13 forward and reverse primers (specific to PTZ57R) to make sure that the fragments are properly placed in plasmids in the correct direction. Selected recombinant clones were cultured and plasmid contents were extracted by Roche plasmid extraction kit.

Digestion of plasmids was performed using the mentioned enzymes in Figure 2. Desirable fragments were isolated from low melting agarose gel (Thermofisher, 16520-050, USA) using Roche gel extraction kit (Roche, 11696505001, Germany). Ligation of fragments was performed using a designed linker and then directly cloned into poly histidine tagged vector: pET28a (+) (Merck, 69864, Germany). Competent cells (*E. coli*, DH5a) were prepared and transformed by the recombinant plasmid pET28a+ containing a fusion sequence of AHEF-Linker-EHEF (ALE) (AHEF: alpha high epitopic region; EHEF: epsilon high epitopic region). Plasmid extraction was performed for the clones with desirable properties. Then, *E. coli* BL21 (DE3) host cells were transformed with these plasmids. To express high amounts of the recombinant proteins, validated clones were inoculated in 10 ml of the LB medium supplemented with kanamycin (50µg/ml) and IPTG (100uM), and incubated at 37ºC for 16-20 hours. Recombinant proteins were released to the culture medium by repeated rounds of freeze (liquid nitrogen, 5 min) and thawing (boiling water, 5 min). Then, the supernatants were used for indirect enzyme-linked immunosorbent assay (ELISA) against histidine tag. Colonies with the highest level of ALE expression were selected for downstream applications.

Fusion protein expression and purification

The selected colony in each experimental group was cultured overnight at 37°C in 500 ml LB medium containing 50µg/ml kanamycin and 100µM IPTG. The cultures were centrifuged and the pellets were collected and cell lysis was performed based on the freeze/thaw method. Briefly, cell pellets were resuspended in the lysis buffer (10 mM Imidazole, 50 mM NaH_2PO_4, 250 mM NaCl, pH=8), Lysozyme was added to the final concentration of 500 ug/ml. Following 40 min incubation on ice, cells were disrupted by sonication (Hielscher, Germany). Subsequently, in each case, 1.5 ml of Ni-NTA agarose (Qiagen, 30210, USA) was added to 10 ml of the lysate and mixed while shaking on ice for 60 min. To purify the target protein, the mixture was loaded on the column with the bottom outlet capped. Then, recombinant proteins were washed with 4 ml of washing buffer (250 mM NaCl, 20 mM Imidazole, 50 mM NaH_2PO_4, pH=8). The 6xHis-tagged recombinant proteins were eluted 4 times with 1 ml of elution buffer (250 mM NaCl, 250 mM Imidazole, 50 mM NaH_2PO_4, pH=8) per column and were collected in 4 separate tubes. Protein Slysates

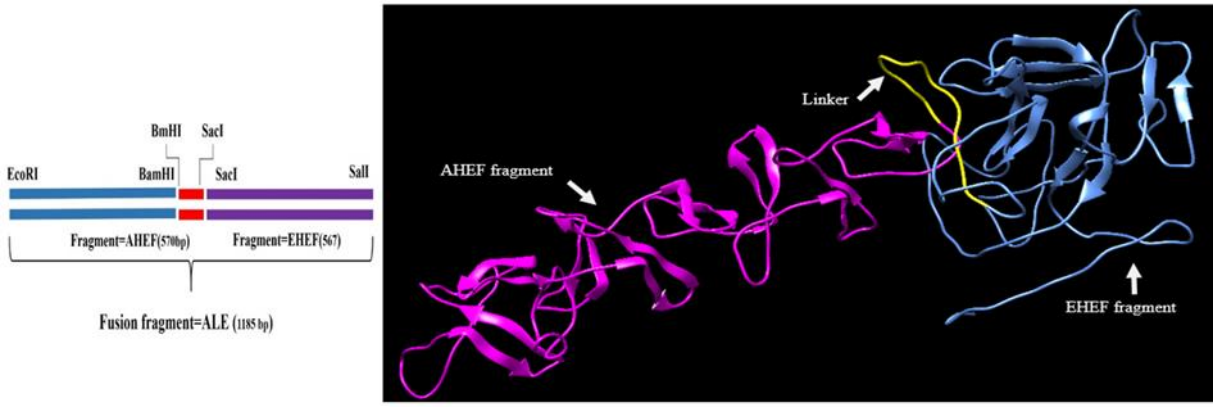

Figure 2. Schematic 3D representation of the designed fusion protein as it was drafted by the I-Tasser …. (A). Restriction map of the recombinant protein ALE (B). Different enzymes including EcoRI, BamHI, SacI, and SalI were applied to connect desirable fragments. The Linker was restricted by BamHI and SalI. In the final structure, AHEF (alpha toxin related fragment: pink-colored structure) is bounded to the EHEF (epsilon toxin related fragment: blue-colored structure) via the yellow-colored linker.

(25 µg/lane) were loaded on a 12% SDS–PAGE and transferred onto nitrocellulose membranes (BioRad Laboratories instrument, USA). The nitrocellulose membranes (Amersham, USA) were blocked with 3% BSA (Bovine serum albumin, Fraction V, Merck, A3311, Germany) and immunoblotting was performed with HRP-conjugated anti-poly Histidin (anti Rabbit, 1:1000) antibodies. The protein bands were visualized by DAB (3, 3'-Diaminobenzidine) staining (Merck, D12384, Germany).

Evaluation of rabbit immune responses against ALE fusion protein

Purified ALE fusion proteins were injected subcutaneousley to New Zealand White rabbits (female, 6 months old, 350-450g) 3 times with 2 weeks intervals. At the end, blood samples were collected and processed to prepare serum samples. Anti-alpha (*Clostridium novyi*) and anti-epsilon (*Clostridium perfringens*) toxins were obtained from Razi Vaccine and Serum Research Institute, Mashhad, Iran Immune responses of the rabbits were evaluated in case of the ALE protein and its cross-reactions with epsilon and alpha toxins. To do so related antibodies were measured based on indirect ELISA experiments.

Results

Bioinformatics studies and recombinant protein design

The best antigenic regions of alpha (EHEF) and epsilon-toxins (AHEF) were selected based on bioinformatics studies. The 3D schematic structure of the recombinant protein and the location of restriction sites are shown in Figure 2. Results from MHC-II peptide binding prediction obtained by IEDB are presented in table 3. The result from docking of ALE and the sequence of protein are being presented in figure 4. For docking studies, the 3D structure of the DRBI was applied as the ligand and the structure of the designed fusion protein was used as the receptor. The results from Pydock program indicated that the maximum affinity score of the fusion protein to DRBI was equal to -611.8, which demonstrated an acceptable level of stimulation for this protein. The binding sites of the MHC-II allele with ALE are shown in figure 4.

Bacterial strains were accurately cultured and identified and their DNA was extracted. Cloning and expression steps were successfully performed and confirmed by the mentioned methods. SDS-PAGE and Western blotting results verified the cloning and transformation steps and the proper expression of the antigenic peptides AHEF, EHEF, and fusion ALE in BL21 DE3 (Figure 3).

Table 3. Predicted B Cell Linear epitopes of the ALE fusion protein identified using Ellipro

Number	Start	End	length	Score*	Peptide sequence
1	1	57	57	0.801	NGELHYKNIPGDTFEYGWINIDSRWYFFDSINLIAKKGYQEIEGERYYFNPNTGVQE
2	371	395	25	0.766	DKKEKSNDSNIVKYRSLSIKAPGIK
3	290	333	44	0.732	NVKLVGQVSGSEWGEIPSYLAFPRDGYKFSLSDTVNKSDLNEDG
4	355	365	11	0.659	VRNLNTNNVQE
5	71	88	18	0.655	TNKHASSKRWGRAINYTG
6	262	276	15	0.624	NVPSQDILVPANTTV
7	100	105	6	0.599	QSNSKA
8	377	353	17	0.596	INGKGNYSAVMGDELIV
9	241	246	6	0.567	LTTSYS
10	194	199	6	0.502	NYNLKS

46

* ElliPro gives each predicted epitope with a score, defined as a PI (Protrusion Index) value averaged over epitope residues. In this method, the protein's 3D shape is approximated by a number of ellipsoids for each residue, a PI value is defined based on each residue's center of mass placed outside the largest possible ellipsoid

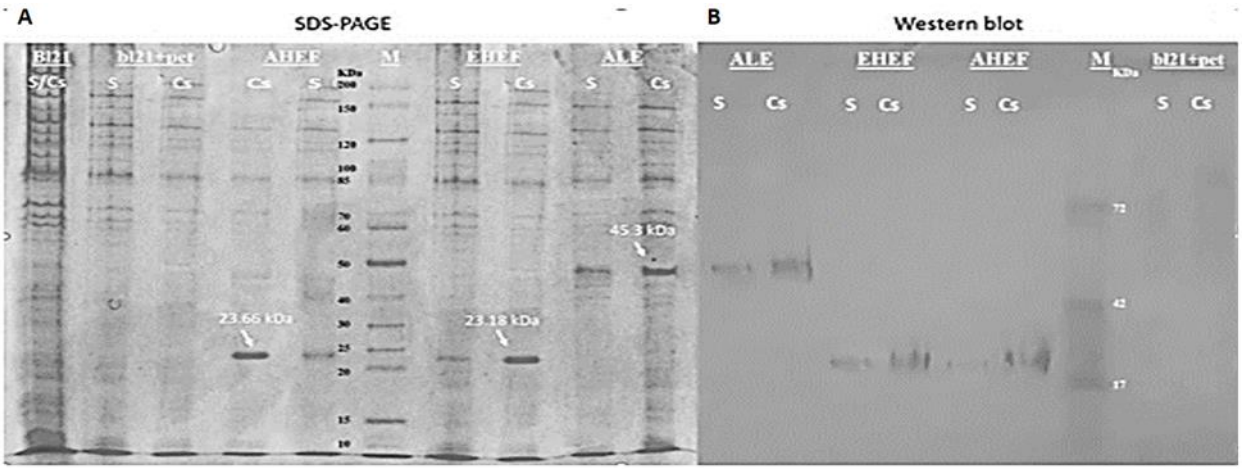

Figure 3. SDS-PAGE (A) and Western blotting (B) results of expressed AHEF (alpha related), EHEF (epsilon related) and ALE fusion fragments. (S: culture supernatant, Cs: cell lysate supernatant).

Antibody responses and cross-reactions analysis

Functional analysis based on ELISA experiments indicated that recombinant AHEF, and EHEF peptides were recognized by anti-native alpha and epsilon-toxin antibodies, respectively (Figure 5). Additionally, the ALE recombinant peptide reacted with both anti-native toxin antibodies due to the presence of AHEF and EHEF fragments in its structure. Cross reactions among anti-ALE antibodies, prepared by injection of the ALE purified peptides to the rabbit, and rabbit anti-alpha and anti-epsilon toxins with various antigens including the alpha-toxin (AT), epsilon-toxin (ET), AHEF, EHEF, and ALE are shown in the Figure 6. The protein content of the *E. coli* BL21 (DE3) containing pET28a (+) with no insertion was injected subcutaneously into a rabbit (150ug/injection). Then, antiserum was isolated and applied as the negative control.

Discussion

Antigenic epitopes are responsible for the interactions between antigens and their specific antibodies. To design effective vaccines against a wide range of pathogens, these epitopic regions, usually identified based on bioinformatics studies, can be utilized. The concurrent application of different algorithms to predict antigenic regions of peptides is a more reliable approach which ensures us about the final results. In the present study to predict highly immunogenic epitopes of both *Clostridium novyi* alpha toxin and *Clostridium perfringens* epsilon toxin, a set of different online and offline bioinformatics softwares were applied. These algorithms use different parameters such as hydrophobicity, hydrophilicity, rate of surface exposure, and etc. To be more efficient instead of

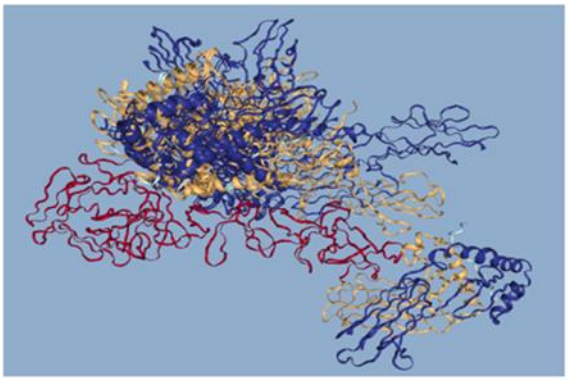

A

NGELHYKNIPGDTFEYGWINIDSRWYFFDSI
NLIAKKGYQEIEGERYYFNPNTGVQESGVFL
TPNGLEYFTNKHASSKRWGRAINYTGWLTL
DGNKYYFQSNSKAVTGLQKISDKYYYFNDN
GQMQIKWQIINNNKYYFDGNTGEAIIGWFNN
NKERYYFDSEGRLLTGYQVIGDKSYYFSDNI
NGNWEEGSGNYNLKSNQYEAELKNTDTVT
ATTTHTVGTSIQATAKFTVPFNETGVSLTTSY
SFANTNTNTNSKEITHNVPSQDILVPANTTVE
VIAYLKKVNVKGNVKLVGQVSGSEWGEIPSY
LAFPRDGYKFSLSDTVNKSDLNEDGTININGK
GNYSAVMGDELIVKVRNLNTNNVQEYVIPVD
KKEKSNDSNIVKYRSLSIKAPGIK

B

Figure 4. A) Results from the molecular docking of DRBI and ALE fusion protein. The output gives the 3D coordinates of two interacting fragments. B) The amino acid sequence of the ALE peptide. Blue: epsilon related fragment (EHEF), Yellow: alpha related fragment and red colored part represents the linker.

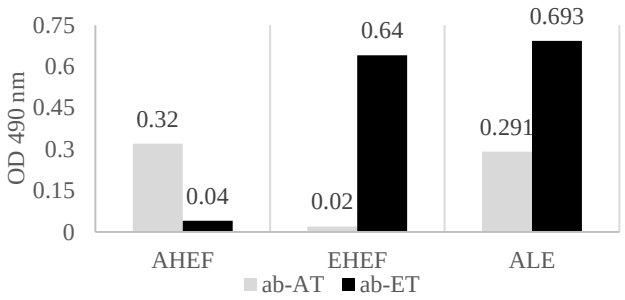

Figure 5. Immunologic assesment of the recombinant EHEF, AHEF, and ALE peptides reactions with specific anti-native alpha and epsilon toxin antibodies, as they were obtained by ELISA experiments (Wavelenght: 490 nm).

using one single epitope of each toxin a fragment which contains the highest scored epitopic region was selected from each structure to build a larger and more immunogenic multi-epitopic fragment. This removes the need for the simultaneous application of the adjuvants or repeated rounds of the injection (Majidi et al., 2020).

Antigenic regions are probably found with a higher frequency in C-terminal regions of the peptides in comparison to the N-terminal sequences with a higher number of beta-sheet structures. It was reported previously based on studies performed using Kolaskar and Willing algorithms and CLC5.5 software (Attasi, 1984). The antigenic fragment of the alpha-toxin (from amino acid 1731 to 1921) was introduced by Noshahri and colleagues (Noshari et al., 2016). Also, in a recent experiment, the epitopic region of the epsilon toxin (aa 531-1098) was reported based on the scores calculated by the Discotope and graphs which were obtained from different softwares (Mehrvarz et al., 2020). By designing multi-epitopic fragments with both B-cell- and T-cell-specific receptors, it would be possible to produce more potent proteins with the capacity for concurrent stimulation of cellular and humoral immune systems. However, direct fusion of different functional domains may lead to many undesirable outcomes such as misfoldings, low yields of protein production, and impaired bioactivities. Hence, designing proper linkers to connect individual fragments is a crucial step since they should have non-polar amino acids which kept the secondary structures, biological activities, and antigenic properties of all fragments, while they are conserving the ORF intact (Chen et al., 2011). Considering all above mentioned criteria a 48 bps linker was designed in which unique BamHI (5´) and SacI (3´) restriction sites were applied. Results from ELISA assay confirmed the desirable properties of the linker, as the ALE fusion protein was recognized with both anti-alpha and anti-epsilon antibodies. This confirms that both fragments of the protein maintained their natural secondary structures, biological activities, and antigenic capacities. Furthermore, according to results obtained during docking experiments, ALE can be recognized and interact with the DRB1 Ovis MHC-II allele.

Cross ELISA assay with anti-epsilon-toxin antibody showed quite noticeable differences between the reactions of the anti-epsilon antibody with alpha-toxin and AHEF compared to its reactions towards EHEF, ALE, and epsilon-toxin. This is an indicative that the anti-epsilon antibody can recognize selected epitopic regions of this toxin

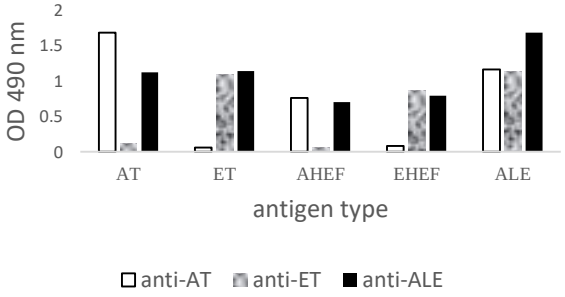

Figure 6. cross reactions of prepared antibodies against AT, ET and ALE with whole toxins and fragments.

only in native epsilon-toxin, EHEF, and ALE. Similarly, the anti-alpha-toxin antibody could only have noticeable reactions with alpha toxin, AHEF, and ALE but not epsilon-toxin and EHEF. This points out the specificity of antibodies for the epitopic areas of their corresponding toxins in alpha toxin, epsilon-toxin, AHEF, EHEF, and ALE. These results support our bioinformatics studies indicating that our antigenic fragments consist of most epitopic regions of the initial toxins which enables them to be recognized by the antibodies produced against their native toxins.

Rabbits immunized with ALE fusion protein were resulted in high production of related antibody. Results of ELISA assay of the anti-ALE fusion protein with different antigens showed that this antibody could recognize Alpha toxin, Epsilon-toxin, AHEF, EHEF and ALE itself indicating that our designed ALE fusion protein is capable of eliciting an immune response against epitopes of alpha and epsilon-toxins. So this could be a promising strategy to produce multi-purpose vaccines against enterotoxaemia diseases, which to our knowledge has not been reported previously.

In a similar study, a fusion protein of non-toxic regions of A and B toxins of *Clostridium difficile* (*C. diff*) was produced with a proper capacity for strong immune response induction. This recombinant protein protects the animal models against *Clostridium difficile* spores (Karczewski et al., 2014). In another report, non-pathogenic areas of the *Clostridium perfringens* type D epsilon-toxin were cloned and expressed in inclusion bodies of *E. coli* BL21 cells and their immunogenicity were evaluated in the animal models. It was confirmed that the anti-recombinant epsilon antibody could successfully recognize the recombinant peptide as well as the native epsilon-toxin (Souza et al., 2010). In addition, in another study by Uppalapati antibody against their designed fusion protein was specifically against alpha-toxin (one part of the their designed fusion protein) and the fusion protein was studied using cross ELISA method (Uppalapati et al., 2012). The results of our study confirmed the high specificity of the recombinant fusion protein (ALE) for anti-epsilon and anti-alpha toxin antibodies, which makes it a proper candidate for future vaccine examinations against enterotoxaemia and the black disease.

References

Adhikari R. P., Karauzum H., Sarwar J., Abaandou L., Mahmoudieh M., Boroun A. R., et al. (2012) Novel structurally designed vaccine for S. aureus α-hemolysin: protection against bacteremia and pneumonia. PloS one, *7*:6, p.e38567.

Alves G. G., Machado de Avila R. A., Chavez-Olortegui C. D. and Lobato F. C. (2014) Clostridium perfringens epsilon toxin: the third most potent bacterial toxin known. Anaerobe 30:102-107.

Attasi M. Z. (1984) Antigenic structures of proteins: their determination has revealed important aspects of immune recognition and generated strategies for synthetic mimicking of protein binding sites. European journal of biochemistry, 145:1, 1-20.

Busch C., Schomig K., Hofmann F. and Aktories K. (2000) Characterization of the catalytic domain of Clostridium novyi alpha-toxin. Infection and immunity, 68:11, 6378-6383.

Chandran D., Naidu S. S., Sugumar P., Rani G. S., Vijayan S. P., Mathur D., et al. (2010) Development of a recombinant epsilon toxoid vaccine against enterotoxemia and its use as a combination vaccine with live attenuated sheep pox virus against enterotoxemia and sheep pox. Clinical and Vaccine Immunology, 17:6, 1013-1016.

Chen J., Rood J. I. and McClane B. A. (2011) Epsilon-toxin production by Clostridium perfringens type D strain CN3718 is dependent upon the agr operon but not the VirS/VirR two-component regulatory system. MBio 2:6. e00275-11

Karczewski J., Zorman J., Wang S., Miezeiewski M., Xie J., Soring K., et al. (2014) Development of a recombinant toxin fragment vaccine for Clostridium difficile infection. Vaccine, 32:24, 2812-2818.

Majidi B., Fathi Najafi M. and Saeedyan S. (2020) Expression and purification of Brucella spp lumazine synthase decameric carrier in fusion to extracellular domain of influenza M2E protein. Iranian Journal of Chemistry and Chemical Engineering (IJCCE).

Mehrvarz M., Najafi M. F., Salehi T. Z. and Majidi B. (2020) In silico analysis and selection of Clostridium perfringens type D epsilon toxin multiepitope fragment. International Journal of Scientific Research and Engineering Development 2:6, 434-440.

Noshari N. G., Najafi M. F., Kakhki A. m., Majidi

B. and Mehrvarz M. (2016) Identification and cloning of highly epitopic regions of Clostridium novyi alpha toxin. Turkish Journal of Biology, 40:6, 1219-1226.

Oscherwitz J. (2016) The promise and challenge of epitope-focused vaccines. Human vaccines & immunotherapeutics, 12:8, 2113-2116.

Palatnik-de-Sousa C. B., Soares I. d. S. and Rosa D. S. (2018) Epitope discovery and Synthetic Vaccine design. Frontiers in immunology 9:826.

Pilechian L. R., AGHAEI P. K., Shamsara M., Jabbari A., Habibi G., Goudarzi H. et al. (2011) Fusion of Clostridium perfringens type D and B epsilon and beta toxin genes and it's cloning in E. coli, Archives of razavi institute, 66:1, 1-10.

Sambrook J., Green M., Sambrook J. and Sambrook J. (2012) Molecular Cloning: A Laboratory Manual, fourth ed. Cold Spring Harbor Laboratory Press, NewYork.

Schmidt S. R. (2009) Fusion-proteins as biopharmaceuticals–applications and challenges. Curr Opin Drug Discov Devel 12:2, 284-295.

Souza A. M., Reis J. K., Assis R. A., Horta C. C., Siqueira F. F., Facchin S., et al. (2010) Molecular cloning and expression of epsilon toxin from Clostridium perfringens type D and tests of animal immunization. Genetics and Molecular Research 9:1, 266-276.

Uppalapati S., Kingston J., Murali H. and Batra H. (2012) Generation and characterization of an inter-generic bivalent alpha domain fusion protein αCS from Clostridium perfringens and Staphylococcus aureus for concurrent diagnosis and therapeutic applications. Journal of applied microbiology, 113:2, 448-458.

Watts C. (2004) The exogenous pathway for antigen presentation on major histocompatibility complex class II and CD1 molecules. Nature immunology, 5:7, 685-692.

Weimer E. T., Lu H., Kock N. D., Wozniak D. J. and Mizel S. B. (2009) A fusion protein vaccine containing OprF epitope 8, OprI, and type A and B flagellins promotes enhanced clearance of nonmucoid Pseudomonas aeruginosa. Infection and immunity 77:6, 2356-2366.

Journal of Cell and Molecular Research (2021) 12 (2), 65-73 DOI: 10.22067/jcmr.v12i2.2102.1002

Review / Mini-Review

Signal Transduction of Unique RAS Family Member towards Cell Survival

Saeideh Nakhaei-Rad *

Stem Cell Biology and Regenerative Medicine Research Group, Institute of Biotechnology, Ferdowsi University of Mashhad, Mashhad, Iran.

Received 3 February 2021 Accepted 21 February 2021

Abstract

Small GTPases of RAS act as central regulators of intracellular signal transduction and translate external stimuli to the various cellular responses. Embryonic stem cell-expressed RAS (ERAS) is a member of the RAS family that is specifically expressed in undifferentiated mouse embryonic stem cells, hepatic stellate cells and diverse human tumors, such as gastric, breast, brain, pancreatic, melanoma and colorectal tumors. Although ERAS belongs to GTPase family, it is an inefficient enzyme to hydrolyze GTP to GDP. Therefore, it remains mainly in its GTP-bound active form and contributes to sustained signal transduction. In comparison with classical members (HRAS, NRAS and KRAS4B), ERAS is known as a unique member, due to its temporal expression, remarkable amino acid sequence deviations and functional differences. Notably, ERAS has been recently proposed as a potential marker for drug resistance in several human tumors. In this minireview, I compare in great detail the biochemical properties of ERAS with conventional members of RAS family, and discuss the main ERAS function in the control of the PI3K-AKT-mTORC survival pathway. Targeting this pathway may sensitize ERAS expressing cell populations to chemotherapy.

***Keywords*:** Embryonic stem cell-expressed RAS, Signaling, Cancer, Oncogene, Effector, Survival

Hallmarks of ERAS

Embryonic stem cell-expressed RAS (ERAS) is a novel and unique member of small GTPase of RAS. Its expression has been first reported in undifferentiated mouse embryonic stem cells in 2003 (Takahashi et al., 2003). ERAS is meanwhile known as a unique member of RAS family due to its temporal expression and unusual biochemical properties. Unlike classical RAS proteins, it is not ubiquitously expressed in human tissues. In human cells, *ERAS* promotor is silenced by DNA methylation and histone deacetylation. Treatment of cells with inhibitors of DNA methyltransferase and histone deacetylase has been shown to restore *ERAS* expression (Nakhaei-Rad et al., 2016; Yashiro et al., 2009; Yasuda et al., 2007).

Biochemistry of ERAS

Regulation of RAS activity

Small GTPases of RAS act as nodes of intracellular signal transduction and convert external stimuli to the various cellular out-comes, including cell proliferation, differentiation, cell survival, migration, apoptosis and calcium signaling (Nakhaei-Rad et al., 2018). Although, RAS proteins are expressed and available for signal transduction at the cellular membranes, they remain as inactive proteins (GDP-bound) unless they receive external stimuli and transform to active protein (GDP-to-GTP exchange) (Fig. 1A). By the action of two main classes of regulatory proteins, namely guanine nucleotide exchange factors (GEFs) and GTPase activating proteins (GAPs), they cycle between an active (GTP-bound) and inactive (GDP-bound) forms, respectively (Fig. 1A). Oncogenic mutations of RAS proteins in three hotspot residues of G12, G13 and Q61 are found in more than 30% of human tumors (Pylayeva-Gupta et al., 2011). These point mutations are placed at the region of the protein where affect either the intrinsic GTPase activity (Q61) of enzyme or impair GAP function (G12 and G13). ERAS is an oncogenic protein without presence of any of these hotspot mutations. ERAS has a natural amino acid deviation at the position of G12S (HRAS numbering; ERAS S50) which renders it GAP insensitive (Takahashi et al., 2003) (Fig. 1B). Substitution of critical residue of glycine 12 for any other amino acids rather than glycine impairs GAP function on RAS proteins, which affects the cycle of RAS from active form (GTP-bound) to inactive form (GDP-bound) (Scheffzek et al., 1997) (Fig. 1A and

* Corresponding author's E-mail address: s.nakhaeirad@ferdowsi.um.ac.ir

B). Among amino acids, glycine possesses the smallest side chain and this small side chain provides a space for arginine finger of GAP proteins to enter the active site of RAS enzymes and accelerate hydrolysis of GTP to GDP (Ahmadian et al., 1997). Therefore, as soon as ERAS is expressed, translates to the active protein which cannot be inactive with conventional GAP proteins (Fig. 1B). Up-to-date, there is not any reports for ERAS specific GAP or inhibitory protein. Thus, the regulation of ERAS at the level of transcription is a critical step on its function.

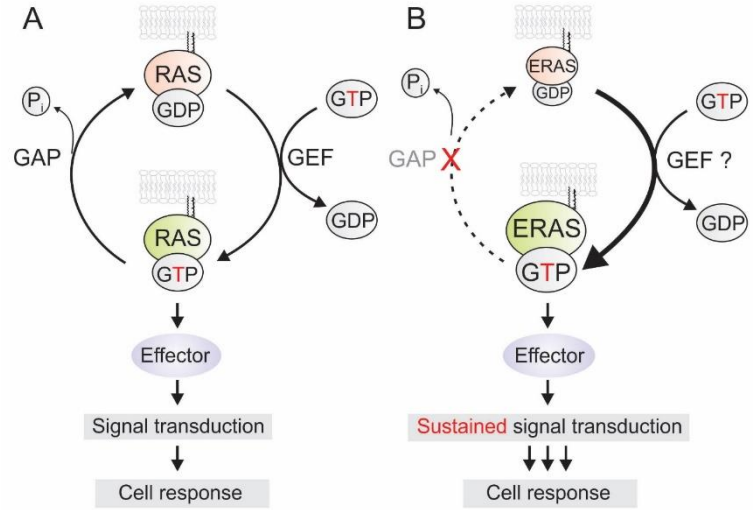

Figure 1. Schematic view of the RAS-GDP/GTP cycle and its comparison with ERAS. A) RAS proteins are cycling between GDP/GTP bound forms by the actions of two main regulatory proteins, GEF, and GAP. Through the interaction with effectors and switching ON the downstream pathways, RAS proteins exert their cellular functions, bottom in gray. B) ERAS harbors a deviation at G12 (S50 ERAS numbering) which impairs natural GTPase cycle to inactive form (GDP-bound) and makes it hyperactive protein with sustained signaling. GAP, GTPase-activating protein; GEF, guanine nucleotide exchange factor.

Structural fingerprints

RAS proteins harbor a conserved G domain with 5 motifs (G1-G5) that is responsible for a high-affinity binding to GTP (Fig1. B) (Bourne et al., 1990; Bourne et al., 1991). G1 with consensus sequence of GxxxxGKS binds to the phosphate groups of GTP, therefore it is known as P-loop (Saraste et al., 1990). Notably, critical residue of G12 is placed in this motif. G2 and G3 or switch I and switch II, respectively, are the flexible regions of the protein which upon binding to GTP or GDP move and provide a docking site for effector proteins (Vetter, 2001; Herrmann, 2003). G4 and G5 are differential motifs among GTPases and ATPases which covalently and specifically bind to the guanine base (Schmidt et al., 1996; Wittinghofer and Vetter, 2011). Although, ERAS protein as a member of RAS family owns conserved G domain with its essential motifs, it cannot efficiently hydrolyze GTP to GDP due to G12S (50 ERAS numbering) deviation in P-loop.

Effector selection by ERAS

Amino acid composition of switch I and switch II regions determine the specificity of RAS proteins for effector proteins (Wittinghofer and Vetter, 2011). Effector proteins are known as “effectors”, since RAS proteins alone cannot translate signals to the target proteins. These proteins are enzymes, scaffolds or modulators which upon RAS-GTP binding get activated or deactivated and diverge RAS signaling to the various cellular compartments and translate the RAS signaling to specific cellular out-comes (Nakhaei-Rad et al., 2018; Nakhaeizadeh et al., 2016). The specific RAS-effector interactions determine which pathways and where should be activated. Prototypes of RAS family, HRAS, NRAS and KRAS4B, possess similar sequences in their switch/effector regions which indicates, they could share the same set of downstream effectors (Nakhaeizadeh et al., 2016). In contrast, the sequence of switch regions of ERAS remarkably differs from HRAS, NRAS and KRAS4B. Therefore, ERAS may apply different set of effectors with different binding affinity and consequently emerges not overlapping cellular functions with classical RAS proteins. Among RASs, the phosphoinositide 3-kinase (PI3K) has the

highest affinity for ERAS (Fig. 3). Our mutational analysis of switch I, switch II and interswitch regions of ERAS to HRAS like sequence had revealed that tryptophan 79 of ERAS (arginine 41 of HRAS), within the interswitch region, is a main modulator for the effector selectivity of ERAS not its switch regions themselves (Nakhaei-Rad et al., 2015).

Prominent components of ERAS signal transduction towards cell survival

ERAS selectively and effectively activates PI3K signaling and this is due to the structural features of ERAS (see above). How dose PI3K support ERAS for its oncogenic function? To address this issue, we need to review in great details the components of this signaling pathway.

Lipid kinases

The RAS effector of PI3K belongs to the family of lipid kinases which phosphorylates phosphatidylinositol and phosphoinositides at inner leaflet of cellular membranes. According to the sequence homology and lipid substrates, three classes of PI3Ks are recognized: Class I, II and III. These kinases get activated either upon ligand binging to the receptor tyrosine kinases and G protein-coupled receptors or direct interaction with RAS proteins which targets them to the plasma membrane where they can interact with their substrates (Vanhaesebroeck et al., 2010). Class I PI3K consists of four heterodimeric proteins with two different functional subunits: catalytic and regulatory subunit. Based on the regulatory subunit, class I PI3K is subdivided in two categories; class IA p110α, p110β and p110δ that are associated with p85-like regulatory subunit (p85α/β, p50α and p55α/γ); class IB has a unique member, p110γ, which forms a heterodimer with regulatory subunits of p101 and p84 (Jean and Kiger, 2014; Vadas et al., 2011; Vanhaesebroeck et al., 2010). The catalytic subunits of class I, p110, exhibit differential expression patterns where p110α and β are ubiquitously expressed in human tissues but expression of p110γ and δ are imitated mainly to the hematopoietic lineages (Fritsch et al., 2013; Fritsch and Downward, 2013; Kok et al., 2009; Vanhaesebroeck et al., 2005).

The phosphorylates 3-hydroxyle of the phosphoinositide (4,5) bisphosphate (PIP_2) is a substrate of p110 catalytic subunit. Upon phosphorylation it is converted to a second messenger of phosphoinositide (3,4,5) trisphosphate (PIP_3) (Fig. 3). PIP_3 acts as a docking site for recruiting the proteins which harbors pleckstrin homology (PH) domain to the membrane. These PH containing proteins include adaptor proteins, protein kinases (*e.g.*, AKT and PDK1), RAS regulatory proteins of GEFs or GAPs (Vanhaesebroeck et al., 2001). Spatial localization of these protein through PH-PIP3 interactions, place them to the specific membrane nanoclusters where they could be in close approximately to their substrates.

Protein kinase B (PKB)

Protein kinase B (PKB) or AKT is a member of AGC subfamily of protein kinases and the most investigated target of PI3K-PIP3 axis. PI3K-PIP3-AKT activation results in cell proliferation, metabolic changes, cell growth, autophagy inhibition, and cell survival (Hers et al., 2011; Pearce et al., 2010). Activity of AKT is regulated by two critical posttranslational covalent modifications on its active site (T308) and hydrophobic motifs, S473 (Andjelkovic et al., 1997). AKT gets phosphorylated at position T308 by PDK1 enzyme (Alessi et al., 1997). Notably, both PDK1 and AKT share a PH domain that cluster them at the same membrane region via binding to PIP3. Phosphorylation of AKT at T308 position activates its kinase activity towards tuberous sclerosis 1/2 (TSC1/2) proteins (Fig. 3). TSC1/2 are GAP for a member of RAS family, RHEB, and their phosphorylation by AKT inhibits their GAP function. Consequently, RHEB could bind to its effector known as mammalian target of rapamycin (mTOR) complex 1 (Fig. 3) (Inoki et al., 2003; Inoki et al., 2002). A kinase for second key phosphorylation site of AKT (S473) is second mTOR complex (mTORC2) (see below for further information).

Composition of mammalian target of rapamycin (mTOR) complex 1 and 2

Two separate protein complexes of mTORC1 and mTORC2 share a same kinase, mTOR that is responsible for their catalytic activities (Zoncu et al., 2010). In addition to mTOR, these complexes have some negative and positive regulatory proteins in common such as DEP domain-containing mTOR-interacting protein (DEPTOR) and mammalian lethal with SEC13 protein 8 (mLST8), respectively (Loewith et al., 2002; Peterson et al., 2009)(Fig. 3). The main differences and accordingly specificity of mTORC1 and mTORC2 emerge from their accessory proteins of regulatory-associated protein of mTOR (RAPTOR) (Hara et al., 2002) and

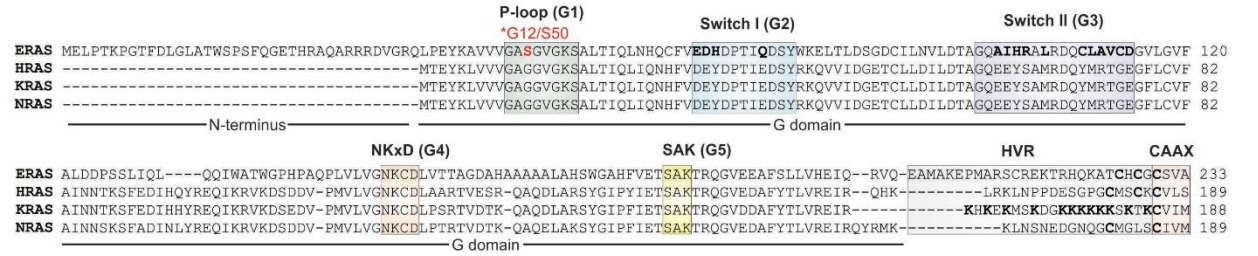

Figure 2. Overall sequence comparison of ERAS protein and classical RAS paralogs. ERAS contains an extended N-terminus (aa 1-38), which is not present in H, K, and NRAS. The P-loop (G1) of ERAS contains a serine (red) instead of a glycine (codon 12, HRAS numbering). Several residues in switch I (G2) and switch II (G2) regions that are responsible for effector recognition are different between ERAS and HRAS (bold letters). ERAS contains, like HRAS, a CAAX motif and two cysteines at the C-terminal hypervariable region (HVR), which is the site for posttranslational modifications by farnesylation and palmitoylation, respectively.

rapamycin-insensitive companion of mTOR (RICTOR), respectively (Sarbassov et al., 2004) (Fig. 3).

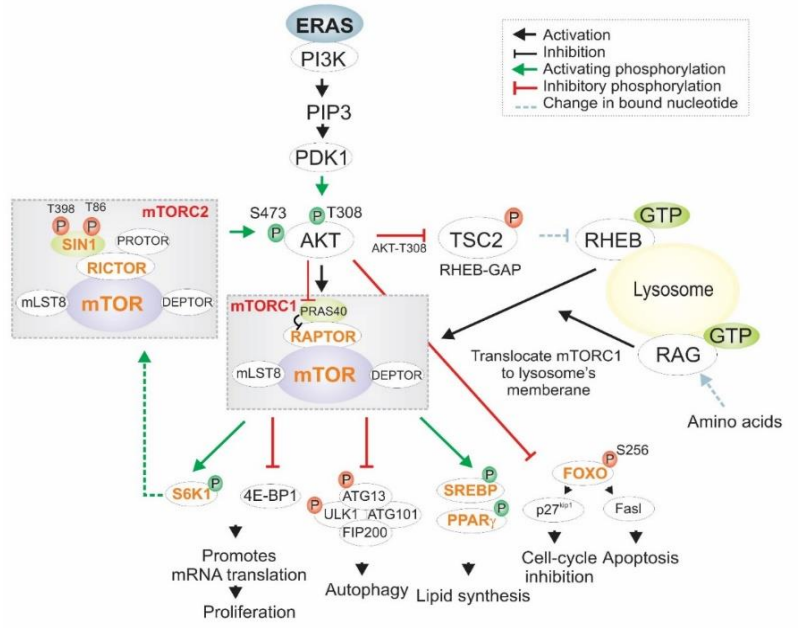

Figure 3. Schematic view of ERAS signaling towards mammalian target of rapamycin (mTOR) complexes. ERAS-PI3K-PDK1-AKT-mTORC signaling, its stimulation, regulation, substrates and cellular outcomes are illustrated. DEPTOR, DEP domain-containing mTOR-interacting protein; FIP200, FAK family kinase-interacting protein of 200 kDa; 4E-BP1, eukaryotic translation initiation factor 4E binding protein 1; FOXO1, forkhead transcription factor; GAP, GTPase activating protein; mLST8, mammalian lethal with SEC13 protein 8; mSIN1, mammalian stress-activated MAP kinase-interacting protein 1; mTORC, mammalian target of rapamycin; PDK1, 3-phosphoinositide-dependent protein kinase; PI3K, phosphoinositide 3-kinase; PKC, protein kinase C; PPARγ, peroxisome proliferator-activated receptor γ; PRAS40, 40 kDa Pro-rich AKT substrate; PROTOR, protein observed with RICTOR; RAPTOR, regulatory-associated protein of mTOR; RAS, rat sarcoma; RHEB, RAS homologue enriched in brain; RICTOR, mTORC2 rapamycin-insensitive companion of mTOR; TSC, tuberous sclerosis; ULK, Unc-51 like autophagy activating kinase 1.

Moreover, they are associated with other regulatory subunits, 40-kDa Proline-rich AKT substrate (PRAS40; mTORC1), mammalian stress-activated MAP kinase-interacting protein 1 (mSIN1/MAPKAP1; mTORC2) and protein observed with RICTOR (PROTOR; mTORC2) (Frias et al., 2006; Pearce et al., 2007; Sancak et al., 2007; Yang et al., 2006).

Regulators and targets of the mTOR complex 1

Since ERAS-PI3K-PDK1 signaling converges on mTORCs, here as cellular outputs of ERAS signaling, we specifically discuss targets of mTORC1/2. Signal transduction from PI3K-PDK1 towards mTORC1 occurs through inhibitory phosphorylation of TSC1/2 by AKT (phosphorylated at position T308) (Huang and Manning, 2008; Sancak et al., 2008). As a GAP, TSC1/2 is the negative regulator of RHEB GTPase (Tee et al., 2003) (Fig. 3). mTORC1 is an effector of RHEB, however, in physiological conditions mTORC is not located on the lysosomes. Therefore, one requirement of RHEB-mTORC1 interaction and its activation is translocation of mTORC1 to the endomembrane. Another GTPase, RAG resides together with RHEB on the lysosome/endosome surface. Changes in amino acid concentrations provide signals to stimulate RAG, which is responsible for endomembrane localization of mTORC1 (Sancak et al., 2008). Upon the TSC1/2 inactivation, RHEB stays in its GTP-loaded form and interacts and activates mTORC1 (Avruch et al., 2009; Inoki et al., 2003; Zoncu et al., 2010). mTORC1 phosphorylates wide range of substrates and regulates the ribosome biogenesis, mRNA translation, lipid synthesis and autophagy (Fig. 3) (Gentilella et al., 2015; Iadevaia et al., 2012; Kim and Chen, 2004; Porstmann et al., 2008; Yu et al., 2010). The best studies kinase downstream of mTORC1 is S6 kinase 1 (S6K1). S6K1 phosphorylates ribosomal protein S6, mTOR itself at position S2448, eukaryotic elongation factor 2 kinase (eEF2) and eIF4B (Hara et al., 1997; Ma and Blenis, 2009; Ma et al., 2008; Wang et al., 2001).

Regulators and targets of mTOR complex 2

Although, the growth factor signaling and mTORC2 association with ribosome are reported to control mTORC2 activity and assembly, the main upstream regulators of mTORC2 still remain as big puzzles (Zinzalla et al., 2011). Upon activation by mTORC1, p-S6K phosphorylates mSIN1 at two positions. mSIN1 is regulatory subunit of mTORC2 and it is essential for the integrity and substrate recruitment by mTORC2 (e.g. AKT) (Fig. 3). Therefore, mTORC1 through S6K regulates mSIN1-mTORC2 (Liu et al., 2013; Liu et al., 2014; Xie and Proud, 2013). Activated mTORC2 has a wide range of substrates rather than AKT (p-AKT473) and phosphorylates AGC kinases, serum and glucocorticoid-regulated kinase (SGK) and protein kinase C (PKC) (Garcia-Martinez and Alessi, 2008; Ikenoue et al., 2008; Sarbassov, 2005; Su and Jacinto, 2011). mTORC2 regulates cellular processes such as cell survival, cell cycle progression, anabolism and actin cytoskeleton organization (Jacinto et al., 2004). Second phosphorylation of AKT kinase at the hydrophobic motifs (S473) stimulates its full activity towards special substrates rather than TSC1/2, such as FOXO1 and 3. FOXO1/3 are two transcription factors that induce the expression from apoptotic genes (Fig. 3). Phosphorylation of FOXO1/3 by p-AKT (S473) sequester them in the cytoplasm. In this regards, it impairs nuclear translocation of FOXO1/3 and prevents their binding to the apoptotic gene promoters and induction of apoptosis. Therefore, mTORC2-AKT473-FOXO1/3 axis favorites the cell survival by inhibiting apoptosis (Wang et al., 2014). Co-immunoprecipitation analysis of the p110 isoforms with overexpressed ERAS and HRAS in Cos-7 cells indicted ERAS has highest affinity for p110α where HRAS binds mainly to p110δ isoform (Nakhaei-Rad et al., 2016). Cells which endogenously or exogenously express ERAS, have significantly higher levels of p-AKT308, p-mTORC, p-S6K, p-S6, p-mSIN1, p-AKT473 and p-FOXO1 (Nakhaei-Rad et al., 2016; Nakhaei-Rad et al., 2015). Collectively, ERAS through binding to PI3K and activation of this axis could regulate stem cell and cancer cell survival.

Concluding remarks

ERAS has been originally detected in undifferentiated embryonic stem cells and later in hepatic stellate cells as well as in several human tumors, including gastric, breast, brain, pancreatic, and colorectal tumors. Functional analysis of ERAS in tumors and stem cells, revealed its expression and signal transduction are important for tumor growth and cell survival responses. ERAS is a candidate gene for drug resistance in various human Establishes Cancer Cell Lines (ECCLs) as well as primary tumors derived from human tissues. To learn more about ERAS function in stemness and drug resistance in tumors, we need comprehensive

studies of ERAS binding partners in various cellular concepts. PI3K-AKT signaling pathway is one of the best-studied pathway controlled by ERAS, however, ERAS-specific effectors and upstream regulators remain unclear. Studying ERAS functions in the human stem cell pluripotency, and cancer cell growth will provide valuable insights into the control mechanisms of ERAS signaling during development, cancerogenesis and resistance to chemotherapies.

Acknowledgement
This study was supported by Ferdowsi University of Mashhad (grant numbers 49795) and Institute of Biotechnology (letter number, 4772474). I am grateful to Prof. Dr. Reza Ahmadian from the Institute of Biochemistry and Molecular Biology II of the Medical Faculty of the Heinrich-Heine University Düsseldorf for his helpful advices, and stimulating discussions.

References

Ahmadian M. R., Stege P., Scheffzek K. and Wittinghofer A. (1997) Confirmation of the arginine-finger hypothesis for the GAP-stimulated GTP-hydrolysis reaction of Ras. Nature Structural Biology 4:9, 686-689.

Alessi D. R., James S. R., Downes C. P., Holmes A. B., Gaffney P. R., Reese C. B. and et al. (1997) Characterization of a 3-phosphoinositide-dependent protein kinase which phosphorylates and activates protein kinase Balpha. Current Biology 7:261-269.

Andjelkovic M., Alessi D. R., Meier R., Fernandez A., Lamb N. J., Frech M. and et al. (1997) Role of translocation in the activation and function of protein kinase B. Journal of Biological Chemistry 272:50, 31515-31524.

Avruch J., Long X., Lin Y., Ortiz-Vega S., Rapley J., Papageorgiou A. and et al. (2009) Activation of mTORC1 in two steps: Rheb-GTP activation of catalytic function and increased binding of substrates to raptor1. Biochemical Society Transactions 37:1, 223-226.

Frias M. A., Thoreen C. C., Jaffe J. D., Schroder W., Sculley T., Carr S. A. and et al. (2006) mSin1 is necessary for Akt/PKB phosphorylation, and its isoforms define three distinct mTORC2s. Current Biology 16:18, 1865-1870.

Fritsch R., de Krijger I., Fritsch K., George R., Reason B., Kumar Madhu S. and et al. (2013) RAS and RHO Families of GTPases Directly Regulate Distinct Phosphoinositide 3-Kinase Isoforms. Cell 153:5, 1050-1063.

Fritsch R. and Downward J. (2013) SnapShot: Class I PI3K Isoform Signaling. Cell 154:4, 940-940.

Garcia-Martinez J. M. and Alessi D. R. (2008) mTOR complex 2 (mTORC2) controls hydrophobic motif phosphorylation and activation of serum- and glucocorticoid-induced protein kinase 1 (SGK1). Biochemistry Journal 416:3, 375-385.

Gentilella A., Kozma S. C. and Thomas G. (2015) A liaison between mTOR signaling, ribosome biogenesis and cancer. Biochimica et Biophysica Acta (BBA)-Gene Regulatory Mechanisms, 1849:7, 812-820.

Hara K., Maruki Y., Long X., Yoshino K., Oshiro N., Hidayat S., and et al. (2002) Raptor, a binding partner of target of rapamycin (TOR), mediates TOR action. Cell 110:2, 177-189.

Hara K., Yonezawa K., Kozlowski M. T., Sugimoto T., Andrabi K., Weng Q. P., and et al. (1997) Regulation of eIF-4E BP1 phosphorylation by mTOR. Journal of Biological Chemistry, 272:42, 26457-26463.

Hers I., Vincent E. E. and Tavaré J. M. (2011) Akt signalling in health and disease. Cellular signalling, 23:10, 1515-1527.

Huang J. and Manning B. D. (2008) The TSC1-TSC2 complex: a molecular switchboard controlling cell growth. Biochemical Journal, 412:2, 179-190.

Iadevaia V., Huo Y., Zhang Z., Foster L. J. and Proud C. G. (2012) Roles of the mammalian target of rapamycin, mTOR, in controlling ribosome biogenesis and protein synthesis. Biochemical Society Transactions, 40:1, 168-172.

Ikenoue T., Inoki K., Yang Q., Zhou X. and Guan K. L. (2008) Essential function of TORC2 in PKC and Akt turn motif phosphorylation, maturation and signalling. The EMBO journal, 27:14,1919-1931.

Inoki K., Li Y., Xu T. and Guan K. L. (2003) Rheb GTPase is a direct target of TSC2 GAP activity and regulates mTOR signaling. Genes & development, 17:15, 1829-1834.

Inoki K., Li Y., Zhu T., Wu J. and Guan K. L. (2002) TSC2 is phosphorylated and inhibited by Akt and suppresses mTOR signalling. Nature cell biology, 4:9, 648-657.

Jacinto E., Loewith R., Schmidt A., Lin S., Ruegg M. A., Hall A. and et al. (2004) Mammalian TOR complex 2 controls the actin cytoskeleton and is rapamycin insensitive. Nature cell biology, 6:11, 1122-1128.

Jean S. and Kiger A. A. (2014) Classes of phosphoinositide 3-kinases at a glance. Journal of cell science, 127:5, 923-928.

Kim J. E. and Chen J. (2004) regulation of peroxisome proliferator-activated receptor-gamma activity by mammalian target of rapamycin and amino acids in adipogenesis. Diabetes 53:11, 2748-2756.

Kok K., Geering B. and Vanhaesebroeck B. (2009) Regulation of phosphoinositide 3-kinase expression in health and disease. Trends in biochemical sciences, 34:3, 115-127.

Liu P., Gan W., Inuzuka H., Lazorchak A. S., Gao D., Arojo O., and et al. (2013) Sin1 phosphorylation impairs mTORC2 complex integrity and inhibits downstream Akt signalling to suppress tumorigenesis. Nature cell biology, 15:11, 1340-1350.

Liu P., Guo J., Gan W. and Wei W. (2014) Dual phosphorylation of Sin1 at T86 and T398 negatively regulates mTORC2 complex integrity and activity. Protein & cell, 5:3, 171-177.

Loewith R., Jacinto E., Wullschleger S., Lorberg A., Crespo J. L., Bonenfant D., and et al. (2002) Two TOR complexes, only one of which is rapamycin sensitive, have distinct roles in cell growth control. Molecular cell, 10:3, 457-468.

Ma X. M. and Blenis J. (2009) Molecular mechanisms of mTOR-mediated translational control. Nature reviews Molecular cell biology, 10:5, 307-318.

Ma X. M., Yoon S. O., Richardson C. J., Julich K. and Blenis J. (2008) SKAR links pre-mRNA splicing to mTOR/S6K1-mediated enhanced translation efficiency of spliced mRNAs. Cell 133:2, 303-313.

Nakhaei-Rad S., Haghighi F., Nouri P., Rezaei Adariani S., Lissy J., Kazemein Jasemi N. S., and et al. (2018) Structural fingerprints, interactions, and signaling networks of RAS family proteins beyond RAS isoforms. Critical reviews in biochemistry and molecular biology, 53:2, 130-156.

Nakhaei-Rad S., Nakhaeizadeh H., Götze S., Kordes C., Sawitza I., Hoffmann M. J., and et al. (2016) The Role of Embryonic Stem Cell-expressed RAS (ERAS) in the Maintenance of Quiescent Hepatic Stellate Cells. Journal of Biological Chemistry, 291:16, 8399-8413.

Nakhaei-Rad S., Nakhaeizadeh H., Kordes C., Cirstea I. C., Schmick M., Dvorsky R., and et al. (2015) The Function of Embryonic Stem Cell-expressed RAS (E-RAS), a Unique RAS Family Member, Correlates with Its Additional Motifs and Its Structural Properties. Journal of Biological Chemistry, 290:25, 15892-15903.

Nakhaeizadeh H., Amin E., Nakhaei-Rad S., Dvorsky R. and Ahmadian M. R. (2016) The RAS-Effector Interface: Isoform-Specific Differences in the Effector Binding Regions. PLoS One 11:12, e0167145.

Pearce L. R., Huang X., Boudeau J., Pawlowski R., Wullschleger S., Deak M., and et al. (2007) Identification of Protor as a novel Rictor-binding component of mTOR complex-2. Biochemical Journal, 405:3, 513-522.

Pearce L. R., Komander D. and Alessi D. R. (2010) The nuts and bolts of AGC protein kinases. Nature reviews Molecular cell biology, 11:1, 9-22.

Peterson T. R., Laplante M., Thoreen C. C., Sancak Y., Kang S. A., Kuehl W. M., and et al. (2009) DEPTOR is an mTOR inhibitor frequently overexpressed in multiple myeloma cells and required for their survival. Cell 137:5, 873-886.

Porstmann T., Santos C. R., Griffiths B., Cully M., Wu M., Leevers S., and et al. (2008) SREBP activity is regulated by mTORC1 and contributes to Akt-dependent cell growth. Cell metabolism, 8:3, 224-236.

Pylayeva-Gupta Y., Grabocka E. and Bar-Sagi D. (2011) RAS oncogenes: weaving a tumorigenic web. Nature Reviews Cancer, 11:11, 761-774.

Sancak Y., Peterson T. R., Shaul Y. D., Lindquist R. A., Thoreen C. C., Bar-Peled L. and et al. (2008) The Rag GTPases bind raptor and mediate amino acid signaling to mTORC1. Science 320:5882, 1496-1501.

Sancak Y., Thoreen C. C., Peterson T. R., Lindquist R. A., Kang S. A., Spooner E., and et al. (2007) PRAS40 is an insulin-regulated inhibitor of the mTORC1 protein kinase. Molecular cell, 25:6, 903-915.

Sarbassov D. D. (2005) Phosphorylation and Regulation of Akt/PKB by the Rictor-mTOR Complex. Science 307:5712, 1098-1101.

Sarbassov D. D., Ali S. M., Kim D. H., Guertin D. A., Latek R. R., Erdjument-Bromage H., and et al. (2004) Rictor, a novel binding partner of mTOR, defines a rapamycin-insensitive and raptor-independent pathway that regulates the cytoskeleton. Current biology, 14:14, 1296-1302.

Scheffzek K., Ahmadian M. R., Kabsch W., Wiesmuller L., Lautwein A., Schmitz F. and et al. (1997) The Ras-RasGAP complex: structural basis for GTPase activation and its loss in oncogenic Ras mutants. Science 277:5324, 333-338.

Su B. and Jacinto E. (2011) Mammalian TOR signaling to the AGC kinases. Critical reviews in biochemistry and molecular biology, 46:6, 527-547.

Takahashi K., Mitsui K. and Yamanaka S. (2003) Role of ERas in promoting tumour-like properties in mouse embryonic stem cells. Nature 423:6939, 541-545.

Tee A. R., Manning B. D., Roux P. P., Cantley L. C. and Blenis J. (2003) Tuberous sclerosis complex gene products, Tuberin and Hamartin, control mTOR signaling by acting as a GTPase-activating protein complex toward Rheb. Current biology, 13:15, 1259-1268.

Vadas O., Burke J. E., Zhang X., Berndt A. and Williams R. L. (2011) Structural basis for activation and inhibition of class I phosphoinositide 3-kinases. Science Signaling 4:195, re2.

Vanhaesebroeck B., Ali K., Bilancio A., Geering B. and Foukas L. C. (2005) Signalling by PI3K isoforms: insights from gene-targeted mice. Trends in biochemical sciences, 30:4, 194-204.

Vanhaesebroeck B., Leevers S. J., Ahmadi K., Timms J., Katso R., Driscoll P. C., and et al. (2001) Synthesis and function of 3-phosphorylated inositol lipids. Annual review of biochemistry, 70:1, 535-602.

Vanhaesebroeck B., Vogt P. K. and Rommel C. (2010) PI3K: from the bench to the clinic and back. Current Topics in Microbiology and Immunology 347:1-19.

Vanhaesebroeck B., Vogt P. (eds) Phosphoinositide 3-kinase in Health and Disease. Current Topics in Microbiology and Immunology, vol 347. Springer, Berlin, Heidelberg.

Wang X., Li W., Williams M., Terada N., Alessi D. R. and Proud C. G. (2001) Regulation of elongation factor 2 kinase by p90(RSK1) and p70 S6 kinase. The EMBO journal, 20:16, 4370-4379.

Xie J. and Proud C. G. (2013) Crosstalk between mTOR complexes. Nature cell biology, 15:11, 1263-1265.

Yang Q., Inoki K., Ikenoue T. and Guan K. L. (2006) Identification of Sin1 as an essential TORC2 component required for complex formation and kinase activity. Genes & development, 20:20, 2820-2832.

Yashiro M., Yasuda K., Nishii T., Kaizaki R., Sawada T., Ohira M. and et al. (2009) Epigenetic regulation of the embryonic oncogene ERas in gastric cancer cells. International journal of oncology, 35:5, 997-1003.

Yasuda K., Yashiro M., Sawada T., Ohira M. and Hirakawa K. (2007) ERas oncogene expression and epigenetic regulation by histone acetylation in human cancer cells. Anticancer Research 27:6b, 4071-4075.

Yu L., McPhee C. K., Zheng L., Mardones G. A., Rong Y., Peng J., and et al. (2010) Termination of autophagy and reformation of lysosomes regulated by mTOR. Nature 465: 7300, 942-946.

Zinzalla V., Stracka D., Oppliger W. and Hall Michael N. (2011) Activation of mTORC2 by Association with the Ribosome. Cell 144:5, 757-768.

Zoncu R., Efeyan A. and Sabatini D. M. (2010) mTOR: from growth signal integration to cancer,

diabetes and ageing. Nature reviews Molecular cell biology, 12:1, 21-35.

Journal of Cell and Molecular Research (2021) 12 (2), 74-86 DOI: 10.22067/jcmr.2021.69000.1004

Review / Mini-Review

Immunological Window of Myocardial Infarction

Azadeh Haghighitalab [1], Mahboubeh Kazemi-Noughabi [1], Shima Minaee [2], Ahmad Amin [3], Ahmad Reza Bahrami [1,4,*]

[1] *Department of Biology, Faculty of Science, Ferdowsi University of Mashhad, Mashhad, Iran*
[2] *Department of Cardiovascular Diseases, Razavi Hospital, Mashhad, Iran*
[3] *Rajaie Cardiovascular, Medical and Research Center, Iran University of Medical Sciences, Tehran, Iran*
[4] *Industrial Biotechnology Research Group, Institute of Biotechnology, Ferdowsi University of Mashhad, Mashhad, Iran*

Received 19 February 2021 Accepted 13 March 2021

Abstract

Acute myocardial infarction (MI) describes as an irreversible death of heart muscle which is initiated by a shortage of myocardium oxygen supply and accompanies by a complex of pro- and anti-inflammatory events. During the last decades, innate and adaptive immune responses are considered more serious for controlling myocardial infarction. As, it was confirmed that deregulated immune system which triggers excessive local and systemic inflammatory events is responsible for serious adverse effects associated with acute MI. Bone marrow activation, spleen monocytopoiesis, a remarkable increase of circulating cytokines and adhesion molecules, in addition to elevated levels of active peripheral leukocytes and platelets are playing significant roles in determining the clinical outcome of patients with MI. The previous experience demonstrated the failure of traditional harsh anti-inflammatory strategies. High mortality rate and poor quality of life observed for survivors of MI despite current progress in the field highlight the urgent need for such interdisciplinary studies in the context of molecular cardiology. Hence, unraveling the cellular and molecular events which are involved in the management of inflammatory responses post-MI is of special focus. The concept of immune regulation after myocardial infarction is not new, but our perception for dealing with the challenge has been changed during the last decades with gaining more in-depth molecular/immunological knowledge. It seems that fine-tuning the interplay between innate and adaptive immune responses and regulating their cross-talk should be in special focus to establish effective therapeutic strategies.

***Keywords*:** Cardiovascular diseases, Myocardial infarction, Innate and adaptive immune systems, Autoimmunity, Inflammation

Background

Cardiovascular diseases (CVDs) are the first cause of death in the world, count for more than 34% of the total number of death per year. In the United States of the America cardiovascular diseases take million lives in each year exclusively. According to the American Heart Association's Heart and Stroke Statistics 48% of all adults in this country develop some type of CVD (Benjamin et al., 2019). CVDs are also the leading cause of death in the European Union countries (Tadayon et al., 2019). Statistical analysis indicates that 43000 cases with CVD have been reported in Iran annually and cardiac complications take 300 lives daily. Prevalence, mortality and morbidity of CVD during recent decades in Iran were reported previously (Sarrafzadegan and Mohammmadifard, 2019). The official statistics of the Ministry of Health and Medical Education of Iran show that 33-38% of total deaths are somehow due to the cardiovascular complications. These pieces of information about CVDs worldwide have made it a universal challenge. The last revision of the World Health Organization CVD risk prediction charts from 21 global regions was published in 2019 (WHO CVD Risk Chart Working Group) and was applied for risk assessment in various populations (Babatunde et al., 2020; Islam et al., 2020; Samaniyan Bavarsad et al., 2020). Furthermore, a higher risk of coronary heart disease and stroke during the last year of worldwide Coronavirus disease (COVID-19) pandemic was reported recently (Gronewold and Hermann, 2021).

In parallel with advancements in therapeutic

*Corresponding author's E-mail address: *ar-bahrami@um.ac.ir*

strategies, various cardio-protective strategies were also introduced and applied in pre-clinical studies and clinical settings. However, translational medicine has no success as much as the pre-clinical studies does (Hoeeg et al., 2021; Zhao et al., 2020).

This could be due to the multifactorial nature of MI which is associated with functional modification of different cell types including tissue-specific and non-specific cells such as cardiomyocytes, smooth muscle cells, fibroblasts, endothelial cells, platelets and effector cells of both innate and adaptive immune systems. Therefore, a better strategy could be a combination of therapies with synergistic effects (Davidson et al., 2019). In such strategy, the role of immune system and its modifications during the pathogenesis of MI seem to be of crucial importance (Hausenloy et al., 2017).

Myocardial infarction: Definition, causes and routine treatments

Myocardial infarction (MI) (also called heart attack) is the direct result of coronary artery disease (CAD) and described as the irreversible death of heart muscle. It is mainly established by exposure of the tissue to prolonged lack of oxygen supply (Zafari et al., 2017). Molecular mechanisms responsible for development and progression of the cardiac remodeling were described in great details (Ayoub et al., 2017; Qiu and Liu, 2019; Schirone et al., 2017; Schüttler et al., 2019). Recently, some genes, lipidomic markers, and microRNAs were introduced as potent biomarkers for diagnosis of the acute MI (Condrat et al., 2020; Horváth et al., 2020; Li et al., 2019; Liu et al., 2019; Samouillan et al., 2020). Furthermore, the crucial role of exosomes in modulating the micro-communications among different cell types of cardiac tissue was discussed during cardiovascular diseases, myocardial infarction and their therapeutic strategies (Chen et al., 2021; Chistiakov et al., 2016; Ma et al., 2020; Pan et al., 2019; Sahoo and Losordo, 2014; Tan et al., 2020; Wu et al., 2019; Yuan et al., 2016).

There are some classifications for myocardial infarction, among which the most famous one was released in 2007 dividing the failures to 5 groups including MI types I to V (Thygesen et al., 2007). This classification was updated 4 times and the last one was published in 2018 (Thygesen et al., 2018; Thygesen et al., 2012; Saaby et al., 2013). Pharmaceutical regimes and revascularization strategies including the application of β-blockers and angiotensin-converting enzyme inhibitors (ACEIs), percutaneous transluminal coronary angioplasty (PTCA) and stenting, or surgical strategies such as the insertion of left ventricular assist devices (LVADs), coronary artery bypass graft (CABG) and cardiac transplantation are the most common therapeutic methods applied for patients with acute myocardial infarction and congestive heart failure (CHF)(Kuo and Tseng, 2009; Panahi et al., 2018). Although routine revascularization strategies make sense to help the remained viable cells of the myocardium, it may lead to ischemia/reperfusion (I/R) injury (Braunwald and Kloner, 1985; Yellon and Hausenloy, 2007). In addition to modifying the final infarct size and left ventricular ejection fraction (LVEF), this could be extensively responsible for the clinical outcome (Hausenloy and Yellon, 2013).

Various mechanisms are associated with the lethal reperfusion injury including release of reactive oxygen species (Raedschelders et al., 2012; Saparov et al., 2017), collapse of the mitochondrial membrane potential (Griffiths and Halestrap, 1995), restoration of physiological pH (Lemasters et al., 1996), and more recently modifications in lymphocyte kinetics (Boag et al., 2015; Bodí et al., 2009). The latter one will result in microvascular obstruction (MVO) in less than 2 hours following reperfusion in animal studies (Boag et al., 2017; Hausenloy and Yellon, 2013; Reffelmann and Kloner, 2002; Yellon and Hausenloy, 2007). Consequences of MVO, unlike lethal reperfusion injury, could be visualized and quantified by different methods such as echocardiography and magnetic resonance imaging in human subjects and is accompanied with adverse clinical outcomes (Bolognese et al., 2004; Hombach et al., 2005; Ito et al., 1996; de Waha et al., 2010; Wu, 2012; Wu et al., 1998). The temporal dynamics of immune responses following prolonged myocardial ischemia/reperfusion was fully investigated in a previous study (Rusinkevich et al., 2019).

Myocardial infarction: A tolerogenic failure

Heart tissues are believed to be protected against autoimmune-based events by specialized functions of tolerogenic dendritic cells, T regulatory cells, and T cells with the expression of inhibitory molecules such as programmed cell death-1 (PD-1). They are in cross-talk with heart cells' ligands. Different antigens have been proposed for self-tolerance failure and initiating cardiac autoimmunity. Full and in detailed description of these concepts were provided in another studies (Carrillo-Salinas et al., 2019; Salaman et al., 2020).

Atherosclerosis is defined as the inflammatory disease of the arterial wall (Matsuura et al., 2014). In animal and human subjects, atherosclerosis is

responsible for different cardiovascular complications including myocardial infarction in addition to autoimmune diseases established by the activity of autoantigens and autoantibodies, in lymphoid or non-lymphoid tissues (Frostegård, 2013; Meier and Binstadt, 2018; Sattler et al., 2017; Shi, 2010). Apolipoprotein B-100, which is the core protein in the structure of low-density lipoprotein is the target of these autoantibodies (*reviewed in* Ley, 2016). It was demonstrated that the cells from both innate and adaptive immune systems are present in the arterial walls and play key functions in the development of atherosclerosis (Dieterlen et al., 2016; Lee et al., 2020).

Patho-physiologically different cells of the immune system, including T cells, monocytes and dendritic cells are induced by different stimuli (Benagiano et al., 2005; McNiel et al., 1990), leading to secretion of pro-inflammatory cytokines in the atherosclerotic lesions (George et al., 2000). So, atherosclerosis shares many of its aspects with chronic autoimmune diseases accompanied by increased level of inflammatory cytokines, modified T helper 1 to T helper 2 cells ratio, and enhanced macrophage and lymphocyte activity (Shi, 2010). It was previously proposed that unbalanced T- and B-cell dependent adaptive immune responses are in close relationship with cardiomyocytes death and tissue fibrosis (Kino et al., 2020; Sánchez-Trujillo et al., 2017). Progressive form of atherosclerosis is observed in patients with rheumatoid arthritis (Sherer and Shoenfeld, 2006). Also, more than 50 times higher chance of inflammatory coronary events was reported for young female patients with systemic lupus erythematosus (SLE) in comparison to healthy individuals (Asanuma et al., 2003; Manzi et al., 1997).

Considering these facts, proper regimes of autoantigen mucosal immunization via recruiting antigen-specific T regulatory and adaptive immune cells are among effective strategies for inhibition of atherosclerosis progression, plaque inflammation and reactivity of lymph node lymphocytes against autoantigens (George, 2008). Important role of T regulatory cells in plaque instability during atherosclerosis and their stimulation by rapamycin, anti-CD3 antibodies, and indirect activation by dendritic cells were previously demonstrated (Yang et al., 2006; Ait-Oufella et al., 2006). According to pre-clinical studies tolerogenic dendritic cells have a favorable capacity for immune-based regulation of the hostile environment following the myocardial infarction. These cells, as a novel anti-remodeling therapy, following their migration to local lymph nodes, induce infarct-specific T regulatory cells and affect polarization of macrophage populations (Choo et al., 2017; Švajger and Rožman, 2018). Also, the induction of cardiomyocyte proliferation by regulatory T cells was reported following MI (Zacchigna et al., 2018).

Myocardial infarction: Interplay between innate and adaptive immune responses

Myocardial infarction is a complex of metabolic, inflammatory and immunological events (Hausenloy et al., 2009; Jung et al., 2019; Kuroki et al., 1993; Prabhu, 2018; Vinten-Johansen et al., 2004) which is accompanied by strong inflammation, cell death and fibrosis as helper mechanisms for tissue repair. These events are triggered by various mechanisms such as aldosterone- mineralocorticoid receptor (MR) signaling (Boag et al., 2017; Rafatian et al., 2014). However, continued activity of these events may lead to cardiac degeneration and heart failure (Burchfield et al., 2013; Frangogiannis et al., 2002; Frangogiannis, 2014). A rise in programmed cell death (PCD), mostly determined with caspase 3 activity, is observed in the first days following MI (Odörfer et al., 2008; Palojoke et al., 2001; Cheng et al., 1996). Moreover, during the first week strong accumulation of macrophages reported in both infarct and peri-infarct zones, which gradually decreases (Nahrendorf et al., 2013).

Pro-inflammatory and inflammatory resolution/reparative phases were proposed as key immune responses following the MI. These responses are mediated by the effector cells of both innate and adaptive immune cells (Fang et al., 2015; Lai et al., 2019). However, the role of effector cells of adaptive immune system (Lymphocytes) is less clear in comparison to monocytes and neutrophils (Horckman et al., 2018). Unlike previous trend, it is now evident that the presence and function of B and T lymphocytes play a critical role in the sequential events triggered following the myocardial infarction (Lee et al., 2020; Santos-Zas et al., 2019). These effects with either constructive or destructive consequences are time- and subset- dependent (Figure 1)(Boag et al., 2017, Hofmann and Frantz, 2015; Hofmann and Frantz, 2016).

In general, one may propose that lymphocyte activation and secretion of cytokines by these cells, following the myocardial infarction, recruits the active players of innate immune responses to the damaged cardiac tissue in the first 24 hours. Through the induction of inflammatory status this leads to a remarkable activity of macrophages with phagocytic behavior to remove cell remnants

and debris, which reaches its peak in 72 hours (Cheng et al., 2017; Frangogiannis et al., 2002; van den Akker et al., 2013).

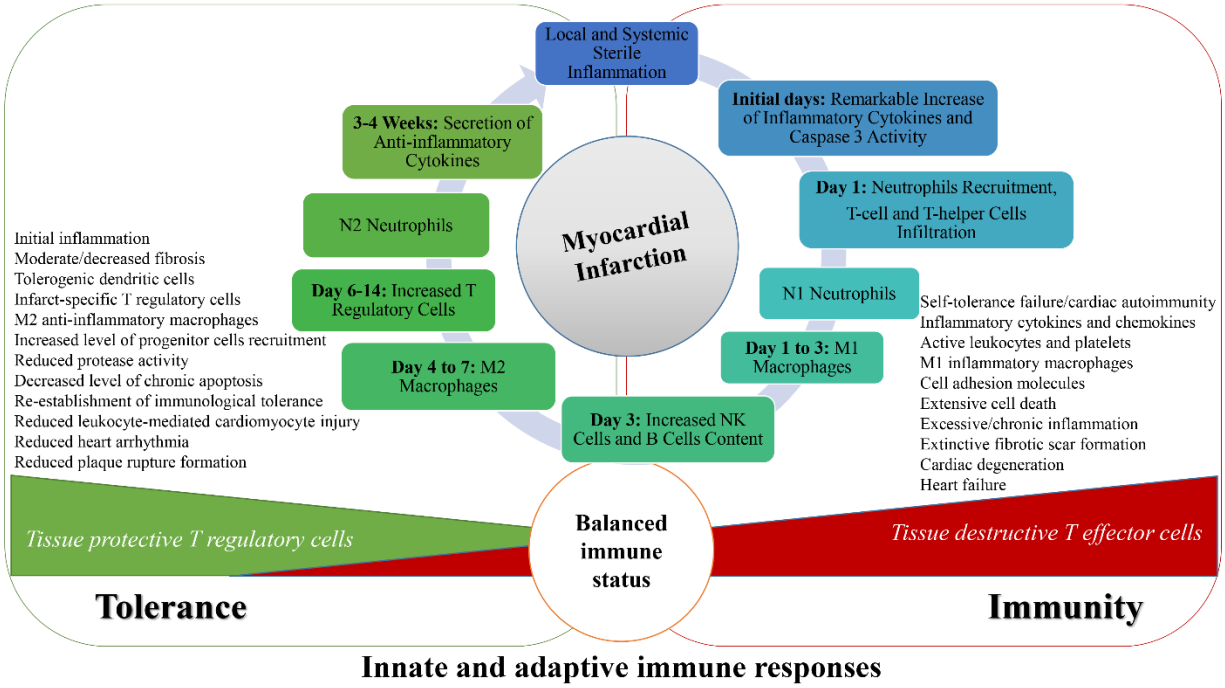

Figure 1. Time-dependent manner of immune cells recruitment to the cardiac tissue following myocardial infarction (MI). The homeostatic activity of innate and adaptive immune cells is crucial for management of local and systemic inflammations in the benefit of tissue regeneration and reparative mechanisms.

These post-MI events are mediated by mobilization of the bone marrow resident hematopoietic progenitor cells into the spleen leading to production of monocyte and neutrophil populations (Gentek and Hoeffel, 2017). Strong adhesive interactions between endothelial cells and leukocytes, induced by different cytokines, chemokines and components of complement system, are responsible for recruitment of inflammatory cells with cytotoxic activities to the infract zone (Nah and Rhee, 2009).

Yolk sac, fetal liver-derived, and monocyte-derived macrophages are main populations of macrophages playing crucial roles during pre- and post-MI events. They are involved in normal and disease situations for maintaining tissue homeostasis and accelerating the reparative process (Engelbertsen et al., 2013; Gomez et al., 2015; Hoeffel et al., 2012; Munshi, 2017; Pinto et al., 2016; Wynn, 2015). M1 macrophages, with cell remnant clearance and extracellular matrix degenerative -capacities, are the dominant population of macrophages in the first 3 days following the MI. Ly-6Clow monocyte-derived M2 macrophages, with wound healing properties, substitute this population during day 4 to 7 following the MI (Yan et al., 2013). M2 macrophages mediate these events through the secretion of anti-inflammatory cytokines, induction of angiogenesis, and collagen deposition (Cheng et al., 2017). Three main interventional methods including drug treatments, cell transplantations, and genetic modifications, were proposed to manage macrophage population switch (Xu et al., 2019).

Innate immune responses are triggered following the MI in order to switch on the tissue repair mechanisms (Aurora et al., 2014; Huang et al., 2013; Lai et al., 2017; Lavine et al., 2014). Similar to other inflammatory conditions, a minimal amount of pro-inflammatory cytokines is necessary for recruiting the main players of the immune system. A contradictory problem occurs when the level of inflammatory cytokines rises above the proper level. In this state, similar to other autoimmune conditions, instead of recruiting the progenitor cells to the damaged sites, the inflammatory mechanisms play as enemies and destroy the tissue structure (Frangogiannis et al., 2002; van den Akker et al., 2013). The roles of inflammatory agents in the pathogenesis of different cardiovascular diseases have been discussed previously (Caligiuri et al., 2000; Hansson, 2005; Hansson and Libby, 2006; Hansson and Hermansson, 2011; Huber et al., 2001; Liuzzo et al., 1999; Liuzzo et al., 2000; Robertson and Hansson, 2006; Song et al., 2001;

Zhou et al., 2000). It should be noticed that during myocardial infarction, unlike pathogen-induced inflammation, we are exposed with a sterile inflammatory status initiated by damage associated molecular patterns (DAMPs) or alarmins (Chen and Nuñez, 2010; Lee et al., 2018). It was proposed that inflammasomes recognize danger signals and mediate sterile inflammatory responses following acute myocardial infarction (AMI) (Fang et al., 2015).

The sequential role of different effector cells of the immune system depicted by van den Akker and colleagues, demonstrated that switching between pro- and anti- inflammatory status happens on day 5 to 7 post MI (van den Akker et al., 2013). B cells, T cells and natural killer (NK) cells are the main players of adaptive immune system with specialized functions (Boag et al., 2017; Boehm, 2011; Iwasaki and Medzhitov, 2015; Nutt et al., 2015; Owen et al., 2013; Pieper et al., 2013; Vivier et al., 2008). It was described by Horckmans and colleagues that the creation and functional properties of fat-associated lymphoid clusters (FALCs) can be modified upon the release of inflammatory cytokines following the MI (Horckmans et al., 2018). These secondary lymphoid organs which contain populations of B and T cells could be found with high frequencies in the pericardium (Bénézech et al., 2015). Based on recent findings they could be considered as the regulation sites for rapid immune responses following acute MI.

The role of T-cells in the pathogenesis of acute coronary syndrome was fully discussed previously (Yu et al., 2014). Furthermore, the importance of a subpopulation of cytotoxic T-cells (CD8+CD57+ cells) following myocardial infarction was confirmed which propose its prognostic features. Moreover, it was demonstrated that Foxp3+ CD4+ T cells are responsible for differentiation of monocytes and macrophages following MI (Weirather et al., 2014). Also, in a separate review paper, the detailed roles of lymphocytes and T regulatory cells during post MI events were fully described (Hofmann and Frantz, 2015), including the concept of tolerance and its important role in the pathogenesis and consequences of MI. Based on available information, the existence of T regulatory cells is necessary for proper healing of the damaged tissue following MI.

Recently, the relationship between epicardial adipose tissue (EAT) lymphocytes and coronary artery disease (CAD) was reported and confirmed that a higher amount of lymphocytes is present in the epicardial adipose tissue (EAT) of both CAD and non-CAD human subjects, in comparison to subcutaneous adipose tissue (SAT). However, the number of CD3 positive T cells indicates remarkable increase in epicardial adipose tissue of CAD subjects in comparison to non- CAD individuals. This is accompanied with decreased number of NK cells. Development of local inflammation and coronary atherosclerosis could be considered as main downstream events of such changes (Mráz et al., 2019).

It was indicated by Boag and colleagues that in human cases in less than one hour and half following the reperfusion, T cells and B cells are recruited to the myocardium with considerable decrease in peripheral levels of the cells. It was proposed that these cells may be accumulated in the epicardial adipose tissue, due to the shared microcirculation (Boag et al., 2015). In fact, epicardial adipose tissue could act as the central compartment to regulate post MI events via players of both adaptive and innate immune systems (Horckmans et al., 2018).

Although myocardial infarction has its own physiological reasons (Francis, 2001; Oerlemans et al., 2012; Roubille and Barrere-Lemaire, 2013) and routine therapeutic methods, the application of immunomodulatory agents such as standard immunosuppressive drugs and stem/progenitor cells will be also effective due to the critical role of T lymphocytes during MI (van den Akker et al., 2013). Cyclosporine, an immunosuppressive drug prescribed for patients with MI, triggers the function and viability of T-cells (Piot et al., 2008). It is noteworthy that replacement of the immunosuppressive drugs with cell based therapies or their cell-free counterparts would be a significant step to introduce novel clinical approaches (Guo et al., 2020; Lee and Kang, 2020).

The therapeutic modulation of inflammatory events following the MI, could lead to the reduced leukocyte-mediated cardiomyocyte injury in the border zone, decreased level of chronic apoptosis in the remodeling area, reduced protease activation, lower inflammation-driven fibrogenic signaling, increased level of progenitor cells recruitment, reduced heart arrhythmia, and reduced plaque rupture formation. These interventions are classified to broad and targeted anti- inflammatory strategies. They are encountered with some challenges including the overlap between the function of some effector molecules during different phases and heterogeneous post-infarction remodeling process in different patients (Huang and Frangogiannis, 2018). In addition, attempts to rejuvenate the aging immune system was recently proposed as another anti-inflammatory therapeutic strategy in the benefit of

effective heart regeneration following myocardial infarction (Tobin et al., 2020).

Myocardial infarction and cardiac regeneration as evolutionary and developmentally dependent traits

From developmental perspective, myocardial infarction is completely different in adult mammals in comparison to neonates as strong cardiac regenerative capacities have been reported during neonatal life. However, this ability is diminished upon the development of the immune system (Fan et al., 2020; Haubner et al., 2018; Santos et al., 2021). It was also demonstrated that the multi-potential ability of epicardial resident cells reduced after birth (Cai et al., 2019). The functional recovery of injured neonatal cardiac tissue is the result of preexisting cardiomyocyte proliferation and is mediated by various immunological, metabolic and environmental factors. As described by Lai and colleagues, in adult cardiac tissue monocyte derived macrophages are found following MI, which promote fibrosis. These data highlighted the importance of immune-modulating therapeutic strategies for treating patient with MI (Lai et al., 2019; Lam and Sadek, 2018).

Conclusion

In conclusion, to introduce better therapeutic strategies which reduce the progressive events following the MI in the benefit of tissue regeneration, multi-target methods are proposed. Among these strategies, the ones which restore immune tolerance to cardiac tissue could be more effective. These strategies will reduce complications for patients with cardiovascular disease.

Acknowledgement

This study was supported by the National Institute for Medical Research Development (NIMAD, Grant number 957797) of Iran and Ferdowsi University of Mashhad (Grant numbers 41827 and 50793).

Conflict of Interest

The authors have no conflicts of interest.

References

Ait-Aissa K., Blaszak S. C., Beutner G., Tsaih S. W., Morgan G., Santos J. H., et al. (2019) Mitochondrial oxidative phosphorylation defect in the heart of subjects with coronary artery disease. Scientific Reports 9(1): 7623.

Ait-Oufella H., Salomon B. L., Potteaux S., Robertson A. K., Gourdy P., Zoll J., et al. (2006) Natural regulatory T cells control the development of atherosclerosis in mice. Nature Medicine 12(2): 178-80.

Amit U., Kain D., Wagner A., Sahu A., Nevo-Caspi Y., Gonen N., et al. (2017) New role for interleukin- 13 receptor α1 in myocardial homeostasis and heart failure. Journal of the American Heart Association 6(5): e005108.

van den Akker F., Deddens J. C., Doevendans P. A. and Sluijter J. P. (2013) Cardiac stem cell therapy to modulate inflammation upon myocardial infarction. Biochimica et Biophysica Acta 1830(2): 2449-2458.

Angajala A., Lim S., Phillips J. B., Kim J. H., Yates C., You Z., et al. (2018) diverse roles of mitochondria in immune responses: novel insights into immuno-metabolism. Frontiers in Immunology 9: 1605.

Asanuma Y., Oeser A., Shintani A. K., Turner E., Olsen N., Fazio S., et al. (2003) Premature coronary-artery atherosclerosis in systemic lupus erythematosus. The New England Journal of Medicine 349(25): 2407-2415.

Aurora A. B., Porrello E. R., Tan W., Mahmoud A. I., Hill J. A., Bassel-Duby R., et al. (2014) Macrophages are required for neonatal heart regeneration. Journal of Clinical Investigation 124(3): 1382-1392.

Ayoub K. F., Pothineni N. V. K., Rutland J., Ding Z. and Mehta J. L. (2017) Immunity, inflammation, and oxidative stress in heart failure: emerging molecular targets. Cardiovascular Drugs and Therapy 31(5-6): 593-608.

Babatunde O. A., Olarewaju S. O., Adeomi A. A., Akande J. O., Bashorun A., Umeokonkwo C. D., et al. (2020) 10-year risk for cardiovascular diseases using WHO prediction chart: findings from the civil servants in south-western Nigeria. BMC cardiovascular disorders 20(1): 154.

Ballinger S. W., Patterson C., Knight-Lozano C. A., Burow D. L., Conklin C. A., Hu Z., et al. (2002) Mitochondrial integrity and function in atherogenesis. Circulation 106(5): 544-549.

Benagiano M., D'Elios M. M., Amedei A., Azzurri A., van der Zee R., Ciervo A., et al. (2005) Human 60-kDa heat shock protein is a target

autoantigen of T cells derived from atherosclerotic plaques. Journal of Immunology 174(10): 6509-6517.

Benjamin E. J., Muntner P., Alonso A., Bittencourt M. S., Callaway C. W., Carson A. P., et al. (2019) American heart association council on epidemiology and prevention statistics committee and stroke statistics subcommittee. Heart disease and stroke statistics-2019 update: a report from the American heart association. Circulation 139(10): e56-e528.

Bénézech C., Luu N. T., Walker J. A., Kruglov A. A., Loo Y., Nakamura K., et al. (2015) Inflammation-induced formation of fat-associated lymphoid clusters. Nature Immunology 16(8): 819-828.

Boag S. E., Andreano E. and Spyridopoulos I. (2017) Lymphocyte communication in myocardial ischemia/reperfusion injury. Antioxidants & Redox Signaling 26(12): 660-675.

Boag S. E., Das R., Shmeleva E. V., Bagnall A., Egred M., Howard N., et al. (2015) T lymphocytes and fractalkine contribute to myocardial ischemia/reperfusion injury in patients. Journal of Clinical Investigation 125(8): 3063-3076.

Boehm T. (2011) Design principles of adaptive immune systems. Nature Reviews Immunology 11(5): 307-317.

Bodí V., Sanchis J., Núñez J., Rumiza E., Mainar L., López-Lereu M. P., et al. (2009) Post-reperfusion lymphopenia and microvascular obstruction in ST-segment elevation acute myocardial infarction. Revista Española de Cardiología 62(10): 1109-1117.

Bolognese L., Carrabba N., Parodi G., Santoro G. M., Buonamici P., Cerisano G., et al. (2004) Impact of microvascular dysfunction on left ventricular remodeling and long-term clinical outcome after primary coronary angioplasty for acute myocardial infarction. Circulation 109(9): 1121-1126.

Bostan M. M., Stătescu C., Anghel L., Șerban I. L., Cojocaru E. and Sascău, R. (2020) Post-myocardial infarction ventricular remodeling biomarkers-the key link between pathophysiology and clinic. Biomolecules 10(11): 1587.

Braunwald E. and Kloner R. A. (1985) Myocardial reperfusion: a double-edged sword? Journal of Clinical Investigation 76(5): 1713-1719.

Breda C. N. S., Davanzo G. G., Basso P. J., Saraiva Câmara. N. O. and Moraes-Vieira P. M. M. (2019) Mitochondria as central hub of the immune system. Redox Biology 26:101255.

Burchfield J. S., Xie M. and Hill J. A. (2013) Pathological ventricular remodeling: mechanisms: part 1 of 2. Circulation 128(4): 388-400.

Cai W., Tan J., Yan J., Zhang L., Cai X., Wang H., et al. (2019) Limited regeneration potential with minimal epicardial progenitor conversions in the neonatal mouse heart after injury. Cell Reports 28(1):190–201.

Carrillo-Salinas F. J., Ngwenyama N., Anastasiou M., Kaur K. and Alcaide P. (2019) Heart inflammation: immune cell roles and roads to the heart. The American Journal of Pathology 189(8):1482-1494.

Chen P., Wang L., Fan X., Ning X., Yu B., Ou C., et al. (2021) Targeted delivery of extracellular vesicles in heart injury. Theranostics 11(5): 2263–2277.

Chen G. Y. and Nuñez G. (2010) Sterile inflammation: sensing and reacting to damage. Nature Reviews Immunology 10(12): 826-837.

Cheng B., Chen H. C., Chou I. W., Tang T. W. and Hsieh P. C. (2017) Harnessing the early post-injury inflammatory responses for cardiac regeneration. Journal of Biomedical Science 24(1): 7.

Cheng W., Kajstura J., Nitahara J. A., Li B., Reiss K., Liu Y., et al. (1996) Programmed myocyte cell death affects the viable myocardium after infarction in rats. Experimental Cell Research 226(2): 316-327.

Chistiakov D. A., Orekhov A. N. and Bobryshev Y. V. (2016) Cardiac extracellular vesicles in normal and infarcted heart. International Journal of Molecular Sciences 17(1): pii: E63.

Choo E. H., Lee J. H., Park E. H., Park H. E., Jung N. C., et al. (2017) Infarcted myocardium-primed dendritic cells improve remodeling and cardiac function after myocardial infarction by modulating the regulatory T cell and macrophage polarization. Circulation 135(15): 1444-1457.

Condrat C. E., Thompson D. C., Barbu M. G., Bugnar O. L., Boboc A., Cretoiu D., et al. (2020) miRNAs as biomarkers in disease: latest findings regarding their role in diagnosis and prognosis. Cells 9(2): 276.

Corral-Debrinski M., Shoffner J. M., Lott M. T. and

Wallace D. C. (1992) Association of mitochondrial DNA damage with aging and coronary atherosclerotic heart disease. Mutation Research 275(3-6): 169-180.

Corral-Debrinski M., Stepien G., Shoffner J. M., Lott M. T., Kanter K. and Wallace D. C. (1991) Hypoxemia is associated with mitochondrial DNA damage and gene induction. Implications for cardiac disease. JAMA 266(13): 1812-1816.

Davidson S. M., Ferdinandy P., Andreadou I., Bøtker H. E., Heusch G., Ibáñez B., et al. Cardioprotection cost action (CA16225). (2019) Multitarget strategies to reduce myocardial ischemia/reperfusion injury: JACC review topic of the week. Journal of the American College of Cardiology 73(1): 89-99.

Dieterlen M. T., John K., Reichenspurner H., Mohr F. W. and Barten M. J. (2016) Dendritic cells and their role in cardiovascular diseases: a view on human studies. Journal of Immunology Research 2016: 5946807.

Engelbertsen D., Andersson L., Ljungcrantz I., Wigren M., Hedblad B., Nilsson J., et al. (2013) T-helper 2 immunity is associated with reduced risk of myocardial infarction and stroke. Arteriosclerosis, Thrombosis, and Vascular Biology 33(3): 637-644.

Fan Y., Cheng Y., Li Y., Chen B., Wang Z., Wei T., et al. (2020) Phosphoproteomic analysis of neonatal regenerative myocardium revealed important roles of checkpoint Kinase 1 via activating mammalian target of rapamycin C1/ribosomal protein S6 Kinase b-1 pathway. Circulation 141(19): 1554–1569.

Fang L., Moore X. L., Dart A. M. and Wang L. M. (2015) Systemic inflammatory response following acute myocardial infarction. Journal of Geriatric Cardiology 12(3): 305–312.

Frangogiannis N. G. (2014) The inflammatory response in myocardial injury, repair, and remodelling. Nature Reviews Cardiology 11(5): 255-265.

Frangogiannis N. G., Smith C. W. and Entman M. L. (2002) The inflammatory response in myocardial infarction. Cardiovascular Research 53(1): 31-47.

Frostegård J. (2013) Immunity, atherosclerosis and cardiovascular disease. BMC Medicine 11:117.

Gentek R. and Hoeffel G. (2017) The innate immune response in myocardial infarction, repair, and regeneration. Advances in Experimental Medicine and Biology 1003: 251-272.

George J. (2008) Mechanisms of disease: the evolving role of regulatory T cells in atherosclerosis. Nature Clinical Practice Cardiovascular Medicine 5(9): 531-540.

George J., Harats D., Gilburd B., Afek A., Shaish A., Kopolovic J., et al. (2000) Adoptive transfer of beta (2)-glycoprotein I-reactive lymphocytes enhances early atherosclerosis in LDL receptor-deficient mice. Circulation 102(15):1822-7.

Gomez Perdiguero E., Klapproth K., Schulz C., Busch K., Azzoni E., Crozet L., et al. (2015) Tissue-resident macrophages originate from yolk-sac-derived erythro-myeloid progenitors. Nature 518(7540): 547-551.

Griffiths E. J. and Halestrap A. P. (1995) Mitochondrial non-specific pores remain closed during cardiac ischemia, but open upon reperfusion. Biochemical Journal 307: 93-98.

Gronewold J. and Hermann D. M. (2021) Social isolation and risk of fatal cardiovascular events. Lancet Public Health S2468-2667(21)00008-6.

Guo Y., Yu Y., Hu S., Chen Y. and Shen Z. (2020) The therapeutic potential of mesenchymal stem cells for cardiovascular diseases. Cell Death and Disease 11(5): 349.

Guzzardi M. A. and Iozzo P. (2011) Fatty heart, cardiac damage, and inflammation. Review of Diabetic Studies 8(3): 403-417.

Haubner B. J., Schuetz T. and Penninger J. M. (2018) Cardiac regeneration in a newborn: what does this mean for future cardiac repair research? Expert Review of Cardiovascular Therapy 16(3): 155-157.

Hausenloy D. J., Garcia-Dorado D., Bøtker H. E., Davidson S. M., Downey J., Engel F. B., et al. (2017) Novel targets and future strategies for acute cardioprotection: position paper of the European society of cardiology working group on cellular biology of the heart. Cardiovascular research 113(6): 564–585.

Hausenloy D. J. and Yellon D. M. (2013) Myocardial ischemia-reperfusion injury: a neglected therapeutic target. Journal of Clinical

Investigation 123(1): 92-100.

Hausenloy D. J., Ong S. B. and Yellon D. M. (2009) The mitochondrial permeability transition pore as a target for preconditioning and post conditioning. Basic Research in Cardiology 104(2): 189-202.

Henrichot E., Juge-Aubry C. E., Pernin A., Pache J. C., Velebit V., Dayer J. M., et al. (2005) Production of chemokines by perivascular adipose tissue: a role in the pathogenesis of atherosclerosis? Arteriosclerosis, Thrombosis, and Vascular Biology 25(12): 2594-2599.

Hoeffel G., Wang Y., Greter M., See P., Teo P., Malleret B., et al. (2012) Adult Langerhans cells derive predominantly from embryonic fetal liver monocytes with a minor contribution of yolk sac-derived macrophages. Journal of Experimental Medicine 209(6): 1167-1181.

Hoeeg C., Dolatshahi-Pirouz A. and Follin B. (2021) Injectable hydrogels for improving cardiac cell therapy-in vivo evidence and translational challenges. Gels 7(1): 7.

Hofmann U. and Frantz S. (2016) Role of T-cells in myocardial infarction. European Heart Journal 37(11): 873-879.

Hofmann U. and Frantz S. (2015) Role of lymphocytes in myocardial injury, healing, and remodeling after myocardial infarction. Circulation Research 116(2): 354-367.

Hombach V., Grebe O., Merkle N., Waldenmaier S., Höher M., Kochs M., et al. (2005) Sequelae of acute myocardial infarction regarding cardiac structure and function and their prognostic significance as assessed by magnetic resonance imaging. European Heart Journal 26(6): 549-557.

Horckmans M., Bianchini M., Santovito D., Megens R. T. A., Springael J. Y., Negri I., et al. (2018) Pericardial adipose tissue regulates granulopoiesis, fibrosis, and cardiac function after myocardial infarction. Circulation 137(9): 948-960.

Horváth M., Horváthová V., Hájek P., Štěchovský C., Honěk J., Šenolt L., et al. (2020) MicroRNA-331 and microRNA-151- 3p as biomarkers in patients with ST-segment elevation myocardial infarction. Scientific Reports 10: 5845.

Huang S. and Frangogiannis N. G. (2018) Anti-inflammatory therapies in myocardial infarction: failures, hopes and challenges. British Journal of Pharmacology 175(9): 1377–1400.

Huang W. C., Yang C. C., Chen I. H., Liu Y. M., Chang S. J. and Chuang Y. J. (2013) Treatment of glucocorticoids inhibited early immune responses and impaired cardiac repair in adult zebrafish. PLoS One 8(6):e66613.

Islam J. Y., Zaman M. M., Moniruzzaman M., Ara Shakoor S. and Hossain A. (2020) Estimation of total cardiovascular risk using the 2019 WHO CVD prediction charts and comparison of population-level costs based on alternative drug therapy guidelines: a population-based study of adults in Bangladesh. BMJ open 10(7): e035842.

Ito H., Maruyama A., Iwakura K., Takiuchi S., Masuyama T., Hori M., et al. (1996) Clinical implications of the 'no reflow' phenomenon. A predictor of complications and left ventricular remodeling in reperfused anterior wall myocardial infarction. Circulation 93(2): 223-228.

Iwasaki A. and Medzhitov R. (2015) Control of adaptive immunity by the innate immune system. Nature Immunology 16(4): 343-353.

Jung M., Dodsworth M. and Thum T. (2018) Inflammatory cells and their non-coding RNAs as targets for treating myocardial infarction. Basic Research in Cardiology 114(1):4.

Kino T., Khan M. and Mohsin S. (2020) The regulatory role of T cell responses in cardiac remodeling following myocardial infarction. International Journal of Molecular Sciences 21(14): 5013.

Knight-Lozano C. A., Young C. G., Burow D. L., Hu Z. Y., Uyeminami D., Pinkerton K. E., et al. (2002) Cigarette smoke exposure and hypercholesterolemia increase mitochondrial damage in cardiovascular tissues. Circulation 105(7): 849-854.

Kubin T., Pöling J., Kostin S., Gajawada P., Hein S., Rees W., et al. (2011) Oncostatin M is a major mediator of cardiomyocyte dedifferentiation and remodeling. Cell Stem Cell 9(5): 420–432.

Kuroki S., Miyahara K. and Uematsu T. (1993) Immunological aspects in patients with acute myocardial infarction. Japanese Circulation Journal 57(1): 37-46.

Lai S. L., Marín-Juez R. and Stainier D. Y. R. (2019) Immune responses in cardiac repair and

regeneration: a comparative point of view. Cellular and Molecular Life Sciences 76(7): 1365-1380.

Lai S. L., Marín-Juez R., Moura P. L., Kuenne C., Lai J. K. H., Tsedeke A. T., et al. (2017) Reciprocal analyses in zebrafish and medaka reveal that harnessing the immune response promotes cardiac regeneration. Elife 6: e25605.

Lam N. T. and Sadek H. A. (2018) Neonatal heart regeneration: comprehensive literature review. Circulation 138(4): 412–423.

Lavine K. J., Epelman S., Uchida K., Weber K. J., Nichols C. G., Schilling J. D., et al. (2014) Distinct macrophage lineages contribute to disparate patterns of cardiac recovery and remodeling in the neonatal and adult heart. Proceedings of the National Academy of Sciences of the United States of America 111(45): 16029-16034.

Lee S., Bartlett B. and Dwivedi G. (2020) Adaptive immune responses in human atherosclerosis. International Journal of Molecular Sciences 21(23): 932.

Lee B. C. and Kang K. S. (2020) Functional enhancement strategies for immunomodulation of mesenchymal stem cells and their therapeutic application. Stem Cell Research and Therapy 11(1): 397.

Lee J. S., Jeong S. J., Kim S., Chalifour L., Yun T. J., Miah M. A., et al. (2018) Conventional dendritic cells impair recovery after myocardial infarction. Journal of Immunology 201(6):1784-1798.

Lemasters J. J., Bond J. M., Chacon E., Harper I. S., Kaplan S. H., Ohata H., et al. (1996) The pH paradox in ischemia-reperfusion injury to cardiac myocytes. Experientia Supplementum 76: 99-114.

Ley K. (2016) 2015 Russell Ross memorial lecture in vascular biology: protective autoimmunity in atherosclerosis. Arteriosclerosis, Thrombosis, and Vascular Biology 36(3): 429-438.

Li Y., He X. N., Li C., Gong L. and Liu M. (2019) Identification of candidate genes and microRNAs for acute myocardial infarction by weighted gene coexpression network analysis. BioMed Research International 2019: 5742608.

Liu Z., Ma C., Gu J. and Yu M. (2019) Potential biomarkers of acute myocardial infarction based on weighted gene co-expression network analysis. BioMedical Engineering OnLine 18(1): 9.

Ma Z. J., Yang J. J., Lu Y. B., Liu Z. Y. and Wang X. X. (2020) Mesenchymal stem cell-derived exosomes: Toward cell-free therapeutic strategies in regenerative medicine. World Journal of Stem Cells 12(8): 814–840.

Manzi S., Meilahn E. N., Rairie J. E., Conte C. G., Medsger T. A. Jr., Jansen- McWilliams L., et al. (1997) Age-specific incidence rates of myocardial infarction and angina in women with systemic lupus erythematosus: comparison with the Framingham Study. American Journal of Epidemiology 145(5): 408-415.

Matsuura E., Atzeni F., Sarzi-Puttini P., Turiel M., Lopez L. R. and Nurmohamed M. T. (2014) Is atherosclerosis an autoimmune disease? BMC Medicine 12:47.

McNeil H. P., Simpson R. J., Chesterman C. N. and Krilis S. A. (1990) Anti-phospholipid antibodies are directed against a complex antigen that includes a lipid-binding inhibitor of coagulation: beta 2-glycoprotein I (apolipoprotein H). Proceedings of the National Academy of Sciences of the United States of America 87(11): 4120-4124.

Mráz M., Cinkajzlová A., Kloučková J., Lacinová Z., Kratochvílová H., Lipš M., et al. (2019) Coronary artery disease is associated with an increased amount of T lymphocytes in human epicardial adipose tissue. Mediators of Inflammation 2019: 4075086.

Meier L. A. and Binstadt B. A. (2018) The contribution of autoantibodies to inflammatory cardiovascular pathology. Frontiers of Immunology 9: 911.

Munshi N. V. (2017) Resident macrophages: near and dear to your heart. Cell 169(3): 376-377.

Murdolo G. and Smith U. (2006) The dysregulated adipose tissue: a connecting link between insulin resistance, type 2 diabetes mellitus and atherosclerosis.Nutrition, Metabolism & Cardiovascular Diseases 1: S35- S38.

Nah D. Y. and Rhee M. Y. (2009) The inflammatory response and cardiac repair after myocardial infarction. Korean Circulation Journal 39(10): 393-398.

Nahrendorf M. and Swirski F. K. (2013) Monocyte and macrophage heterogeneity in the heart.

Circulation Research 112(12): 1624-1633.

Neels J. G. and Olefsky J. M. (2006) Inflamed fat: what starts the fire? Journal of Clinical Investigation 116(1): 33-35.

Nutt S. L., Hodgkin P. D., Tarlinton D. M. and Corcoran L. M. (2015) The generation of antibody-secreting plasma cells. Nature Reviews Immunology 15(3): 160-171.

Odörfer K. I., Walter I., Kleiter M., Sandgren E. P. and Erben R. G. (2008) Role of endogenous bone marrow cells in long-term repair mechanisms after myocardial infarction. Journal of Cellular and Molecular Medicine 12(6B): 2867-2874.

Ohman M. K., Wright A. P., Wickenheiser K. J., Luo W. and Eitzman D. T. (2009) Visceral adipose tissue and atherosclerosis. Current Vascular Pharmacology 7(2): 169-179.

Owen J., Punt J. and Stranford S. (2013) Kuby Immunology: International Edition. New York: W. H. Freeman.

Palojoki E., Saraste A., Eriksson A., Pulkki K., Kallajoki M., Voipio-Pulkki L. M., et al. (2001) Cardiomyocyte apoptosis and ventricular remodeling after myocardial infarction in rats. American Journal of Physiology-Heart and Circulatory Physiology 280(6): H2726-H2731.

Pan W., Zhu Y., Meng X., Zhang C., Yang Y. and Bei Y. (2019) Immunomodulation by exosomes in myocardial infarction. Journal of Cardiovascular Translational Research 12 (1): 28-36.

Panahi M., Vadgama N., Kuganesan M., Ng F. S. and Sattler S. (2018) Immunopharmacology of post-myocardial infarction and heart failure medications. Journal of Clinical Medicine 7(11): 403.

Pieper K., Grimbacher B. and Eibel H. (2013) B-cell biology and development. The Journal of Allergy and Clinical Immunology 131(4): 959-971.

Pinto A. R., Ilinykh A., Ivey M. J., Kuwabara J. T., D'Antoni M. L., Debuque R., et al. (2016) Revisiting cardiac cellular composition. Circulation Research 118(3): 400-409.

Prabhu S. D. (2018) The cardiosplenic axis is essential for the pathogenesis of ischemic heart failure. Transactions of the American Clinical and Climatological Association 129: 202-214.

Qiu L. and Liu X. (2019) Identification of key genes involved in myocardial infarction. European Journal of Medical Research 24(1): 22.

Raedschelders K., Ansley D. M. and Chen D. D. (2012) The cellular and molecular origin of reactive oxygen species generation during myocardial ischemia and reperfusion. Pharmacology & Therapeutics 133(2): 230-255.

Rafatian N., Westcott K. V., White R. A. and Leenen F. H. (2014) Cardiac macrophages and apoptosis after myocardial infarction: effects of central MR blockade. The American Journal of Physiology - Regulatory, Integrative and Comparative Physiology 307(7): R879- R887.

Reffelmann T. and Kloner R. A. (2002) Microvascular reperfusion injury: rapid expansion of anatomic no reflow during reperfusion in the rabbit. The American Journal of Physiology-Heart and Circulatory Physiology 283(3): H1099-H1107.

Rusinkevich V., Huang Y., Chen Z. Y., Qiang W., Wang Y. G., Shi Y. F., et al. (2019) Temporal dynamics of immune response following prolonged myocardial ischemia/reperfusion with and without cyclosporine A. Acta Pharmacologica Sinica 40(9): 1168–1183.

Sahoo S. and Losordo D. W. (2014) Exosomes and cardiac repair after myocardial infarction. Circulation Research 114(2): 333-344.

Salaman M. R. and Gould K. G. (2020) Breakdown of T-cell ignorance: the tolerance failure responsible for mainstream autoimmune diseases?. Journal of Translational Autoimmunity 3: 100070.

Samaniyan Bavarsad P., Kheiri S. and Ahmadi A. (2020) Estimation of the 10-year risk of cardiovascular diseases: using the SCORE, WHO/ISH, and Framingham models in the Shahrekord cohort study in southwestern Iran. Journal of Tehran University Heart Center 15(3): 105–112.

Samouillan V., Martinez de Lejarza Samper I. M., Amaro A. B., Vilades D., Dandurand J., Casas J., et al. (2020) Biophysical and lipidomic biomarkers of cardiac remodeling post- myocardial infarction in humans. Biomolecules 10(11): 1471.

Sánchez-Trujillo L., Vázquez-Garza E., Castillo E. C., García-Rivas G. and Torre-Amione G. (2017) Role of adaptive immunity in the development and

progression of heart failure: new evidence. Archives of Medical Research 48(1):1-11.

Santos F., Correia M., Nóbrega-Pereira S. and Bernardes de Jesus B. (2021) Age-related pathways in cardiac regeneration: a role for lncRNAs?. Frontiers in Physiology 11: 583191.

Santos-Zas I., Lemarié J., Tedgui A. and Ait-Oufella H. (2019) Adaptive immune responses contribute to post-ischemic cardiac remodeling. Frontiers in Cardiovascular Medicine 5:198.

Saparov A., Ogay V., Nurgozhin T., Chen W. C. W., Mansurov N., Issabekova A., et al. (2017) Role of the immune system in cardiac tissue damage and repair following myocardial infarction. Inflammation Research 66(9): 739-751.

Sarrafzadegan N. and Mohammmadifard N. (2019) Cardiovascular disease in Iran in the last 40 years: prevalence, mortality, morbidity, challenges and strategies for cardiovascular prevention. Archives of Iranian Medicine 22(4): 204-210.

Sattler S., Fairchild P. Watt F. M., Rosenthal N. and Harding S. E. (2017) The adaptive immune response to cardiac injury-the true roadblock to effective regenerative therapies? NPJ Regenerative Medicine 2:19.

Schirone L., Forte M., Palmerio S., Yee D., Nocella C., Angelini F., et al. (2017) A review of the molecular mechanisms underlying the development and progression of cardiac remodeling. Oxidative Medicine and Cellular Longevity 2017:3920195.

Schüttler D., Clauss S., Weckbach L. T. and Brunner S. (2019) Molecular mechanisms of cardiac remodeling and regeneration in physical exercise. Cells 8(10): 1128.

Sherer Y. and Shoenfeld Y. (2006) Mechanisms of disease: atherosclerosis in autoimmune diseases. Nature Clinical Practice Rheumatology 2(2): 99-106.

Shi G. P. (2010) Immunomodulation of vascular diseases: atherosclerosis and autoimmunity. European Journal of Vascular and Endovascular Surgery 39(4): 485-494.

Švajger U. and Rožman P. (2018) Induction of tolerogenic dendritic cells by endogenous biomolecules: an update. Frontiers in Immunology 9: 2482.

Tadayon S., Wickramasinghe K. and Townsend N. (2019) Examining trends in cardiovascular disease mortality across Europe: how does the introduction of a new European standard population affect the description of the relative burden of cardiovascular disease? Population Health Metrics 17(1):6.

Tan S., Floriano J. F., Nicastro L., Emanueli C. and Catapano F. (2020) Novel applications of mesenchymal stem cell-derived exosomes for myocardial infarction therapeutics. Biomolecules 10(5): 707.

Thygesen K., Alpert J. S., Jaffe A. S., Chaitman B. R., Bax J. J., Morrow D. A., et al. (2018) Fourth universal definition of myocardial infarction. Journal of the American College of Cardiology 72(18): 2231–2264.

Tobin S. W., Alibhai F. J., Weisel R. D. and Li R. K. (2020) Considering cause and effect of immune cell aging on cardiac repair after myocardial infarction. Cells 9(8): 1894.

Veloso C. D., Belew G. D., Ferreira L. L., Grilo L. F. F., Jones J. G., Portincasa P., et al. (2019) A mitochondrial approach to cardiovascular risk and disease. Current Pharmaceutical Design 25(9): 3175-3194.

Vinten-Johansen J. (2004) Involvement of neutrophils in the pathogenesis of lethal myocardial reperfusion injury. Cardiovascular Research 61(3): 481-497.

Vivier E., Tomasello E., Baratin M., Walzer T. and Ugolini S. (2008) Functions of natural killer cells. Nature Immunology 9(5):503-510.

de Waha S., Desch S., Eitel I., Fuernau G., Zachrau J., Leuschner A., et al. (2010) Impact of early vs. late microvascular obstruction assessed by magnetic resonance imaging on long-term outcome after ST-elevation myocardial infarction: a comparison with traditional prognostic markers. European Heart Journal 31(21): 2660-2668.

Weirather J., Hofmann U. D., Beyersdorf N., Ramos G. C., Vogel B., Frey A., et al. (2014) Foxp3+ CD4+ T cells improve healing after myocardial infarction by modulating monocyte/macrophage differentiation. Circulation Research 115(1): 55-67.

World health organization cardiovascular disease risk charts: revised models to estimate risk in 21 global regions. The Lancet Global Health 7(10): e1332–e1345.

Wu R., Gao W., Yao K. and Ge J. (2019) Roles of exosomes derived from immune cells in cardiovascular diseases. Frontiers in Immunology 10: 648.

Wu K. C. (2012) CMR of microvascular obstruction and hemorrhage in myocardial infarction. Journal of Cardiovascular Magnetic Resonance 14: 68.

Wu K. C., Zerhouni E. A., Judd R. M., Lugo-Olivieri C. H., Barouch L. A., Schulman S. P., et al. (1998) Prognostic significance of microvascular obstruction by magnetic resonance imaging in patients with acute myocardial infarction. Circulation 97(8):765-772.

Wynn T. A. (2015) Type 2 cytokines: mechanisms and therapeutic strategies. Nature Reviews Immunology 15(5): 271-282.

Xu J. Y., Xiong Y. Y., Lu X. T. and Yang Y. J. (2019). Regulation of type 2 immunity in myocardial infarction. Frontiers in Immunology 10: 62.

Yan X., Anzai A., Katsumata Y., Matsuhashi T., Ito K., Endo J., et al. (2013) Temporal dynamics of cardiac immune cell accumulation following acute myocardial infarction. Journal of Molecular and Cellular Cardiology 62: 24-35.

Yang K., Li D., Luo M. and Hu Y. (2006) Generation of HSP60-specific regulatory T cell and effect on atherosclerosis. Cellular Immunology 243(2): 90-95.

Yellon D. M. and Hausenloy D. J. (2007) Myocardial reperfusion injury. New England Journal of Medicine 357(11):1121-1135.

Yuan M. J., Maghsoudi T. and Wang T. (2016) Exosomes mediate the intercellular communication after myocardial infarction. International Journal of Medical Sciences 13(2): 113-116.

Zacchigna S., Martinelli V., Moimas S., Colliva A., Anzini M., Nordio A., et al. (2018) Paracrine effect of regulatory T cells promotes cardiomyocyte proliferation during pregnancy and after myocardial infarction. Nature communications 9(1): 2432.

Zhao W., Zhao J. and Rong J. (2020) Pharmacological modulation of cardiac remodeling after myocardial infarction. Oxidative Medicine and Cellular longevity 2020: 8815349.

Journal of Cell and Molecular Research (2021) 12 (2), 87-96 DOI: 10.22067/jcmr.v12i2.89670

Research Article

Comparative *in silico* Survey of Retinoic Acids as Putative Biomolecules Against VEGF Receptors: A Glycomics-based Approach

Ali Fallah, Esmaeil Samadian, Azadeh Mohammad-Hasani, Abasalt Hosseinzadeh Colagar*

Department of Molecular and Cell Biology, Faculty of Basic Sciences, University of Mazandaran, Babolsar, Iran

Received 17 November 2020 Accepted 3 January 2021

Abstract

In this study, putative interactions between all of the retinoic acid (RA) ligands (all-trans (At), 9-cis (9c), and 13-cis (13c)), and VEGF receptors (VEGFR-1, -2 and -3) were investigated. It was performed considering the glycosylation status of the receptors to achieve a more reliable mode of interactions based on glycomics. We found that RAs may have a higher affinity for ligand-binding domains in VEGFRs. Furthermore, all RA isomers can strongly attach to VEGFR-3 receptor in comparison to other ones. It was also demonstrated that receptor dimerization of RAs may be less targeted. Moreover, regarding post-translational modifications, glycosylated structures showed conflicting binding energies. RAs may target the human vasculature, specifically lymph vessels, through VEGFR-3. In addition, the ligand binding-mediated activation of VEGFRs may be affected by these agents. Also, the glycosylation status of the receptors can interfere with these manners. Furthermore, our results confirmed that the consideration of carbohydrates in crystal structures is essential for a better interpretation of ligand/receptor interactions during drug discovery studies. Even though these observations improved our understanding of the binding patterns of RAs to VEGFRs, validation of these results needs further analysis to introduce these biomolecules as anti-VEGF remedies.

***Keywords*:** Retinoic acids, Angiogenesis, VEGF receptors, Glycomics, *in silico*

Introduction

Organization of blood and lymphatic vessels, vasculogenesis and angiogenesis, is critical to provide whole-body with fresh oxygen and nutrient supply and remove catabolites. At the cellular level, activation of vascular endothelial growth factor receptors (VEGFR-1, -2, and -3) by their cognate ligands (different isotypes of VEGF) is the most important receptor tyrosine kinase/RTK-related signaling pathway. This pathway adjusts multiple processes which are essential for developmental, physiological, and pathological neovascularization (Christensen et al. 2017; Lee et al. 2017; Qiao et al. 2006; Shibuya 2013). The VEGFs are signal proteins which are produced by cells to trigger the formation of vessel networks via binding to their corresponding RTKs. All isoforms of VEGF-A can bind to VEGFR-1 and VEGFR-2, while VEGF-B is special for VEGFR-1 (Álvarez-Aznar et al. 2017; Goel and Mercurio 2013; Jeltsch et al. 2006; Leppänen et al. 2010). VEGF-C and VEGF-D isoforms with cleaved C-terminal domain are high-affinity ligands for VEGFR-3. Upon elimination of both pro-peptides, they obtain binding affinity for VEGFR-2. VEGF-E which exists in poxviruses can specifically bind to VEGFR-2 (Mercer et al. 2002).

As the ligand binding to the extracellular domain (ECD) of VEGFRs is required for their stimulation, the disruption of these ligand/receptor complexes deregulates their RTK and normal physiological activities. For this reason, ligand trapping from VEGFR-1 is resulted in the placental loss of preeclampsia and abnormalities in retinal and corneal vascularization (Markovic-Mueller et al. 2017). In contrast, VEGFR-1 traps the main angiogenic ligand VEGF-A from VEGFR-2 and displays a negative regulatory role against VEGFR-2-induced blood vessel sprouting. Alternatively, VEGFR-2/VEGFR-3 heterodimerization is an additional signal to facilitate this sprouting. Moreover, VEGFR-3 homodimers mediate lymphogenesis. So, a defective VEGFR-3 cascade results embryonic death (Leppänen et al. 2013; Qiao et al. 2006).

Considering the fact that classical anti-VEGF compounds are clinically administrated to prevent

*Corresponding author's e-mail address:
ahcolagar@umz.ac.ir, acolagar@yahoo.com

particular disease (cancer, retinopathy, endometriosis, and so forth)-associated neovascularization, the discovery of detailed molecular mechanisms of blood vessel formation is essential to design advanced anti-angiogenic remedies (Hegde et al. 2018; Ma & Ning 2019).

The glycome is the entire complement of sugars, whether free or present in more complex molecules of an organism. Glycomics is a comprehensive and multi-aspect study of glycome (Rudd et al. 2017). 32 types of sugar linkages were reported in various Saccharides. These building blocks can increase the degree of complexity. Sugar structures, are highly branched. Glycans are highly dynamic as they can bound to proteins or conjugate with lipids to form modified structures (Aizpurua-Olaizola et al. 2018). Glycans play significant roles during viral/bacterial recognition, cell signaling events, intrinsic immunity modulation, prohibition of cell proliferation, cancer expansion, cell fate determination, invasion, circulation arrangement, protein folding and other important biological procedures (Aizpurua-Olaizola et al. 2018; Rudd et al. 2017). Hence, glycomics is widely applicable in the clinic as it was reported previously (Reid et al. 2012).

Currently, we know that glycosylation facilitates signal transfer from the surrounding microenvironment to inside the cell. The structure of carbohydrates has direct impact on ligand/receptor binding, dimerization, and internalization of various signaling complexes, and, thus activation of different cell receptors. RTKs are the most prevalent type of Asparagine (N)-linked glycans that transduce signals which are important for cell communications. Accordingly, it could be concluded that VEGFRs mediate main functional properties of the vascular endothelial cells during angiogenesis. There are 13, 18, and 12 N-glycosylation sites with different carbohydrate side-chains in VEGFR-1, -2, and -3, respectively (Contessa et al. 2010; Itkonen and Mills 2013; Lopez-Sambrooks et al. 2016). Although it has not been fully understood so far, these sugar residues, which are not completely detected in crystal structures, may also affect the conformational features of VEGFRs. Therefore, comprehending the effects of the sugar structures on the binding of a candidate drug VEGFRs improves our knowledge about the binding mode of action of drug/VEGFRs such complexes. also, this direct impact is important for a glycomics-based point of view in drug design against VEGFRs.

Retinoids are physiological derivatives of vitamin A which have several positive impacts on normal cell growth and differentiation, tissue homeostasis, developmental organogenesis, and visual performance (Khalil et al. 2017; Mallipattu and He 2015; Zhu et al. 2015). However, they may have destructive effects on the morphogenesis during human embryogenesis (Gudas, 1994; Rönn et al., 2015). All retinoids including all-trans (At), 9-cis (9c), and 13-cis (13c) retinoic acids (RAs) emerge more recently as antineoplastic agents. Accordingly, on the contrary to the harmful influence of At-RA, a main active isomer of RA, (Rühl et al. 2018; Tsuji et al. 2015; Hu et al., 2020) that frequently causes embryonic death due to developmental deformity, it has been used in cancer therapy towards acute promyelocytic leukemia (Huang et al., 1988) colorectal cancer, pancreatic cancer, oral leukoplakia and skin cancer (Applegate and Lane 2015; Di Masi et al. 2015; Lodi et al. 2016; Moon et al. 1997; Tarapcsák et al. 2017; Uray et al. 2016; Szymański et al., 2020).

Interestingly, although we know that RAs are diffusible biomolecules (Minkina et al. 2017) and exert their impressions on gene regulation via nuclear receptor RAR/RXR. However, several studies demonstrated that RAs can tune-up the angiogenesis through binding to VEGFRs with an unclear pattern (Njar et al. 2019; Simandi et al. 2018; Urushitani et al. 2018; Costantini et al., 2020).
In the present study, via a computational-based approach we investigated the binding manner of At-RA, 9c-RA, and 13c-RA with the extracellular regions of three human VEGFRs (R-1, R-2, and R-3). We found an alternative mechanism which is responsible for the VEGFR-mediated inhibitory implications of RAs during angiogenesis. Furthermore, regarding the importance of VEGFRs' saccharide residues inactivation, we also compared the possible binding sites of three isoforms of RAs to both glycosylated and unglycosylated crystal structures of VEGFRs introduced so far.

Materials and Methods

Preparation of structures

Retinoic acids are small biomolecules with an average mass of about 300.435 kDa. The structures of interest isoforms (At-RA, 9c-RA, and 13c-RA) have been retrieved from PubChem database (http://pubchem.ncbi.nlm.nih.gov/) in structure-Data file (SDF) format which is an acceptable input for our docking program. Identifier (ID)s of retrieved isoforms from public repository were as

follows: 6419707; 449171, and 5282379, respectively (Dunning 2018). Also, the PDB files of human VEGFR1-3 have been obtained from the Protein Database (http://www.pdb.org). All structures were prepared by WebLab (http://weblab.cbi.pku.edu.cn) (Liu et al., 2009) and the visual molecular dynamics (VMD 1.9.3) package (www.ks.uiuc.edu/Research/vmd/) (Zhang 2015). The Swiss-PdbViewer modeling program was applied to perform energy minimization of all investigated structures (http://www.expasy.org/swissmod) (Guex et al. 2009). As the cut-off for bond, torsion, angle, improper angles, non-bounded and electrostatic functions was set for 10 Å by default, energy (E) exchanges between two steps was stopped below 0.05 kJ/mol, and the acting forces between any atom stopped below 10 Å.

The structural details including PDB IDs, domains, length, and glycosylation status of the extracellular regions of our studied VEGF receptors are summarized in the Table 1.

In order to minimize the energy of all 3D structures prepared by the Web Lab, we performed the energy minimization procedure using Swiss-PdbViewer (DeepView). The first (E1) and the end (E2) energy amounts for each molecule were listed in the Table 2. Moreover, docking energies obtained for different RA-VEGFR complexes using HEX 8.0 were described in Table 1.

A comparison of assessed docking energies for various RA-VEGFR complexes in this work indicated that At-RA, 9c-RA, and 13c-RA (-256.10, -256.11, and -248.56 kJ/mol, respectively) are highly bound to VEGFR-3 4BSK (Table 1). This is also occurred at different amino acid residues in VEGFR-3 D2 (OA-133: ARG-CA to OA-190: GLY-CA) (Figure 2).

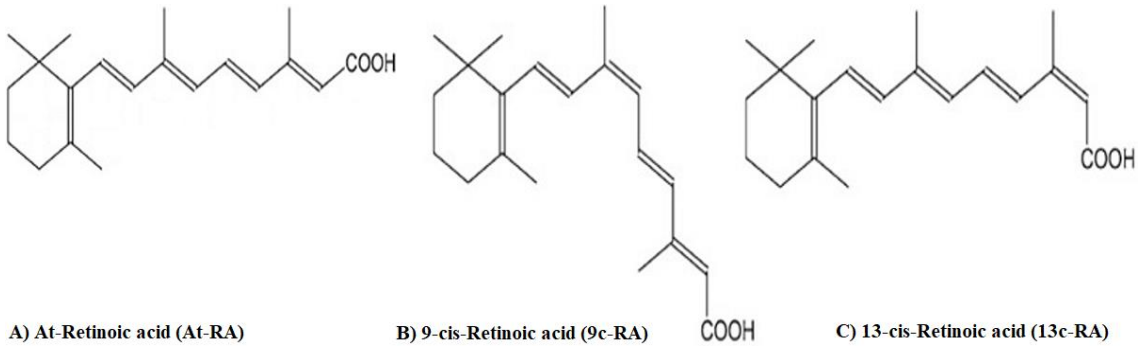

Figure 1. Schematic structural representation of retinoic acid isoforms including all-trans (At), 9-cis (9c), and 13-cis (13c) retinoic acids (RAs). At-RA is the main active isomer of RA (http://pubchem.ncbi.nlm.nih.gov/).

Docking parameters

Docking studies were carried out using HEX 8.0 (http://hexserver.loria.fr), which is an interactive molecular graphics program to calculate and display feasible docking modes of pairs of protein and ligand molecules (Roudini et al. 2020). Moreover, it can predict the position of ligand-receptor contacts approximately. All docking parameters were left as their default values (Pourhashem et al. 2017).

Results

The molecular structures of retinoic acid isoforms including At-RA, 9c-RA, and 13c-RA were represented in Figure 1 as they were obtained from PubChem. Chemical differences and reactive groups are shown for each structure.

Besides, our ligands can attach to other investigated structures with lower tendencies and they have the lowest binding mode in complex with VEGFR-1 D2 (1QTY), as demonstrated in Table 1. Also, we found At-RA, 9c-RA, and 13c-RA bind slightly to VEGFR-2 and VEGFR -1 D3 (residues from [O] R-143: ASN-CA to [O] R-278: LYS-CA and [O] X-241: LYS-CA to [O] X-331: LYS-CA, respectively) (Figure 2). In addition, as it was demonstrated in Figure 3 regarding the trends of binding energies for RA-VEGFR complexes, a decreased binding mode was detected for VEGFR-1 D3 (5T89) in comparison to VEGFR-2 D3 (2X1X) and also for VEGFR-2 D3 (2X1X) in comparison to

Table 1. Structural details (Chain, Domain, Glycosylation status) for VEGFRs and docking simulations for RAs-VEGFRs.

Receptors	PDB IDs	Chain	Domain (amino acid positions)	Glycosylation status		Docking Energy (kJ/mol)		
				Sugars and aa positions	Number of glycosylation sites	At-RA	9c-RA	13c-RA
VEGFR1	1FLT	95aa (Phe X135-Thr X226)	D2 (aa151 – aa 214)	-	-	-228.38	-223.9	-209.82
	1QTY	101aa (Phe T135-Gln T225)	D2 (aa151 – aa 214)	-	-	-15.76	-17.29	-18.19
	5T89	646aa (Asp 31-Thr Y654)	D1 (aa32-aa123), D2 (aa151-aa214), D3 (aa230-aa327), D4 (aa335-aa421), D5 (aa428-aa553), D6 (aa556-aa 654)	ASN X 100 (NAG X 701 & NAG X 702), ASN X 196 (NAG X 703), ASN X 251 (NAG X 704), ASN X 323 (NAG X 705), ASN X 402 (NAG X 706), ASN X 417 (NAG X 707 & NAG X 710), ASN X 574 (NAG X 708), ASN X 625 (NAG X 709) / ASN Y 100 (NAG Y 701), ASN Y 164 (NAG Y 702), ASN Y 196 (NAG Y 703 & NAG Y 704), ASN Y 251 (NAG Y 705), ASN Y 402 (NAG Y 707), ASN Y 417 (NAG Y 708), ASN Y 547 (NAG Y 709), ASN Y 625(NAG Y 710)	16	-217.79	-231.50	-218.01
VEGFR2	2X1W	213aa (Phe L 125-Glu L 326)	D2 (aa141-aa207), D3 (aa224-aa320)	ASN L 143 (NAG L 2401), ASN L 245 (NAG L 2601 & NAG L 2602), ASN L 318 (NAG L 2701)/ ASN M 245 (NAG M 1201 & NAG M 1201), ASN M 318 (NAG M 1301, NAG M 1302 & BMA M 1303)/ ASN N 143 (NAG N 1401), ASN N 245 (NAG N 1601), ASN N 318 (NAG N 1701 & NAG N 1702)/ ASN O 143 (NAG O 2001), ASN O 158 (NAG O 2101), ASN O 245 (NAG O 2201 & NAG O 2202), ASN O 318 (NAG O 2301).	12	-244.06	-244.45	-241.28
	2X1X	213aa (Pro R124-Glu R326)	D2 (aa141-aa207), D3 (aa224-aa320)	ASN R 143 (NAG R 404), ASN R 245 (NAG R 402 & NAG R 403), ASN R 318 (NAG R 405 & NAG R 406).	3	-251.99	-245.43	-242.62
	3KVQ	108aa (Ile A669-Gly A756)	D7 (aa667-aa753)	-	-	-241.31	-247.96	-240.43
	3V6B	424aa (His R131-Phe R329)	D2 (aa141-aa207), D3 (aa224-aa320)	-	-	-189.43	-206.67	-186.63
VEGFR3	4BSJ	232aa (Asp A328-His A554)	D4 (aa331-aa415), D5 (aa422-aa552)	ASN A 411 (NAG A 601), ASN A 515 (NAG A 602)	2	-51.50	-49.20	-43.38
	4BSK	214aa (Pro A30-Ile A224)	D1 (aa30-aa127), D2 (aa151-aa213)	ASN A 33 (NAG A 301), ASN A 104 (NAG A 302), ASN A 166 (NAG A 303)	3	-256.10	-256.11	-248.56

*ASN: Asparagine

* NAG: N-acetyl glucose

Table 2. Energy minimization (first and end energy) for VEGFRs.

Receptor	PDB IDs	Chain	E_1 (first energy minimization kJ/mol)	E_2 (end energy minimization kJ/mol)
VEGFR1	1FLT	X, Y	-6040.213	-10363.84
	1QTY	T, U, X, Y	-4588.174	-22151.435
	5T89	X, Y	-40754.605	-71025.164
VEGFR2	2X1W	L, M, N, O	-23284.633	-37331.891
	2X1X	R	+343794.188	-11717.921
	3KVQ	A	-1688.371	- 4945.834
	3V6B	R	-2886.585	-10666.744
VEGFR3	4BSK	A	16982.123	-9005.400
	4BSJ	A	-7782.256	-12937.562

Figure 2. Docking of three retinoid types (At-RA, 9c-RA, and 13c-RA) with VEGFR-1, 2, and 3 complexes: A1-3, B1-3, and C1-3 are docking results of retinoid types with VEGFR-1 (PDB-ID 5T89), VEGFR-2 (PDB-ID 2X1X), and VEGFR-3 (PDB-ID 4BSK), respectively. RA isoforms differentially bind to different domains of VEGFRs.

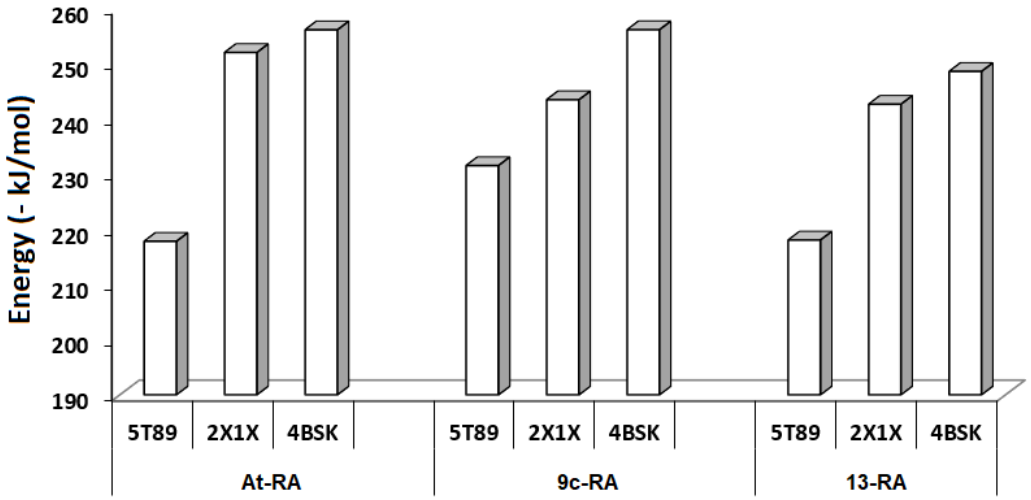

Figure 3. Docking energy amounts are shown for various complexes of At-RA, 9c-RA, and 13c-RA isoforms with different VEGF receptors, including VEGFR-1 D3 (5T89), VEGFR-2 D3 (2X1X), and VEGFR-2 D3 (2X1X).

VEGFR-3 D2 (4BSK) in a gradual mode in case of 9cRA isoform. A similar trend was observed for both At-RA and 13-RA isoforms, while differences were more remarkable for 5T89 in comparison to 2X1X and 4BSK. According to crystal structures of three VEGFRs, structures 5T89, 2X1W, and 4BSK, for VEGFR-1, -2, and -3, have resolved the higher number of carbohydrate residues among other structures studded up-to-now, respectively (Table 1). Considering the glycosylated VEGFR-2 structures, 2X1W (with a higher glycosylation status) has a lower docking tendency (At-RA: -244.06; 9c-RA: -244.45; 13c-RA: -241.28, kJ/mol) in comparison to a less glycosylated structure 2X1X (At-RA: -251.99; 9c-RA: -245.43; 13c-RA: -242.62, kJ/mol). These observations were not confirmed for other receptors such as glycosylated 2X1X with a lower energy versus non-glycosylated 3V6B with a higher energy (Table 1).

Discussion

The regulatory function of the VEGF signaling system has comprehensively been established in normal *de novo* and pathological revascularization. This cascade is modulated by the activation of VEGF receptor family members (VEGFR-1, -2, and -3). VEGFR-2 triggers the blood vessels organization whereas VEGFR-1 plays a negative feedback for VEGFR-2 function (Greenberg et al. 2008; Stuttfeld and Ballmer-Hofer 2009). In VEGFR-3-related signaling pathways, VEGFR-3 (only) induces lymphatic vascularization and also in co-operation with VEGFR-2 mediates blood angiogenesis (Leppänen et al. 2013). These trans-membrane RTKs have seven extra-cellular immunoglobulins (Ig)-like domains (D1-7) and their activation process involves the ligand binding through D1-3, dimerization through D4-7, and auto-phosphorylation of the cytoplasmic kinase domains. The ligand-mediated induction mode via a membrane-distal domain 2 (D2) is conserved for all VEGF receptors. Additionally, for both VEGFR-1 and 2, D3 (not mainly) is used for ligand attachment (Leppänen et al. 2010; Leppänen et al. 2013; Markovic-Mueller et al. 2017).

Recent studies disclose the potential of retinoids to interrupt with angiogenic processes. Weninger et al. in 1993 illustrated that retinoids are potent inhibitors of VEGF/VPF production by normal human keratinocytes. These cells may contribute to the therapeutic effects of retinoids (Weninger et al. 1998). Also, in 2007 Noonan et al. showed that the synthetic retinoid 4-hydroxy fenretinide (4HPR) displays anti-angiogenic effects (Noonan et al. 2007). In addition, microarray data by Albini et al. demonstrated that some anti-angiogenic agents, such as N-acetyl-cysteine and 9c-RA, induce molecular indices in endothelial cells which mimic *in vitro* senescence (Albini et al. 2012). Tsuji et al. showed evident data for the binding of retinoic acid isomers (At-RA, 9c-RA, and 13c-RA) with RXRs and RARs (Tsuji et al. 2015). Moreover, Zhong et al. confirmed that CYP26C1 is a 4-oxo-atRA hydroxylase and probably be important for adjusting the condensation of active retinoids in human tissues (Zhong et al. 2018).

Taken together, there is no clear data indicating that how RAs affect VEGFRs from outside the cell.

Here for the first time, the binding patterns of RAs with VEGFRs were clarified using a docking-based approach. Results revealed that all three RA isomers (At-, 9c-, and 13c-RA) can remarkably bound to VEGFR-3. In comparison to interactions with other domains, RAs have a higher affinity to D2 in VEGFR-3 (Figure 2). This may suggest a novel mechanism for these agents which targets the vasculature, especially through the ligand (VEGF-C) detachment from its respective receptor which leads to the lymph/blood vessels deterioration. These biomolecules can also interfere with blood vessels formation through the inhibition of VEGF-A-VEGFR-2 and (with a lower affinity) VEGFR-1 (Table 1). Although RAs may have strong contacts with similar domains, as depicted in VEGFR-3 D2 (Figure 2) or VEGFR-1/-2 D3 (Figure 2), they can't interact with similar residues, may be owing to variations in RA isomers (Figure 1). Actually, structural remodeling for receptor dimerization in D4-7 could not be sharply affected by RAs, considering the competed energies which were demonstrated in Table 1. As the kinase activity of VEGFRs is fundamentally concerted by their glycosylation status (Gomes Ferreira et al. 2018), their glycosylated 3D structures were also considered in the current study. In this regard, glycosylation may lead to a lower affinity of RAs for VEGFR-2 (2X1W) when compared with 2X1X. Conversely, glycosylation may affect the 5T89 folding in a way that different modes achieve in RA-VEGFR-1 docking assessments. These inconsistencies in binding energies between glycosylated and unglycosylated structures suggest that sugar residues can alter the ligand-binding manners. Accordingly, post-translational modifications like glycosylation should be considered in such docking studies to reach a reliable behavior. It implies the importance of glycomics-based approaches in ligand/receptor binding studies.

Taking a computational analysis, instead of a real experiment, is easy and cost-benefit, though, validation of the outputs by real experiments are inevitable. It is clear that all factors applied during simulations are based on approximation and are under control by users. Currently, by advances in computational biology docking of several thousands of ligands were performed which can be applied in pharmaceutical industries to design improved structure-dependent drugs (Yadav et al. 2018). Nevertheless, we can have a better interpretation of the applications of RAs in tissue regeneration, wound repair, and cancer therapy or other VEGF-associated system uses in the future. thus, molecular dynamics and experimental analysis in further investigations may confirm our findings.

Acknowledgments
Thanks to Zeinab Pourhashem (School of Advanced Technologies in Medicine, Golestan University of Medical Sciences, Gorgan, Iran) for their scientific support. We are grateful to our colleagues for the critical reviews of the manuscript.

Conflicts of interest
The authors declare that they have no conflict of interest.

References

Aizpurua-Olaizola O., Toraño J.S., Falcon-Perez J.M., Williams C., Reichardt N. and Boons G-J. (2018) Mass spectrometry for glycan biomarker discovery. TrAC Trends in Analytical Chemistry 100: 7-14.

Albini A., Tosetti F., Li V.W., Noonan D.M. and Li W.W. (2012) Cancer prevention by targeting angiogenesis. Nature reviews Clinical oncology 9(9): 498.

Álvarez-Aznar A., Muhl L. and Gaengel K. (2017) VEGF receptor tyrosine kinases: key regulators of vascular function. In Current topics in developmental biology (Vol. 123: pp. 433-482): Elsevier.

Applegate C.C. and Lane M.A. (2015) Role of retinoids in the prevention and treatment of colorectal cancer. World journal of gastrointestinal oncology 7(10): 184.

Christensen S.T., Morthorst S.K., Mogensen J.B. and Pedersen L.B. (2017) Primary cilia and coordination of receptor tyrosine kinase (RTK) and transforming growth factor β (TGF-β) signaling. Cold Spring Harbor perspectives in biology 9(6): a028167.

Contessa J.N., Bhojani M.S., Freeze H.H., Ross B.D., Rehemtulla A. and Lawrence T.S. (2010) Molecular imaging of N-linked glycosylation suggests glycan biosynthesis is a novel target for cancer therapy. Clinical Cancer Research 16(12): 3205-3214.

Costantini L., Molinari R., Farinon B., and Merendino N. (2020) Retinoic acids in the treatment of most lethal solid cancers. Journal of clinical medicine 9(2): 360.

Di Masi A., Leboffe L., De Marinis E., Pagano F., Cicconi L., Rochette-Egly C. and et al. (2015) Retinoic acid receptors: from molecular mechanisms to cancer therapy. Molecular aspects of medicine 41: 1-115.

Dunning M.W. (2018) Quantification and Profiling of Hepatic Retinoid in Freshwater Fishes by Liquid Chromatography–Tandem Mass Spectrometry (Master's thesis, University of Waterloo).

Goel H.L. and Mercurio A.M. (2013) VEGF targets the tumour cell. Nature Reviews Cancer 13(12): 871-882.

Gomes Ferreira I., Pucci M., Venturi G., Malagolini N., Chiricolo M. and Dall'Olio F. (2018) Glycosylation as a main regulator of growth and death factor receptors signaling. International journal of molecular sciences 19(2): 580.

Greenberg J.I., Shields D.J., Barillas S.G., Acevedo L.M., Murphy E., Huang J. and et al. (2008) A role for VEGF as a negative regulator of pericyte function and vessel maturation. Nature 456(7223): 809-813.

Gudas L.J. (1994) Retinoids and vertebrate development. Journal of Biological Chemistry 269(22): 15399-15402.

Guex N., Peitsch M.C. and Schwede T. (2009) Automated comparative protein structure modeling with SWISS-MODEL and Swiss-PdbViewer: A historical perspective. Electrophoresis 30(S1): S162-S173.

Hegde P.S., Wallin J.J. and Mancao C. (2018) Predictive markers of anti-VEGF and emerging role of angiogenesis inhibitors as immunotherapeutics. Paper presented at the Seminars in cancer biology.

Huang M., Ye Y-c., Chen S., Chai J-R., Lu J-X., Gu L-J. and Wang Z-Y. (1988) Use of all-trans retinoic acid in the treatment of acute promyelocytic leukemia.

Hu P., van Dam A. M., Wang Y., Lucassen P. J. and Zhou J. N. (2020) Retinoic acid and depressive disorders: Evidence and possible neurobiological mechanisms. Neuroscience & Biobehavioral Reviews 112: 376-391.

Itkonen H.M. and Mills I.G. (2013) N-linked glycosylation supports cross-talk between receptor tyrosine kinases and androgen receptor. PloS one 8(5).

Jeltsch M., Karpanen T., Strandin T., Aho K., Lankinen H. and Alitalo K. (2006) Vascular endothelial growth factor (VEGF)/VEGF-C mosaic molecules reveal specificity determinants and feature novel receptor binding patterns. Journal of Biological Chemistry 281(17): 12187-12195.

Khalil S., Bardawil T., Stephan C., Darwiche N., Abbas O., Kibbi A.G. and et al. (2017) Retinoids: a journey from the molecular structures and mechanisms of action to clinical uses in dermatology and adverse effects. Journal of Dermatological Treatment 28(8): 684-696.

Lee J.M., Cimino-Mathews A., Peer C.J., Zimmer A., Lipkowitz S., Annunziata C.M. and et al. (2017) Safety and clinical activity of the programmed death-ligand 1 inhibitor durvalumab in combination with poly (ADP-ribose) polymerase inhibitor olaparib or vascular endothelial growth factor receptor 1-3 inhibitor cediranib in women's cancers: a dose-escalation, phase I study. Journal of Clinical Oncology 35(19): 2193.

Leppänen V.M., Prota A.E., Jeltsch M., Anisimov A., Kalkkinen N., Strandin T. et al. (2010) Structural determinants of growth factor binding and specificity by VEGF receptor 2. Proceedings of the National Academy of Sciences 107(6): 2425-2430.

Leppänen V.M., Tvorogov D., Kisko K., Prota A.E., Jeltsch M., Anisimov A. and et al. (2013) Structural and mechanistic insights into VEGF receptor 3 ligand binding and activation. Proceedings of the National Academy of Sciences 110(32): 12960-12965.

Liu X., Wu J., Wang J., Liu X., Zhao S., Li Z. and et al. (2009) WebLab: a data-centric, knowledge-sharing bioinformatic platform. Nucleic acids research 37(suppl_2): W33-W39.

Lodi G., Franchini R., Warnakulasuriya S., Varoni E.M., Sardella A., Kerr A.R. et al. (2016)

Interventions for treating oral leukoplakia to prevent oral cancer. Cochrane Database of Systematic Reviews(7).

Lopez-Sambrooks C., Shrimal S., Khodier C., Flaherty D.P., Rinis N., Charest J.C. and et al. (2016) Oligosaccharyltransferase inhibition induces senescence in RTK-driven tumor cells. Nature chemical biology 12(12): 1023.

Ma X. and Ning S. (2019) Cyanidin-3-glucoside attenuates the angiogenesis of breast cancer via inhibiting STAT3/VEGF pathway. Phytotherapy research 33(1): 81-89.

Mallipattu S.K. and He J.C. (2015) The beneficial role of retinoids in glomerular disease. Frontiers in medicine 2, 16.

Markovic-Mueller S., Stuttfeld E., Asthana M., Weinert T., Bliven S., Goldie K.N. and et al. (2017) Structure of the Full-length VEGFR-1 Extracellular Domain in Complex with VEGF-A. Structure 25(2): 341-352.

Mercer A.A., Wise L.M., Scagliarini A., McInnes C.J., Büttner M., Rziha H.J. and et al. (2002) Vascular endothelial growth factors encoded by Orf virus show surprising sequence variation but have a conserved, functionally relevant structure. Journal of General Virology 83(11): 2845-2855.

Minkina A., Lindeman R.E., Gearhart M.D., Chassot A.A., Chaboissier M.C., Ghyselinck N.B. and et al. (2017) Retinoic acid signaling is dispensable for somatic development and function in the mammalian ovary. Developmental biology 424(2): 208-220.

Moon T.E., Levine N., Cartmel B., Bangert J.L., Rodney S., Dong Q. and et al. (1997) Effect of retinol in preventing squamous cell skin cancer in moderate-risk subjects: a randomized, double-blind, controlled trial. Southwest Skin Cancer Prevention Study Group. Cancer Epidemiology and Prevention Biomarkers 6(11): 949-956.

Njar V., Mbatia H., Ramamurthy V. and Ramalingam S. (2019) 13-Cis-Ramba Retinamides That Degrade Mnks For Treating Cancer. In: Google Patents.

Noonan D.M., Benelli R. and Albini A. (2007) Angiogenesis and cancer prevention: a vision. In Cancer Prevention (pp. 219-224): Springer.

Pourhashem Z., Mehrpouya M., Yardehnavi N., Eslamparast A. and Kazemi-Lomedasht F. (2017). An in-silico approach to find a peptidomimetic targeting extracellular domain of HER3 from a HER3 Nanobody. Computational biology and chemistry 68: 39-42.

Qiao J., Huang F., Naikawadi R.P., Kim K.S., Said T. and Lum H. (2006) Lysophosphatidylcholine impairs endothelial barrier function through the G protein-coupled receptor GPR4. American Journal of Physiology-Lung Cellular and Molecular Physiology 291(1): L91-L101.

Reid C.W., Twine S.M., and Reid AN. (2012) Bacterial glycomics: current research, technology and applications: Caister Academic Press.

Roudini L., NayebZadeh Eidgahi N., Rahimi H. R., Saberi M. R., Amiri Tehranizadeh Z., Beigoli S. and et al. (2020) Determining the interaction behavior of calf thymus DNA with berberine hydrochloride in the presence of linker histone: a biophysical study. Journal of Biomolecular Structure and Dynamics 38(2): 364-381.

Rönn R.E., Guibentif C., Moraghebi R., Chaves P., Saxena S., Garcia B. and Woods N-B. (2015) Retinoic acid regulates hematopoietic development from human pluripotent stem cells. Stem Cell Reports 4(2): 269-281.

Rudd P., Karlsson N.G., Khoo K-H. and Packer N.H. (2017) Glycomics and glycoproteomics. In Essentials of Glycobiology [Internet]. 3rd edition: Cold Spring Harbor Laboratory Press.

Rühl R., Krężel W. & de Lera A.R. (2018) 9-Cis-13, 14-dihydroretinoic acid, a new endogenous mammalian ligand of retinoid X receptor and the active ligand of a potential new vitamin A category: vitamin A5. Nutrition reviews 76(12): 929-941.

Shibuya M. (2013) VEGFR and type-V RTK activation and signaling. Cold Spring Harbor perspectives in biology 5(10): a009092.

Simandi Z., Horvath A., Cuaranta-Monroy I., Sauer S., Deleuze J-F. and Nagy L. (2018) RXR heterodimers orchestrate transcriptional control of

neurogenesis and cell fate specification. Molecular and cellular endocrinology 471: 51-62.

Stuttfeld E. and Ballmer-Hofer K. (2009) Structure and function of VEGF receptors. IUBMB life 61(9): 915-922.

Szymański Ł., Skopek R., Palusińska M., Schenk T., Stengel S., Lewicki S. ... and Zelent A. (2020) Retinoic Acid and Its Derivatives in Skin. Cells 9(12): 2660.

Tarapcsák S., Szalóki G., Telbisz Á., Gyöngy Z., Matúz K., Csősz É., Nagy P., Holb I.J., Rühl R., Nagy L. and Szabó G. (2017) Interactions of retinoids with the ABC transporters P-glycoprotein and Breast Cancer Resistance Protein. Scientific reports 7(1): 1-11.

Tsuji M., Shudo K. and Kagechika H. (2015) Docking simulations suggest that all-trans retinoic acid could bind to retinoid X receptors. Journal of computer-aided molecular design 29(10): 975-988.

Uray I.P., Dmitrovsky E. and Brown P.H. (2016) Retinoids and rexinoids in cancer prevention: from laboratory to clinic. Paper presented at the Seminars in oncology.

Urushitani H., Katsu Y., Kagechika H., Sousa A.C., Barroso C.M., Ohta Y. and et al. (2018) Characterization and comparison of transcriptional activities of the retinoid X receptors by various organotin compounds in three prosobranch gastropods; Thais clavigera, Nucella lapillus and Babylonia japonica. Aquatic Toxicology 199: 103-115.

Weninger W., Rendl M., Mildner M. and Tschachler E. (1998) Retinoids downregulate vascular endothelial growth factor/vascular permeability factor production by normal human keratinocytes. Journal of investigative dermatology 111(5): 907-911.

Yadav P., Bandyopadhyay A., Chakraborty A. and Sarkar K. (2018) Enhancement of anticancer activity and drug delivery of chitosan-curcumin nanoparticle via molecular docking and simulation analysis. Carbohydrate polymers 182: 188-198.

Zhang J. (2015) The Hybrid Idea of Optimization Methods Applied to the Energy Minimization of (Prion) Protein Structures Focusing on the beta2-alpha2 Loop. arXiv preprint arXiv:1504.03614.

Zhong G., Ortiz D., Zelter A., Nath A. and Isoherranen N. (2018) CYP26C1 is a hydroxylase of multiple active retinoids and interacts with cellular retinoic acid binding proteins. Molecular pharmacology 93(5): 489-503.

Zhu H., Hu J., Li X., Chen L., Zhao H., Zhou W. and et al. (2015). All-trans retinoic acid and arsenic combination therapy benefits low-to-intermediate-risk patients with newly diagnosed acute promyelocytic leukaemia: a long-term follow-up based on multivariate analysis. British journal of haematology 171(2): 277-280.

Journal of Cell and Molecular Research (2021) 12 (2), 97-103 DOI: 10.22067/jcmr.2021.64305.0

Research Article

Identification of Bacterial Proteins in the Gut of Sunn pest, *Eurygaster integriceps*

Mohammad Saadati [1,*], Mahmoud Toorchi [2]

[1] *Faculty of Agriculture, University of Birjand, Birjand, Iran*
[2] *Faculty of Agriculture, University of Tabriz, Tabriz, Iran*

Received 1 November 2020 Accepted 6 March 2021

Abstract

Proteomics is a powerful tool to identify effective proteins in the biochemical reactions of the insect body. Many proteins were reported in the gut lumen and tissues which are essential to complete the physiological role of the alimentary canal of Sunn pest. The gut microbiome of insects has a key role in the digestive process. In this study, for the first time, gut proteins of adult Sunn pest were extracted. These proteins were visualized and identified with two-dimensional polyacrylamide gel electrophoresis and mass spectrometry, respectively. Newly identified proteins include pyruvate dehydrogenase, oxidoreductase FAD-binding protein, hypothetical proteins, glycerol-3 phosphate dehydrogenase, conserved hypothetical proteins, ABC excinucleases, ABC-type transport systems and molecular chaperones. The accumulation of these metabolism proteins in the gut of Sunn pest indicates the importance of symbiotic proteins in the improvement of digestive activities and insect-bacteria interactions. Results suggest that the identified bacterial proteins can be considered as effective proteins in the process of nutrition and provide more gut-derived targets for enzyme engineering and development of biopesticides.

***Keywords*:** Proteomics, Digestive system, Scutelleridae, Biochemistry, Bacteria, Two dimensional gel electrophoresis

Introduction

Many insects are serious pests of the grains, among them Sunn (Critchley, 1998). The active cycle begins in the spring with main devastating consequences on the farms. It includes feeding, reproduction, and appearance of new adults. Inactive phase occurs on the host in the winter shelters on hillsides (Critchley, 1998; Javaheri et al., 2009). The utilization of chemicals is one of the common approaches to control the Sunn pest in the farmers. Although, overuse of insecticides has affected the non-target organisms particularly their biological enemies in the current farms. This lead to the outbreak of secondary pests like wheat trips and some aphids in the grain farms of Iran. Therefore, the introduction of safer pest management methods is amenable. Protein inhibitors are a new class of biopesticides with the capacity for safe control of insect-plant interactions. Insecticidal proteins such as protease inhibitors, α-amylase inhibitors, lectins, and chitinases have been proposed as potential candidates for development of transgenic plants (Jouanian et al., 1998). The comprehensive study of the digestive system could be considered as the first step to find potent targets for toxic proteins.

The basic structure of the digestive canal is similar among various species of insects with some differences related to their adaptation for feeding process (Engel and Moran, 2013). In hemiptera and Sunn pest as special cases, the alimentary canal is composed of foregut, midgut and hindgut, among which foregut and hindgut are smaller than the midgut (Habibi et al., 2008; Saadati et al., 2008). Midgut as the key part of the digestive system contains four parts (Saadati bezdi et al., 2012a). Salivary glands and gut are main parts of the digestive system in the insects, particularly hemipterous insects (Habibi et al., 2008, Saxena, 1963). Sap-feeding hemipterans, and many beetle and ant species which are specialized on nectar or honey dew do not produce peritrophic matrix proteins (Engel and Moran, 2013). Extra oral digestion as a unique approach of feeding was reported from hemiptera. During extra oral digestion, they inject their salivary proteins to the

*Corresponding author's E-mail address:
m-saadati@birjand.ac.ir

target plant tissues to liquefy the food before entering to their gut for final digestive process (Boyd, 2003). The gut as the main part of the digestive system is responsible for converting food particles to small molecules and preparing them for absorption (Pauchet et al., 2008; Hou et al., 2010; Liu et al., 2009). Moreover, gut is the first natural barrier against plant toxins and other xenobiotics that can be taken while feeding (Yao et al., 2009). Hence, gut proteins and their gene expression modifications are key factors which improve efficiency of nutrition.

The term of proteomics was for the first time proposed by Wilkins in 1996 as a similar approach to the genomics. It is defined as the large-scale investigation of proteins, emphasizing on their specialized functions in particular times or situations. The proteome map of midgut of the sunn pest was determined previously by Saadati et al., (2012b). They identified more than 100 protein spots which were classified in 11 various functional categories. They demonstrated some changes in the gut and salivary gland proteins of adult Sunn pests and their fifth instars in a comparative mode (Saadati et al., 2012c). Moreover, in another study, they confirmed that some wheat proteins are accumulated in the gut of adult Sunn pests (Saadati and Toorchi, 2017).

On the other hands, the functional integrity of bacterial proteins with digestive processes was approved in animals. It was proposed that gut microbiome secretions of insects may have different roles in their normal physiology. In the present study we were endeavored to identify gut bacterial proteins of Sunn pest for the first time. This will open up new opportunities to clarify the roles of bacterial proteins in digestive and immune systems of insects and will improve our knowledge about insect-bacteria interactions.

Materials and Methods

Animal sampling and insect dissection

Overwintering adults of Sunn pest (*Eurygaster integriceps Puton*, Hemiptera: Scutelleridae) were collected from Torbat-e Jam, Khorasan Razavi, Iran, in February 2018 and were transferred to insectarium for rearing on the wheat seeds (*Triticium aestivum* L.; Poales: Poaceae) of variety Roshan at 27°C with a 16:8 long-day (L:D) photoperiods. One-day-old new adult insects were selected for dissection of digestive system. Their midguts were then transferred to micro tubes containing a cocktail of protease inhibitors in phosphate buffered saline (PBS, pH: 6.9) (Roche Applied Science, Manneheim, Germany).

Protein extraction

At first, ten dissociated guts were grounded to a fine powder using a mortar and pestle. Then, gut tissues were transferred to a 50 ml tube containing 10 ml of 10% tricholoroacetic acid in acetone and 0.07% of 2-mercaptoethanol. The tube was ultra-sonicated and kept at -20°C for one hour. After one round of centrifugation at 9000 ×*g* for 20 min at 4° C, the supernatant was removed. The pellet was washed with acetone containing 0.07% of 2-mercaptoethanol, air-dried, and resuspended in the lysis buffer (7 M Urea, 2 M Thiourea, 5% 3-[(3-cholamidopropyl) dimethylammonio]-1 propanesulfonate (CHAPS), and 2 mM Tributylphosphine) while vigorously shake. The final step of centrifugation was performed at 20000 ×g for 20 min at room temperature to remove gross materials. The pellet was kept at -80°C until further analysis as it was described previously (Saadati Bezdi et al., 2012 a, b).

Two-dimensional polyacrylamide gel electrophoresis (2-DE) and image analysis

A total of 400 µg of gut proteins were transferred to an immobilized pH gradient (IPG) strip (11 cm, pH 3-10 linear; Bio-Rad, Hercules, CA, USA). The rehydration was performed under the following condition: 50 V for 14 hours at 25 °C. Isoelectric focusing was performed under various conditions including: 250 V for 15 min; and 8000 V for 1 h on a linear ramp; in addition to 8000 V for 4 h on a rapid ramp. The equilibration solution (ES) 1 (6 M urea, 2% Sodium dodecyl sulfate (SDS), 0.375 M Tris-HCl (pH 8.8), 20% glycerol, and 130 mM dithiortheitol (DTT)) was used to float the strips for 30 min. This process was repeated with equilibration solution (ES) 2 in which the DTT was substituted by 135 mM Iodoacetamide. The second dimension electrophoresis with 13% SDS-polyacrylamide gel was begun after isoelectric focusing. The gels were finally stained with Coomassie Brilliant Blue and were scanned with a calibrated densitometer (GS-800, Bio-Rad). Results were analyzed using PDQuest 2-D analysis software (ver. 8.0.1, Bio-Rad). This includes different stages such as image filtration, spot detection, background subtraction and spot matching. The gel with the highest quality was selected as the reference; and was used for spot analysis of other gels. The amounts of protein per spot were expressed as the volume of the spot, which is defined as the sum of detected intensities of all pixels that make up that spot (Saadati bezdi et al.,

2012c). To reduce errors during image analysis, spots volumes were normalized using local regression method.

Protein identification

To identify proteins, gels excised from Coomassie brilliant blue CBB -stained 2-DE gels were subjected to in-gel trypsin digestion (Wako, Osaka, Japan) using automated protein digestion system (Digest Pro 96; Intavis, Koeln, Germany). To prepare spots these steps were performed sequentially: Incubation (acetonitrile), washing (50 mM NH_4HCO_3, 15 min), reduction (10 mM DTT in 50 mM NH_4HCO_3, 20 min), and alkylation (40 mM Iodacetamide in 50 mM NH_4HCO_3,15 min). Finally, samples were digested using trypsin at 37°C for 16 h. Desalting was performed using NuTip C-18 pipet tips (Glygen Inc., Columbia, *NY*). Peptides were then injected with an autosampler into an Ultimate 3000 nanoLC (Dionex, Germering, Gemany) coupled with a nanospray LTQ Orbitrap XL mass spectrometer (Thermo Fisher, San Jose, CA, USA). Peptides (1 µl) were reconstituted in 0.1% formic acid (5 µl) and loaded onto the trap column (PepMap, C18, 300 µm ID × 5 mm, pump at 25 µl/ min flow rate). Then, peptides were eluted and separated from the trap column using 0.1% formic acid in acetonitrile on a 75 µm ID × 12 cm C18 column (Nikkyo Technos, Tokyo, Japan) at a flow rate of 200 nl/ min and sprayed at a voltage of 1.8 kV. The mass spectrometry (MS) was applied in the positive-ion mode using Xcalibur software (ver. 1.4, Thermo Fisher) and data acquisition was set to cover a scan range of 100- 2000 *m/z* that resulted by three MS/MS scans after considering of 60 min as retention time. Tandem mass spectrum data files were converted to MGF files using Bioworks software (ver. 3.3.1, Thermo Fisher). Peptide masses were searched against protein sequences which are available from the National Centre for Biotechnology Information using the Mascot software (ver. 2.3.02, Matrix Science, London, UK). Search parameters were set equal to 0.5 Da for product mass tolerance and 10 ppm for peptide mass accuracy. Only one missed trypsin cleavage was allowed during analysis and carbamidomethylation of cysteins and oxidation of methionines were selected as fixed and variable modifications, respectively (Saadati Bezdi et al., 2012b, c). The three match peptides and at least five percent coverage in the peptides sequences were selected to beginning of evaluations of probably proteins. Finally, the proteins with ion scores greater than 36 which were significant in the NCBI database ($P<0.01$) selected as target proteins.

Results

One-day-old adult sunn pests were selected for dissecting. Crude proteins which were extracted from their guts were separated by 2-DE and visualized by CBB. Protein expression patterns were analyzed using image analysis software and a total of 288 protein spots were detected. The most spots were also identified in previous studies (Saadati et al., 2012a; Saadati et al., 2012b; Saadati et al., 2012c., Saadati and Toorchi, 2017). Fifteen protein spots which were not introduced previously were selected for further analysis via sequencing (Figure 1).

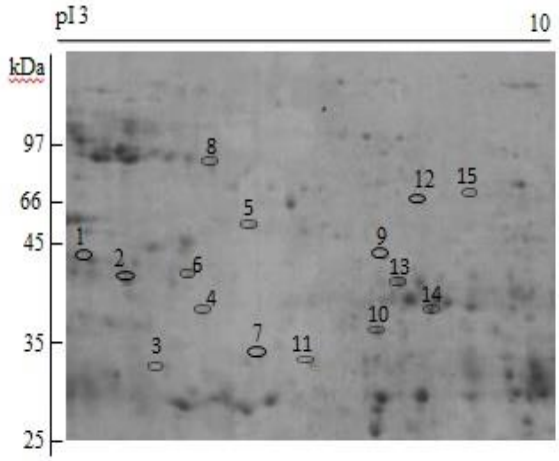

Figure 1. Gut protein expression patterns of Sunn pest adult insects (*Eurygaster integriceps*). One-day-old insects rearing on the wheat seeds were dissected and their gut proteins were extracted, separated by two-dimensional gel electrophoresis, and visualized by CBB staining. Circles indicate positions of accumulated proteins in the guts.

The resulted sequences that prepared with mass spectrometry searched in the different database. In the first step animal database and plant database were used to identify new proteins. Finally, all organism databases used to search new sequence for covering prokaryotes and eukaryotes proteins. Eight proteins were identified for the first time in the present study. Although, they were extracted from sunn pest gut, they had a bacterial origin (Table 1). Newly identified proteins includes: Pyruvate dehydrogenases (spot 1a), oxidoreductase FAD-binding proteins (spot 1b), unidentified proteins (spot 1c), glycerol-3 phosphate dehydrogenases (spot 2a), conserved unidentified proteins (spot 2b), excinuclease ABC (spot 3), ABC-type transport systems (spot 4), and molecular chaperons (spot 5). In the proteomics researches, targets proteins were selected from current database. Hence, there is more chance to this point that unknown proteins (Table 1) be new proteins that not addressed with identified proteins. Some of spots in the gel patterns contain

more than one protein like spot 1 and 2 (Figure 1, Table 1). Cutting of large spot from fresh gels may be reducing quality of target spots. The replicable experiment is necessary action against this challenge. Distribution of appearing spots in the final gels showed that bacteria can be secreted various proteins in the wide range of *pH* in the gut of sunn pest (Figure 1). The most of identified proteins belongs to energy and metabolism proteins such pyruvate dehydrogenases, oxidoreductase FAD-binding proteins, glycerol-3 phosphate dehydrogenases and ABC-type transport systems. The other proteins from this research are effective in the protein and nucleic acid synthesis like unidentified proteins (spot 1c), conserved unidentified proteins (spot 2b), excinuclease ABC (spot 3), and molecular chaperons (spot 5).

(Saadati et al., 2012a). Our results showed that some of bacterial proteins were accumulated in the alimentary canal of adult sunn pest. The function of microbial proteins in the digestive system of insects is improvement of digestive and immune process (Demandel et al., 2020). Alkaline condition in the gut of some insects like Lepidoptera and termites were not proper to symbiotic bacteria, generally. There are new reports from resistant bacteria to alkalinity phase like a *Firmicutes*, *Clostridium*, and *Planctomycetes* in the digestive system of insects (Engel and Moran, 2013). Aerobic and anaerobic conditions are very effective to microbiome variability in the gut of insects. It is reported that anaerobic phase was more occurred in the larger insects in comparison to smaller insects.

The presence of many protists, fungi, archaea, and bacteria was reported in the guts of various insects

Table 1. Expressed proteins with bacterial origins in the gut of adult sunn pest, Eurygaster integriceps, using all entries (organisms) in NCBI database.

Spot no.[a]	Description	Acc. no.[b]	Organism	Theo[c].		Exp[d].	M.P.[e]	Score[f]	Cov[g].
				M_r (kDa)/p*I*		Mr (kDa)			%
1	Pyruvate dehydrogenase	gi| 97898	*E.faecalis*	26.2	4.36	44	15	59	19
1b	Oidoreductase FAD-binding protein	gi| 291333815	*Marine bacterium*	37.8	3.62	44	11	48	17
1c	Hypothetical protein	gi| 145543418	*P.tetraurelia*	35.2	3.88	44	8	45	13
2	Glycerol-3-phosphate dehydrogenase	gi| 28377286	*L.plantarum*	38.2	4.72	41.3	12	44	8
2a	Conserved Hypothetical protein	gi| 303247419	*D.fructosovoranus*	36.40	4.92	41.3	9	38	7
3	Not identified								
4	Not identified								
5	Not identified								
6	Not identified								
7	ABC-type transport system	gi| 237745572	*O.formigenes*	26.17	6.18	34.7	16	64	15
8	Not identified								
9	Molecular Chaperons	gi| 120436429	*G.forsetti*	46.3	7.63	46.2	20	85	11
10	Not identified								
11	Not identified								
12	Excinnuclease ABC	gi| 15892189	*R.conorii*	17.71	6.9	70.2	11	48	8
13		Not identified							
14		Not identified							
15		Not identified							

a) Spot no., the spot numbers as given in the Figure 1.
b) Acc. no., accession numbers according to the NCBI (all entries) database.
c) Theo., theoretical; M_r, molecular weight; *pI*, isoelectric point.
d) Exp., experimental.
e) M.P., number of query matched peptides; the proteins with more than 3 matched peptides were included.
f) Score, ion score of identified protein using NCBI database.
g) Cov., Sequence coverage, the proteins with more than 5% sequence coverage were included.

Discussion

Microbial colonization of the gut lumen depends on the variations of both pH and oxygen levels (Engel and Moran, 2013; Demandel et al., 2020). Our previous data showed that the *pH* along the gut axis of sunn pest is about 5.5 to 6.5 for the midgut

(Dillon and Dillon, 2004). Termits as the main host of protists, xylophage insects as vectors of fungi, and methanogenic archaea and bacteria as common microorganisms in the animal world, are well-known examples of the symbiotic insect-bacteria interactions (Engel and Moran, 2013; Dillon and Dillon, 2004). There are few or no detectable

bacteria in the gut of hemiptera insects. On the other hands, detritivores and wood-feeders are famous groups which have the highest ratios of total gut microbial biomass to the host mass.

Dillon and Dillon (2004) suggested that there is a direct relationship between communities and the compartmentalizations of the gut. They proposed that small communities of microorganisms such as Drosophila, Mosquitoes, and Aphids have a correlation with the narrow gut. Gammaproteobacteria, Alphaproteobacteria, Betaproteobacteria, Bacteroidetes, and Firmicutes such as Lactobacillus and other Bacillus species, Clostridia, Actinomycetes, Spirochaetes, Verrucomicrobia, and Actinobacteria are commonly present in the gut of insects (Engel and Moran, 2013). In a previous study, Baumann showed that heritable symbionts can be divided into two intergrading categories as follows: obligate and facultative endosymbionts (Baumann, 2005).

The presence of the *Ishikawaella capsulate*, as an obligate bacterium, was reported from the midgut of Stink bugs. This bacterium has a key role in the coevolution of the gut-microorganism interactions. During this process some genes which are related to the cell wall synthesis or lipids metabolism were drifted, which indicates the specialization of the microorganisms to the conditions provided by their hosts (Engel and Moran, 2013).

The gastric caeca are special part of digestive system to colonize of bacterial symbionts in the other hemiptera insects. Some of them are transmitted vertically through smearing of eggs by the mother as in *I. capsul*ata, and in the other species environmental acquisition is entrance main way. In the last way, specific symbiont strain may be selected every generation after suitable ingested organisms (Engel and Moran, 2013; Demandel et al., 2020). The southern green stink bug, *Nezara viridula* (Heteroptera: Pentatomidae), contains symbiotic bacteria in the alimentary canal as both way innate and acquiring shelter in every generation (Prado et al., 2006).

Previous data demonstrated the proteome map of the gut and salivary glands of the adult Sunn pests using tube-based 2-dimensional gel electrophoresis (Saadati Bezdi et al., 2012a and 2012b). The previously identified proteins were classified into six functional groups based on their physiological roles including metabolism proteins, musculature proteins, immune related proteins, transport proteins, nutrition storage, and other proteins (Saadati Bezdi et al., 2012b). Various proteins were reported from the gut of Sunn pest: *i)* Proteins associated with the gut muscles such as myosin heavy chain, arginine kinase, actin 3, and tropomyosin; *ii)* effective proteins of the carbohydrate metabolism like glyceraldehyde 3-phosphate dehydrogenase, triose phosphate isomerase, α-amylase, β-galactosidase, glycoside hydrolase, enolase, and aldose reductase; *iii)* protein related to protein metabolism such as aspartate aminotransferase, glyoxylate reductase, glutamate dehydrogenase, and trypsin (Saadati Bezdi et al., 2012b and 2012c). Our data indicated that glyceraldehyde 3-phosphate dehydrogenase, and pyruvate dehydrogenase, two key enzymes in the carbohydrate metabolism, are expressed in the Sunn pest gut with an origin of the *Lactobacillus plantarum* and *Enterococcus faecalis*, respectively. Glyceraldehyde 3-phosphate dehydrogenase breaks down the glucose to produce cellular energy (Chandra et al., 2006; Kunieda et al., 2004). This enzyme is necessary to convert glyceraldehyde 3-phosphate to the 1,3 bisphosphoglycerate during the glycolysis cycle. Through the combination of this data with our previous ones, we can suggest that both innate cells of the host and some symbiotic bacteria have the amenable capacity for the synthesis of key proteins of the carbohydrates metabolism. Furthermore, the supplementary roles of some microorganisms in the nutrition process were approved. The pyruvate dehydrogenase-mediated reaction of pyruvate conversion to the acetyl co enzyme A occurs in the inner membranes of mitochondria (Chandra et al., 2006). The 1c and 2b spots consist of some hypothetical proteins which their existence has been predicted. These proteins are interesting candidates for further biochemical investigations as our current knowledge is not sufficient to identify their properties. Although, in the near future their complete sequences, structures and functional features will be provided based on the molecular dynamic studies in the context of the progressive proteomics. Molecular chaperons (spot 5) are among the critical proteins during the protein synthesis. In fact, most of the times, chaperons are heat shock proteins which are expressed in response to the cellular stress or the elevation of the temperature. Upon activation they can act as foldases, holdases or protein disaggregates (Mahroof et al., 2009). Our results propose that the existence of chaperons with bacterial origins can be considered as an effective folding agent in the conformational determination of the bacterial proteins. Some chaperons of the Sunn pest gut were reported by Saadati bezdi et al., (2012 a, c).

Oxidoreductase FAD-binding protein (spot 1b) is the main protein in the electron transport chain that acts in the redox reaction with flavin adenine

dinucleotide (FADH). This protein is necessary to complete ATP production after the reduction of nicotinamide adenine dinucleotide (NADH) and FADH (Chen et al., 2019). Similar to our previous results, it was demonstrated that this protein is also accumulated in the guts of adult Sunn pests (Saadati Bezdi et al., 2012c). The presence of similar proteins from different origins confirmed the importance of some host reactions in the gut of the Sunn pest. It is interesting that some coevolutionary pathways select proper symbiotic bacteria of the digestive system in the Sunn pests.

ABC-type transporter system (ATP-binding cassette transporter) (Spot 4) is one the largest gene families of animals and prokaryotes. This protein composed of a transmembrane and a membrane-associated ATPase subunit (Chen et al., 2019).
Excinuclease or excision endonuclease (spot 3) is a key enzyme of the DNA repair. The existence of this enzyme with the bacterial origin suggests that the DNA reproductions of symbiotic bacteria is a common mechanism. So far, the digestive system of the Sunn pest was one of the interesting targets for proteome analysis by our research team. We studied the proteome map of the gut and the salivary glands (Saadati bezdi et al., 2012a, 2012b). We compared the proteome contents of adult Sunn pets with their fifth instars (Saadati bezdi et al., 2012c). Also, we demonstrated the accumulation of some plant proteins in the guts of the Sunn pests (Saadati and Toorchi, 2017). These results will complete our knowledge about the gut proteins of Sunn pest in Iran. However, further experiments are essential to find more appropriate approaches to apply these proteins as potential candidates during protein engineering and design of biopesticides against sunn pest populations.

Acknowledgments
We thank Dr. Y. Furusawa and Dr. Kitamura for their critical comments and kind col-laboration. We also appreciate Tanin Naderi and Zahra Rafiei for helping in insect collection. The authors thank University of Birjand of Iran, University of Tabriz and the National Institute of Crop Science of Japan.

References

Babbitt P.C., Hasson M.S., Wedekind J. E., Palmer D. R. J., Barrett W. C., Reed G. H. and et al. (1996) The enolase superfamily: A general strategy for enzyme catalyzed abstraction of the α-protons of carboxylic acids. Biochemistry 35:16489-16501.

Barbehenn R. V. (2002) Gut-based antioxidant enzymes in a polyphagous and a graminivorous grasshopper. Journal of Chemical Ecology 28: 1329-1347.

Baumann P. (2005) Biology bacteriocyte-associated endosymbionts of plant sap-sucking insects. Annual Review of Microbiology 59: 155-189.

Boyd D. W. (2003) Digestive enzymes and stylet morphology of *Deraecoris nigritulus* (Uhler) (Hemiptera: Miridae) reflect adaptions for predatory habits. Annual Entomology Society America 96: 667-671.

Chandra S. B. C., Vik J. L. and Kapatral V. (2006) Comparative insect mithocondrial genomes: Differences despite conserved genome synthenty. African Journal of Biotechnology 5: 1308-1318.

Chen S., Dong Z., Ren X, Zhao D., Zhang Y., Tang M. and et al. (2019) Proteomic Identification of Immune-Related Silkworm Proteins Involved in the Response to Bacterial Infection, Journal of Insect Science 19: 38-51.

Critchley B. R. (1998) Literature review of sunn pest *Eurygaster integriceps* Put. (Hemiptera, Scutelleridae). Crop Protection 17: 271-287.

Demandel S., Lin B., Shi M., Li Y., Xu X. and Jin F. (2020) iTRAQ-Based comparative proteomic analysis of larval midgut from the beet armyworm, *Spodoptera exigua* (Hübner) (Lepidoptera: Noctuidae) challenged with the entomopathogenic bacteria *Serratia marcescens*. Frontiers in Physiology 11:442-454.

Dillon R. J., Dillon V. M. (2004) The gut bacteria of insects: nonpathogenic interactions. Annual Review Entomology 49: 71-92.

Engel P., Moran N. A. (2013) The gut microbiota of insects – diversity in structure and function. Microbiology Review 37: 699-735.

Fransichetii I. B., Lopes A. H, Dias F. A, Pham V.M. and Ribeiro J. M. (2007) An insight into the sialotranscriptome of the seed-feeding bug, *Oncupeltus fasciatus*. Insect Biochemistry and Molecular Biology 37: 903-910.

Habibi J., Courdon T. A, Backus E. A., Brandt S. L, Wagner R M., Wright M. K., et al. (2008). Morphology and histology of the alimentary canal of *Lygus hesperus* (Heteroptera: Cimicomorpha:

Miridae). Annual Entomology Society of America 101: 159-171.

Hou Y., Zou Y., Wang F., Gong J., Zhong X., Xia .Q. and Zhao P. (2010) Comparative analysis of proteome maps of silkworm hemolymph during different developmental stages. Proteome Science 8: 45- 55.

Javaheri M., Scheafer C. W., Lattin J.D. (2009) Shield bugs (Scutelleridae). In: Scheafer C, Panizzi W. (Eds). Heteroptera of economic importance. CRC Press, Washington, USA pp 457-503.

Jouanian L., Bonade-Bottino M., Giard C., Morrot G. and Giband M. (1998) Transgenic plants for insect resistance. Plant Science 131: 1-11.

Kunieda T., Fujiyuki T., Kucharski R., Foret S., Ament S. A., Toth A.L., et al. (2006) Carbohydrate metabolism genes and pathways in insects: insights from the honey bee genome. Insect of Molecular Biology 15: 563-576.

Liu J., Zheng,S., Liu L., Li L. and Feng Q. (2009) Protein profiles of the midgut of *Spodoptera litura* at the sixth instars feeding stage by shutgun ESI-MS approach. Journal of Proteome Research 2010: 2117-2142.

Mahroof R., Zhu K. H., Neven L., Subramanum B. and Bai J. (2005) Experssion patterns of three heat shock protein 70 genes among developmental stages of the red flour beetle, *Tribolium castaneum* (Coleoptera: Tenebrionidae). Comparative Biochemistry and Physiology 141: 247-256.

Pauchet Y., Muck A., Heckel D.G. and Preiss S. (2008) Mapping the larval midgut lumen proteome of *Helicoverpa armigera*, a generalist herbivourous insect. Journal of Proteome Research, 7:1629-1639.

Prado S. S., Rubinoff D. and Almeida R. P. P. (2006) Vertical transmission of a pentatomid caeca-associated symbiont. Annual Entomolgical Society of America 99: 577–585

Saadati M. and Toorchi M. (2017) The study of plant protein accumulation in gut of insect using proteomics technique: Wheat–sunn pest interaction. Journal of the Saudi Society of Agricultural Sciences 16: 205-209

Saadati Bezdi M., Farshbaf Pourabad R., Toorchi M., Zarghami N. and Komatsu S. (2012a) Protein patterns in salivary gland of sunn pest, *Eurygaster integriceps* (put.) (Hem: Scutelleridae). Turkish Journal of Entomology 36: 71-80.

Saadati Bezdi M., Toorchi M., Farshbaf Pourabad R. and Zarghami N. (2012b) Protein map of gut in adult sunn pest, *Eurygaster integriceps* (Put.) (Hem: Scutelleridae): Two-dimensional electrophoresis technique. Munis Entomology and Zoology 7: 229-237.

Saadati Bezdi M., Toorchi M., Farshbaf Pourabad R., Zarghami N., Nouri M. Z. and Komatsu S. (2012c) Proteome analysis of gut and salivary gland proteins of fifth-instar nymphs and adults of the sunn pest. Archives of Insect Biochemistry and Physiology 81: 105-119.

Saxena K. N. (1963) Mode of ingestion in a heteropterous insect *Dysdercus Koenigii* (F.)(Pyrrohocoridae). Journal of Insect Physiology 9: 47-71.

Tunaz H. and Stanley D.W. (2004) Phospholipase A2 in salivary glands isolated from tobacco hornworms, *Manduca sexta*. Comparative Biochemistry and Physiology, 139: 27-33.

Wilkins M., Pasquali C., Appel R., Ou K., Golaz O., Sanchez J., et al. (1996) From proteins to proteomes: large scale protein identification by 2-D electrophoresis and amino acids analysis. Bio/techniques 14: 61–65.

Journal of Cell and Molecular Research (2021) 12 (2), 104-110 DOI: 10.22067/jcmr.v12i2.88457

Research Article

Identification of Suitable Housekeeping Genes for Quantitative Gene Expression Analysis During Retinoic Acid-induced Differentiation of Embryonal Carcinoma NCCIT Cells

Sara Soltanian *, Mahboubeh Sheikhbahaei

Department of Biology, Faculty of Science, Shahid Bahonar University of Kerman, Kerman, Iran

Received 1 September 2020 Accepted 13 November 2020

Abstract

Real-time quantitative PCR (qRT-PCR) is often used as an effective experimental method for analyzing gene expression. In this method, normalization of target gene expression levels must be performed using housekeeping genes (HKGs). HKGs are used to compensate for difference between samples due to diverse quality and quality of RNAs and different reverse transcription yield. For an ideal reference gene, constant expression levels across different samples of one experiment is necessary. In the current study, expression stability of four candidate references genes including Beta actin (ACTB), glyceraldeyde-3-phosphate dehydrogenase (GAPDH), hypoxanthine guanine phosphoribosyl transferase (HPRT1) and Beta-2-Microglobulin (β2M) following retinoic acid (RA) treatment in embryonal carcinoma NCCIT cells were evaluated. NCCIT cells were exposed to RA (10 µM) for 14 days to induce differentiation. RT-qPCR for candidate references genes was performed and normalization between untreated and RA-treated cells was performed using identical sample input amounts. Expression of OCT4, SOX2, NANOG during RA-induced differentiation was assessed by quantitative real-time PCR. RT-qPCR results indicated significant difference in expression level of GAPDH between untreated (Ct mean: 19.36667± 0.28) and RA-treated (Ct mean: 28.94± 0.18) NCCIT cells. However, transcriptional level of ACTB, HPRT and β2M remained unchanged after RA treatment. qRT-PCR analysis using ACTB, HPRT and β2M showed treatment of NCCIT cells with RA lead to significant down regulation of OCT4 (79%), NANOG (71%) and SOX2 (96%) transcript. ACTB, HPRT and β2M were recognized as valid reference genes for analysis of gene expression during RA-induced differentiation of NCCIT cells, while GAPDH was not suitable.

***Keywords*:** Housekeeping genes, NCCIT cell, Retinoic acid, Differentiation, Expression analysis

Introduction

Real-time reverse transcription quantitative PCR (qRT-PCR) has emerged as one of the most powerful tools for quantifying gene expression levels in a variety of gene expression studies. In real time PCR, it is required to normalize variations in quantity and quality of starting RNA and cDNA synthesis efficiency among different samples. For this purpose, internal control, often referred to as a housekeeping or reference gene are widely used (Nygard et al., 2007). Housekeeping genes (HKGs) are constitutive genes that are required for maintenance of basic cellular function (Richly et al., 2003). Since, HKGs play a critical role in accurate normalization of qRT-PCR data, an ideal HKGs must be expressed in a stable and non-regulated constant level across different cell types and experimental situation (Chen et al., 2006; Turabelidze et al., 2010).

Beta actin (ACTB), glyceraldeyde-3-phosphate dehydrogenase (GAPDH), hypoxanthine guanine phosphoribosyl transferase (HPRT1) and Beta-2-Microglobulin (β2M) are among the most commonly used HKGs in qRT-PCR studies (Dheda et al., 2004; Radonić et al., 2004). However, several reports have shown that these HKGs have variable expression levels in different experimental conditions (de Kok et al., 2005; Glare et al., 2002; Selvey et al., 2001). Therefore, there is no universal HKGs having stable expression in all tissues under all experimental conditions and it is clear that suitable HKGs must be selected for particular sample sets and experimental models.

The purpose of our current investigation is to evaluate the expression stability of four candidate HKGs (ACTB, GAPDH, HPRT and β2M) during retinoic acid (RA)-induced differentiation of embryonal carcinoma (EC) NCCIT cells. According

*Corresponding author's E-mail address:
Soltanain@uk.ac.ir; sarasoltanian@gmail.com

to our results, GAPDH showed high variability of expression between untreated and RA-treated NCCIT cells. Therefore, although GAPDH is a common reference gene in many experiments, it cannot be an optimal reference gene in this experiment. On the contrary, expression levels of ACTB, HPRT and β2M remained unchanged in NCCIT cells after RA treatment, so they can be used as a suitable reference gene for analysis of gene expression in NCCIT cells exposed to RA.

Materials and Methods

NCCIT cell culture and RA treatment

NCCIT cells (Pasteur Institute of Iran, Tehran) were cultured in RPMI-1640 medium (Gibco, Grand Island, USA) supplemented with 10% fetal bovine serum (FBS; Biowest, France) and 100 U/mL penicillin and streptomycin (Biowest, France) in the presence of a humidified atmosphere with 5% CO_2 at 37 °C. According to many researches, to induce differentiation, NCCIT cells were treated with 10 µM RA for 2 weeks (Jin et al., 2012; Kooistra et al., 2009; Park et al., 2014).

RNA extraction and cDNA synthesis

RNA isolation kit (DENAzist Asia, Mashhad, Iran) was used to extract total RNA from untreated and RA-treated NCCIT cells. Afterward, quality and quantity of RNA were assessed via nanodrop and agarose gel electrophoresis. To avoid DNA contamination, total RNA was treated with DNase I (Cat. No. EN0521; Thermo Fisher Scientific). For cDNA synthesis, 1 µg RNA was reverse transcribed using 200 U of M-MuLV reverse transcriptase (Cat. No. EP0441; Thermo Scientific) in presence of 5 µM oligo (dt)18 (Cat. No. MAN0013109; Thermo Scientific), 1 mM dNTPs (Cat. No. R0192; Thermo Scientific) in accordance with the manufacturer's instructions.

Quantitative Real-Time PCR

Real time PCR was performed using real-time PCR system (Analytik Jena, Jena, Germany). For each reaction, 12.5 µl of SYBR Green, 0.5 µl of forward and reverse primers (10 µM) and 1µl cDNA in total volume of 25 µl was used. Real time program for all genes **was**: 95°C for 4 min followed by 40 cycles of 95°C for 30 s, 62°C for 20s, and 72°C for 10 s. To derive melting curves, at the end of the PCR run, temperature was increased in steps of 1°C for 10 s from 61°C to 95°C. The sequence of primers and product length are described in Table 1.

Table 1. List of different PCR primers used in the study

Gene name	Sequence (5´ to 3´)	Product size (bp)
POU class 5 homeobox 1 (POU5F1) Alias symbols: OCT4	F:CCGAAAGAGAAAGCGAACCAGTAT R: CCACACTCGGACCACATCCTTC	145
Nanog homeobox (NANOG)	F: AATACCTCAGCCTCCAGCAGATG R: CTGCGTCACACCATTGCTATTCT	149
SRY-box transcription factor 2 (SOX2)	F:GGGAAATGGGAGGGGTGCAAAAGAGG R: TTGCGTGAGTGTGGATGGGATTGGTG	151
Hypoxanthine guanine phosphoribosyl transferase (HPRT)	F: TTTGTTGTAGGATATGCCCTT R: ACATTGATAATTTTACTGGCGAT	168
Beta-actin (ACTB)	F: ACCACCTTCAACTCCATCATG R: CTCCTTCTGCATCCTGTCG	120
Glyceraldehyde-3-phosphatedehydrogenase (GAPDH)	F: GACCACTTTGTCAAGCTCATTTCC R: GTGAGGGTCTCTCTCTTCCTCTTGT	151
Beta-2-Microglobulin (*β2M*)	F: CTCCGTGGCCTTAGCTGTG R: TTTGGAGTACGCTGGATAGCCT	69

Data analysis

Fold change in expression of the HKGs in RA-treated versus the untreated samples

Reverse transcription was performed with the same amount (1 µg) and optimal quality of total RNA from two samples (untreated and RA-treated NCCIT cells), so mean cycle threshold (Ct) values of two samples were used to evaluate expression stability of candidate HKG.

In order to calculate fold change in expression of the HKGs in the treated versus the untreated samples, at first mean Ct values was calculated as 2^{-Ct} and fold change is calculated as Mean 2^{-Ct} $_{\text{treated cell}}$/ Mean 2^{-Ct} $_{\text{untreated cells.}}$

Fold change in expression of pluripotency factors during RA-induced differentiation of NCCIT cells

To assess expression of OCT4, NANOG and SOX2 in RA-exposed cells in comparison with the untreated control cells, B2M, HPRT and ACTB were used as HKGs and data were analyzed by relative quantification using the comparative Ct method: Fold change = $2^{-\Delta\Delta ct}$.

$\Delta\Delta C$ = [ΔCt treated cells (Meant Ct $_{\text{target gene}}$ - Mean Ct $_{\text{reference gene}}$) _ ΔCt control cells (Meant Ct $_{\text{target gene}}$ - Mean Ct $_{\text{reference gene}}$)]

Statistical analysis

In this experiment, NCCIT cells were cultured and treated with RA in three "6 cm cell culture plate" and then differentiated cells were merge and one RNA was extracted from them. The same was done for untreated NCCIT cells. For qPCR, there are three biological repeats for each gene. Mean Ct values are shown in Supplementary table 1. T-test was used to compare expression of genes between treated and control NCCIT cells. P-value less than 0.01 was considered statistically significant.

Results and Discussion

Identification of ideal HKGs that are stably expressed under various experimental conditions and tissues of interest would provide a powerful tool for normalization of target gene expression levels in qRT-PCR. On the contrary, poor selection of HKGs can invalidate the normalization process and lead to the generation of misleading information (Chen et al., 2006; Glare et al., 2002; Haller et al., 2004). Unfortunately, it has been proved that expression of commonly used HKGs is affected with treatment or physiological state (Bustin, 2000; Janovick-Guretzky et al., 2007; Wu and Rees, 2000). Therefore, studies to find suitable HKGs with a relatively stable expression level across many different cell type and conditions have received more attention in gene expression analysis (Vandesompele et al., 2002). In the present paper we have therefore looked at the expression stability of commonly used HKGs including ACTB, HPRT, β2M and GAPDH during RA- induced differentiation of NCCIT cells.

For this purpose, normalization was performed between untreated and RA-treated samples using same amount of RNA (1 µg) in cDNA synthesis and optimal quality of RNAs were confirmed by nanodrop (260/230: 2-2.2 and 260/280: 1.8-2) and electrophoresis (supplementary Figure 1). After qRT-PCR, analysis of melting curves clearly indicated that each of the primer pairs described in Table 1 amplified a single expected product with a distinct Tm (supplementary Figure 2). The accuracy of the amplification reaction was validated by gel electrophoresis (Figure 1).

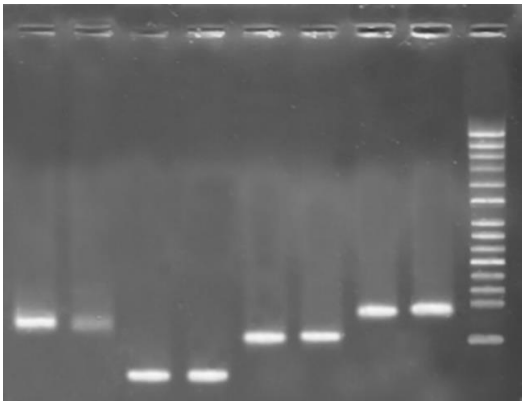

Figure 1. The accuracy of qRT-PCR was further validated by gel electrophoresis. qRT-PCR products from left to right are GAPDH: 151 bp; β2M: 69 bp; ACTB:145 b and HPRT: 168 bp genes for untreated and RA-treated NCCIT cells respectively. A molecular weight marker (100 bp ladder) is used.

Ct values of the candidate HKGs obtained by qRT-PCR in both samples (untreated and RA-treated NCCIT cells) were used to assess their expression levels and stability (supplementary Table 1). In comparison with other HKGs, the average Ct±SD (25.8±0.025) of β2M in untreated NCCIT cells was the highest, meaning it had the lowest expression level than other and the most abundantly expressed gene was *ACTB* and its average Ct±SD (17.78±0.055) was the lowest.
Using the Ct values of each experimental sample, we draw a box-plot for candidate HKGs (Figure 2). The results showed that mean Ct values of HPRT (untreated cells: 22.55± 0.12; RA-treated cells: 22.51±0.18), ACTB (untreated cells:17.785±0.05; RA-treated cells: 17.33±0.17) and β2M (untreated cells: 25.85± 0.02; RA-treated cells: 26±0.06) did not change significantly after treatment with RA. Calculating fold change in expression of the HKGs in the treated versus the untreated samples showed RA treatment changed the expression of β2M, HPRT, GAPDH by 0.86, 1.03 and 1.37 fold. Therefore, they can be regarded as reliable reference genes for expression analysis of target genes in this experiment. On the contrary, expression of GAPDH in NCCIT cells (Ct:19.36±0.28) reduced significantly (around 678-fold) after RA treatment (Ct: 28.94±0.18) and so this gene is not suitable reference gene for expression analysis of target genes after exposure to NCCIT and likely any cell lines to RA.

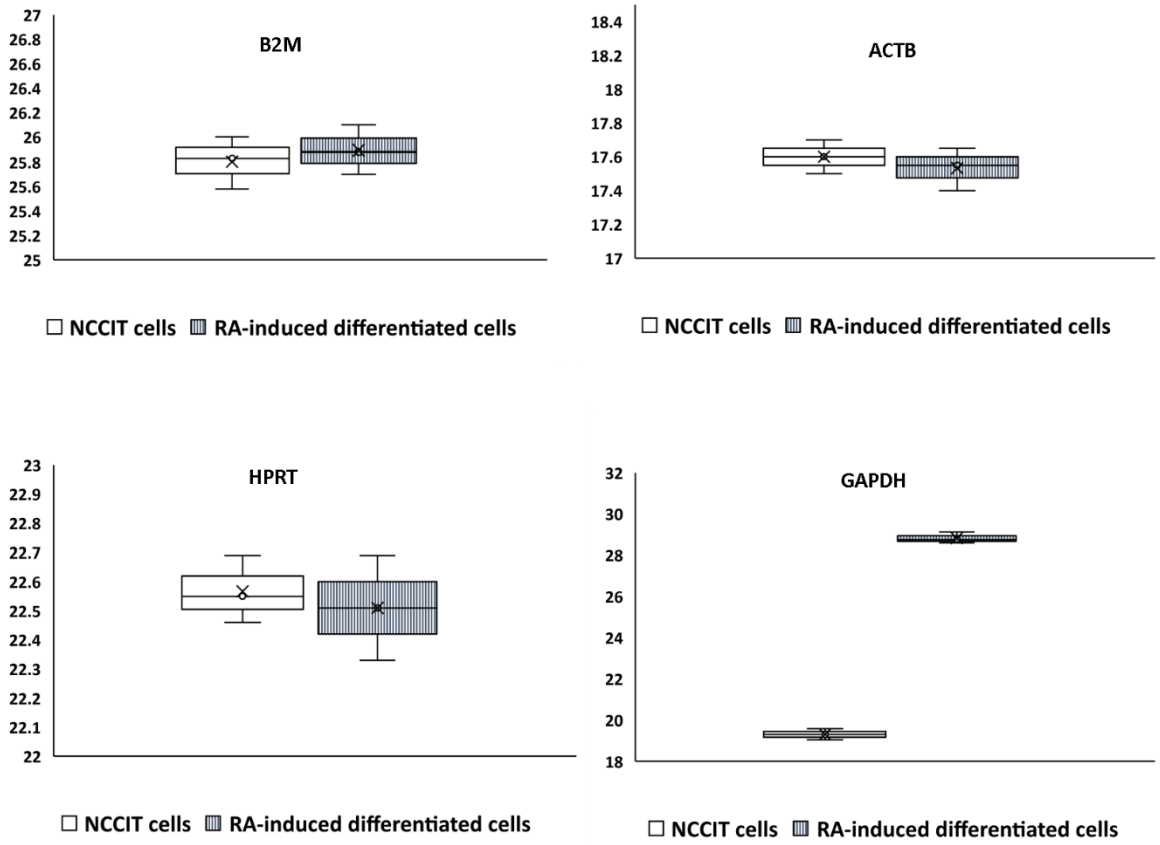

Figure 2. Box-plot based on Ct of 4 candidate HKGs in untreated and RA-treated NCCIT cells. The block diagram represents the quartile range (25th to 75th percentiles) of Ct values; the '×' in the box depicts the median of the Ct value; underline and overline are determined by the minimum and maximum values of the Ct value.

This was the first study that analyzed expression stability of some HKGs during RA-induced differentiation of pluripotent embryonal carcinoma NCCIT cells. In another study, stability of various HKGs during RA-induced differentiation of human embryonic stem (ES) cell was examined and β2M, ribosomal protein L13A and Alu repeats were found to be the most stable for this experimental set-up (Vossaert et al., 2013). According to another report, both HPRT and beta-tubulin mRNA levels varied markedly in spontaneously differentiating and growth factor-

supplemented (TGF-beta) ES cell cultures, while GAPDH expression remained relatively constant (Murphy and Polak, 2002).

RA mediated differentiation and exit from the pluripotent state in NCCIT cells were confirmed via expression analysis of important pluripotency markers including OCT4, NANOG and SOX2 using qRT-PCR. The transcription factors OCT4, SOX2, and NANOG are important factors for maintaining pluripotency and self-renewal of pluripotent cells (Chambers and Tomlinson, 2009). In many researches, down regulation of OCT4, NANOG and SOX2 were reported during differentiation of pluripotent cells and exit from pluripotency state (Rassouli et al., 2013; Soltanian and Dehghani, 2018; Soltanian et al., 2014; Soltanian et al., 2020; Stevanovic, 2003).

Since, β2M, ACTB and HPRT showed stable expression levels during RA treatment, they could be used as reference genes for expression analysis of pluripotency factors between untreated and RA-treated NCCIT cells. Results showed that after RA treatment, expression of OCT4, NANOG and SOX2 decreased to around 79 %, 71 % and 96 % of that of untreated NCCIT cells (Figure 3). Therefore, according to these results, NCCIT cells undergo differentiation by RA treatment.

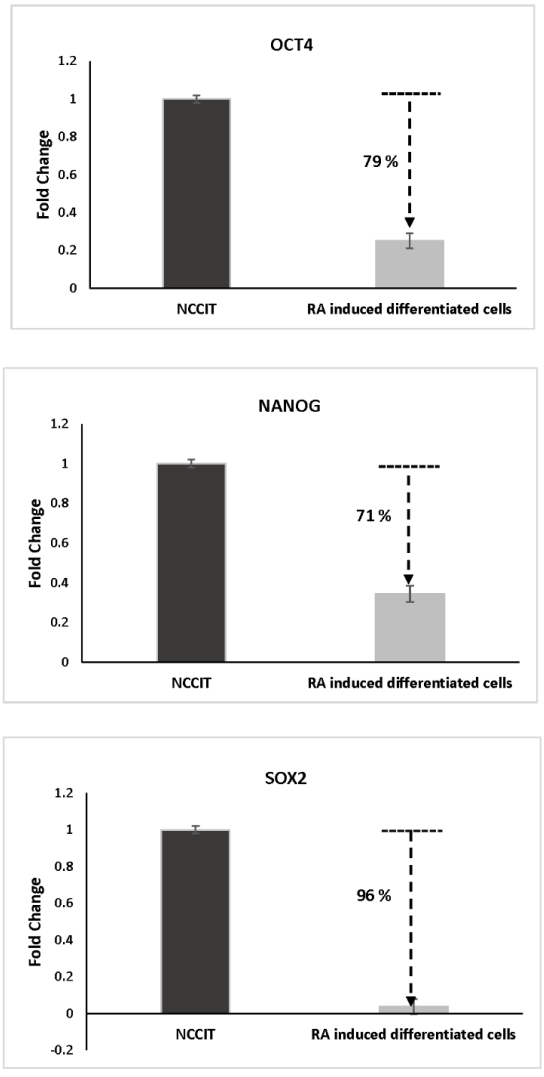

Figure 3. Quantitative RT-PCR analysis of OCT4, NANOG and SOX2 gene expression after treatment of NCCIT with RA. NCCIT cells were treated with RA (10 μM) for 14 days and expression of OCT4, NANOG and SOX2 were measured and compared to untreated cells as control by real time PCR. The graph represents the mean data±SD (error bar) of at least three independent experiments. *$p<0.01$ against control.

In conclusion, selection of a suitable HKG is essential to normalize real-time PCR data. However, the choice of HKGs should be tailored to the nature of the study. For example, although

B2M, ACTB, HPRT and GAPDH are widely used and accepted as reference genes for analysis of gene expression, according to some researches, their expression varies in different situation. Therefore, expression level stability of HKGs must be confirmed in each study (Guénin et al., 2009; Zhang et al., 2005). Furthermore, it has been strongly proposed that more than one stable expressed reference gene should be used to avoid misinterpretation of gene expression data (Hamalainen et al., 2001; Zhong and Simons, 1999).

Acknowledgement
The authors thank Vice Chancellor for Research and Technology, Shahid Bahonar University of Kerman, Kerman, Iran for financial support.

Conflict of Interest
The authors declare that they have no conflict of interest

References

Bustin S. A. (2000) Absolute quantification of mRNA using real-time reverse transcription polymerase chain reaction assays. Journal of molecular endocrinology 25:169-193.

Chambers I. and Tomlinson S. R. (2009) The transcriptional foundation of pluripotency. Development 136:2311-2322.

Chen J., Rider D. A. and Ruan R. (2006) Identification of valid housekeeping genes and antioxidant enzyme gene expression change in the aging rat liver. The Journals of Gerontology Series A: Biological Sciences and Medical Sciences 61:20-27.

de Kok J. B., Roelofs R. W., Giesendorf B. A., Pennings J. L., Waas E. T., Feuth T., Swinkels D. W. and Span P. N. (2005) Normalization of gene expression measurements in tumor tissues: comparison of 13 endogenous control genes. Laboratory investigation 85:154-159.

Dheda K., Huggett J. F., Bustin S. A., Johnson M. A., Rook G. and Zumla A. (2004) Validation of housekeeping genes for normalizing RNA expression in real-time PCR. Biotechniques 37:112-119.

Glare E. M., Divjak M., Bailey M. and Walters E. H. (2002) β-Actin and GAPDH housekeeping gene expression in asthmatic airways is variable and not suitable for normalising mRNA levels. Thorax 57:765-770.

Guénin S., Mauriat M., Pelloux J., Van Wuytswinkel O., Bellini C. and Gutierrez L. (2009) Normalization of qRT-PCR data: the necessity of adopting a systematic, experimental conditions-specific, validation of references. Journal of experimental botany 60:487-493.

Haller F., Kulle B., Schwager S., Gunawan B., von Heydebreck A., Sültmann H. and Füzesi L. (2004) Equivalence test in quantitative reverse transcription polymerase chain reaction: confirmation of reference genes suitable for normalization. Analytical biochemistry 335:1-9.

Hamalainen H., Tubman J., Vikman S., Kyrölä T., Ylikoski E., Warrington J. and Lahesmaa R. (2001) Identification and validation of endogenous reference genes for expression profiling of T helper cell differentiation by quantitative real-time RT-PCR. Analytical biochemistry 299:63-70.

Janovick-Guretzky N., Dann H., Carlson D., Murphy M., Loor J. J. and Drackley J. K. (2007) Housekeeping gene expression in bovine liver is affected by physiological state, feed intake, and dietary treatment. Journal of Dairy Science 90:2246-2252.

Jin B., Ernst J., Tiedemann R. L., Xu H., Sureshchandra S., Kellis M., and et al. (2012) Linking DNA methyltransferases to epigenetic marks and nucleosome structure genome-wide in human tumor cells. Cell reports 2:1411-1424.

Kooistra S. M., Thummer R. P. and Eggen B. J. (2009) Characterization of human UTF1, a chromatin-associated protein with repressor activity expressed in pluripotent cells. Stem cell research 2:211-218.

Murphy C. L. and Polak J. M. (2002) Differentiating embryonic stem cells: GAPDH, but neither HPRT nor β-tubulin is suitable as an internal standard for measuring RNA levels. Tissue engineering 8:551-559.

Nygard A.-B., Jørgensen C. B., Cirera S. and Fredholm M. (2007) Selection of reference genes for gene expression studies in pig tissues using SYBR green qPCR. BMC molecular biology 8:67.

Park S.-W., Do H.-J., Ha W. T., Han M.-H., Song H., Uhm S.-J., and et al. (2014) Differential expression of ETS family transcription factors in NCCIT human embryonic carcinoma cells upon retinoic acid-induced differentiation. Biological and Pharmaceutical Bulletin 37:659-665.

Radonić A., Thulke S., Mackay I. M., Landt O., Siegert W. and Nitsche A. (2004) Guideline to reference gene selection for quantitative real-time PCR. Biochemical and biophysical research communications 313:856-862.

Rassouli F. B., Matin M. M., Bahrami A. R., Ghaffarzadegan K., Cheshomi H., Lari S., Memar B.

and Kan M. S. (2013) Evaluating stem and cancerous biomarkers in CD15+ CD44+ KYSE30 cells. Tumor Biology 34:2909-2920.

Richly E., Chinnery P. F. and Leister D. (2003) Evolutionary diversification of mitochondrial proteomes: implications for human disease. Trends in Genetics 19:356-362.

Selvey S., Thompson E. W., Matthaei K., Lea R. A., Irving M. and Griffiths L. R. (2001) β-Actin—an unsuitable internal control for RT-PCR. Molecular and cellular probes 15:307-311.

Soltanian S. and Dehghani H. (2018) BORIS: a key regulator of cancer stemness. Cancer cell international 18:1-13.

Soltanian S., Dehghani H., Matin M. M. and Bahrami A. R. (2014) Expression analysis of BORIS during pluripotent, differentiated, cancerous, and non-cancerous cell states. Acta Biochim Biophys Sin 46:647-658.

Soltanian S., Sheikhbahaei M. and Ziasistani M. (2020) Phytol Down-Regulates Expression of Some Cancer Stem Cell Markers and Decreases Side Population Proportion in Human Embryonic Carcinoma NCCIT Cells. Nutrition and Cancer:1-14.

Stevanovic M. (2003) Modulation of SOX2 and SOX3 gene expression during differentiation of human neuronal precursor cell line NTERA2. Molecular biology reports 30:127-132.

Turabelidze A., Guo S. and DiPietro L. A. (2010) Importance of housekeeping gene selection for accurate reverse transcription-quantitative polymerase chain reaction in a wound healing model. Wound repair and regeneration 18:460-466.

Vandesompele J., De Preter K., Pattyn F., Poppe B., Van Roy N., De Paepe A. and et al. (2002) Accurate normalization of real-time quantitative RT-PCR data by geometric averaging of multiple internal control genes. Genome biology 3:1-12.

Vossaert L., O'Leary T., Van Neste C., Heindryckx B., Vandesompele J., De Sutter P. and et al. (2013) Reference loci for RT-qPCR analysis of differentiating human embryonic stem cells. BMC molecular biology 14:21.

Wu Y.-Y. and Rees J. L. (2000) Variation in epidermal housekeeping gene expression in different pathological states. Acta dermato-venereologica 80: 2-3

Zhang X., Ding L. and Sandford A. J. (2005) Selection of reference genes for gene expression studies in human neutrophils by real-time PCR. BMC molecular biology 6:4.

Zhong H. and Simons J. W. (1999) Direct comparison of GAPDH, β-actin, cyclophilin, and 28S rRNA as internal standards for quantifying RNA levels under hypoxia. Biochemical and biophysical research communications 259:523-526.

Supplementary Materials:

A

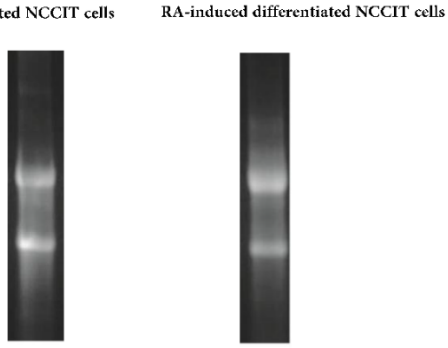

B

Sample	Concentration	260/280	260/230
Undifferentiated NCCIT cells	1000 µg/ml	2.1	1.8
RA- induced differentiated cells	1000 µg/ml	2.2	1.9

Figure S1. Agarose gel electrophoresis of total RNA isolated from undifferentiated and RA- induced differentiated NCCIT cells. A) Intact total RNAs have sharp 28S and 18S rRNA bands. B) Nanodrop analysis of RNA samples isolated from undifferentiated and RA- induced differentiated NCCIT cells.

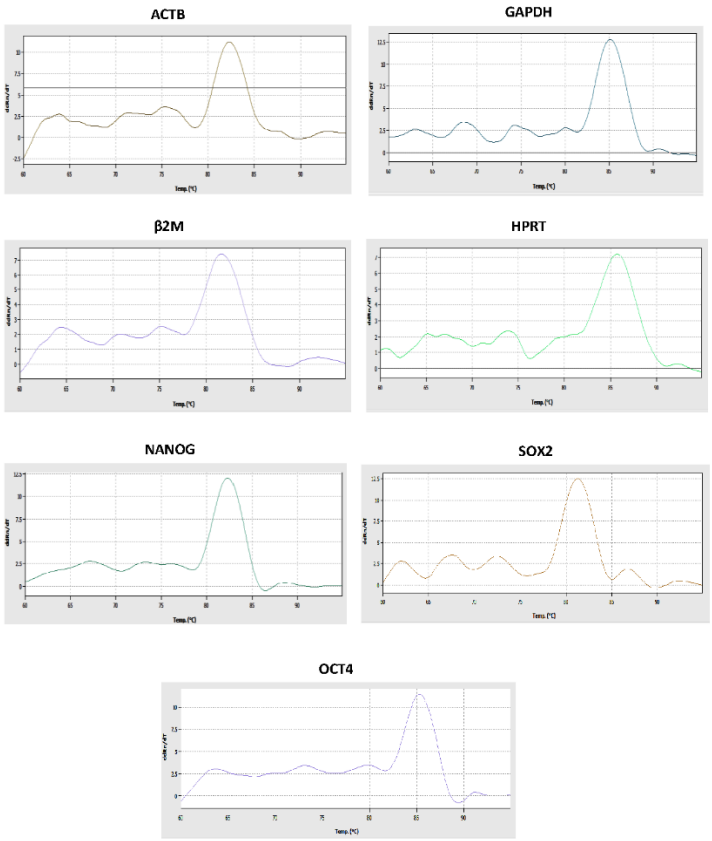

Figure S2. Melt-curve analysis of products from SYBR Green assay for each primer sets.

Table S1. The man Ct value of three biological repeats

Gene Name	β2M	HPRT	GAPDH	ACTB
Ctvalues	25.88	22.69	19.58	17.84
(NCCIT	25.83	22.5	19.04	17.73
untreated	25.85	22.46	19.48	17.785
cells)				
Ctvalues	25.99	22.69	29.12	17.16
(RA-	26.12	22.33	28.76	17.51
treated	26.09	22.51	28.94	17.335
NCCIT				
cells)				

Scientific Reviewers

MANUSCRIPT PREPARATION

Manuscripts should be prepared in accordance with the uniform requirements for Manuscript's Submission to **"Journal of Cell and Molecular Research".**

Language: Papers should be in English (either British or American spelling). The past tense should be used throughout the results description, and the present tense in referring to previously established and generally accepted results. Authors who are unsure of correct English usage should have their manuscript checked by somebody who is proficient in the language; manuscripts that are deficient in this respect may be returned to the author for revision before scientific review.

Typing: Manuscripts must be typewritten in a font size of at least 12 points, double-spaced (including References, Tables and Figure legends) with wide margins (2.5 cm from all sides) on one side of the paper. The beginning of each new paragraph must be clearly indicated by indentation. All pages should be numbered consecutively at the bottom starting with the title page.

Length: The length of research articles should be restricted to ten printed pages. Short communication should not exceed five pages of manuscript, including references, figures and tables. Letters should be 400-500 words having 7-10 references, one figure or table if necessary. Commentaries and news should also be 800-1000 words having 7-10 references and one figure or table if necessary.

Types of Manuscript: JCMR is accepting original research paper, short communication reports, invited reviews, letters to editor, biographies of scientific reviewers, commentaries and news.

Statement of Human and Animal Rights: Author's should declare regulatory statement regarding the experiments using animals, human cells/tissues that all in vivo experiments have been performed according to the guidelines (explained by WHO, international animal rights federations or your respective institute) to use animals in their research work.

Conflict of Interest Statement: Authors or corresponding author should declare statement of conflict of interest at the last of manuscript.

Manuscript Evaluation Time: All submitted manuscripts will be evaluated and reviewed according to following evaluation schedule.
Pre-Editorial Evaluation: All submitted manuscripts, right after their submission to JCMR will be evaluation by Editors for being according to the journal scope and format. This evaluation can take 2-7 days of submission.
Reviewer's Evaluation: Selected manuscripts after pre-editorial evaluation will be sent to minimum two blind reviewers assigned by Editor-in-Chief. This process may take 21-27 days.
Post Editorial Evaluation: After receiving reviewer's comments, editors evaluate the manuscripts considering the comments and decide their first decision. This process takes 3-5 days and then authors are informed regarding the editorial decision.

GENERAL ARRANGEMENT OF PAPERS

Title: In the first page, papers should be headed by a concise and informative title. The title should be followed by the authors' full first names, middle initials and last names and by names and addresses of

laboratories where the work was carried out. Identify the affiliations of all authors and their institutions, departments or organization by use of Arabic numbers (1, 2, 3, etc.).

Footnotes: The name and full postal address, telephone, fax and E-mail number of corresponding author should be provided in a footnote.

Abbreviations: The Journal publishes a standard abbreviation list at the front of every issue. These standard abbreviations do not need to be spelled out within paper. However, non-standard and undefined abbreviations used five or more times should be listed in the footnote. Abbreviations should be defined where first mentioned in the text. Do not use abbreviations in the title or in the Abstract. However, they can be used in Figures and Tables with explanation in the Figure legend or in a footnote to the Table.

Abstract: In second page, abstract should follow the title (no authors' name) in structured format of not more than 250 words and must be able to stand independently and should state the Background, Methods, Results and Conclusion. Write the abstract in third person. References should not be cited and abbreviations should be avoided.

Keywords: A list of three to five keywords for indexing should be included at bottom of the abstract. Introduction should contain a description of the problem under investigation and a brief survey of the existing literature on the subject.

Materials and Methods: Sufficient details must be provided to allow the work to be repeated. Correct chemical names should be given and strains of organisms should be specified. Suppliers of materials need only be mentioned if this may affect the results. Use System International (SI) units and symbols.

Results: This section should describe concisely the rationale of the investigation and its outcomes. Data should not be repeated in both a Table and a Figure. Tables and Figures should be selected to illustrate specific points. Do not tabulate or illustrate points that can be adequately and concisely described in the text.

Discussion: This should not simply recapitulate the Results. It should relate results to previous work and interpret them. Combined Results and Discussion sections are encouraged when appropriate.

Acknowledgments: This optional part should include a statement thanking those who assisted substantially with work relevant to the study. Grant support should be included in this section.

References: References should be numbered and written in alphabetical order. Only published, "in press" papers, and books may be cited in the reference list (see the examples below). References to work "in press" must be accompanied by a copy of acceptance letter from the journal. References should not be given to personal communications, unpublished data, manuscripts in preparation, letters, company publications, patents pending, and URLs for websites. Abstracts of papers presented at meetings are not permissible. These references should appear as parenthetical expressions in the text, e.g. (unpublished data). Few example of referencing patterns are given as follows:
Examples of text references:

Cite a source written by one author: (Kikuchi, 2014)

Cite a source written by two authors: (Rinn and Chang, 2012)

Cite a source written by three or more authors: (Mead et al., 2015)

Examples of end references:

Bongso A., Lee E. H. and Brenner S. (2005) Stem cells from bench to bedside. World Scientific Publishing Co. Singapore, 38-55 pp.

Kikuchi K. (2014) Advances in understanding the mechanism of zebrafish heart regeneration. Stem Cell Research 13:542-555.

Irfan-Maqsood M. (2013) Stem Cells of Epidermis: A Critical Introduction. Journal of Cell and Molecular Research 5:1, 1-2.

(6 authors:) Mead B., Berry M., Logan A., Scott R. A., Leadbeater W. and Scheven B. A. (2015) Stem cell treatment of degenerative eye disease. Stem Cell Research 14:243-257.

Rinn J. L. and Chang H. Y. (2012) Genome regulation by long noncoding RNAs. Annual Review of Biochemistry 81:1-9.

Note: When citing more than six authors, give the name of the first six authors and abbreviate the others to et al.

(more than 6 authors:) Vaculik C., Schuster C., Bauer W., Iram N., Pfisterer K., Kramer G., et al. (2012) Human dermis harbors distinct mesenchymal stromal cell subsets. Journal of Investigative Dermatology 132:563-574.

Tables and Figures: Tables and Figures should be numbered (1, 2, 3, etc.) as they appear in the text. Figures should preferably be the size intended for publication. Tables and Figures should be carefully marked. Legends should be typed single-spaced separately from the figures. Photographs must be originals of high quality. Photocopies are not acceptable. Those wishing to submit color photographs should contact the Editor regarding charges.

JCMR Open Access Policy: Journal of Cell and Molecular Research follows the terms outlined by the Creative Common's Attribution-Only license (CC-BY) to be the standard terms for Open Access. Creative Commons License.

Note: All manuscripts submitted to JCMR are tracked by using "iThenticate" or "small tools" for possible plagiarism before acceptance to JCMR.

Table of Contents

Journal of Cell and Molecular Research

Volume 12, Number 2, (Winter) 2021